Nuclear effects in neutrino interactions

Marco Martini
Ghent University

Neutrino - nucleus interaction @ $E_\nu \sim O$ (1 GeV)

[MiniBooNE, T2K energies]

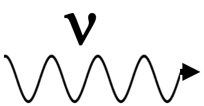

Quasielastic (QE)

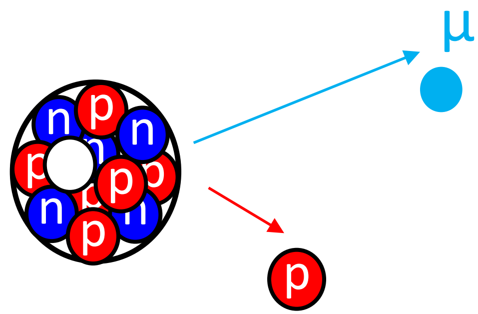

Two Nucleons knock-out (2p-2h)

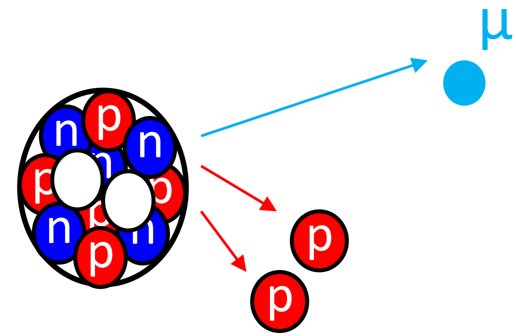

Incoherent π production

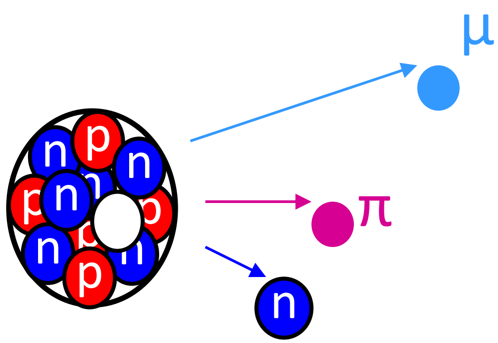

Coherent π production

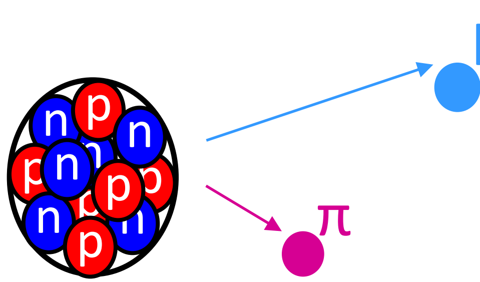

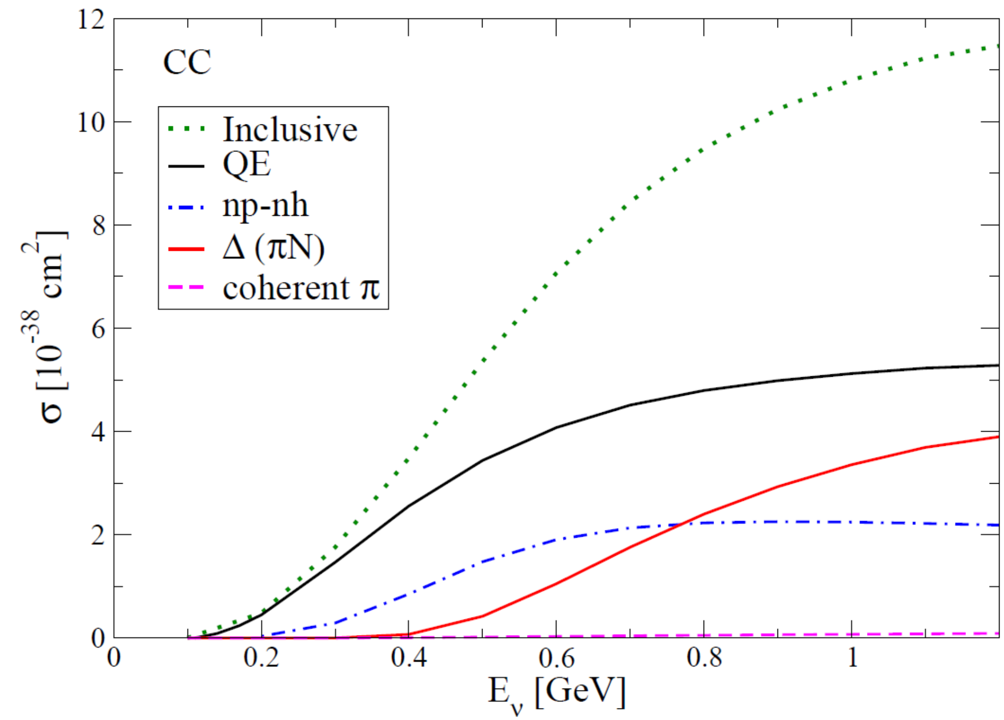

M. Martini, M. Ericson, G. Chanfray, J. Marteau, PRC 80 065501 (2009)

Neutrino-nucleus interaction

$$\mathcal{L}_W = \frac{G_F}{\sqrt{2}} \cos(\theta_C) l_\mu h^\mu$$

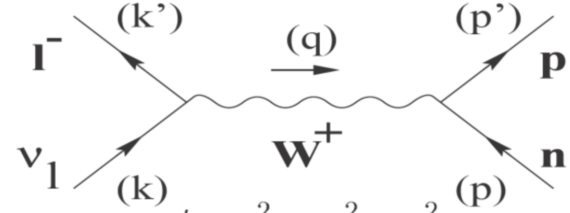

$$t = q^2 = \omega^2 - \boldsymbol{q}^2$$

lepton

$$\langle k', s'|l_\mu|k, s\rangle = e^{-iqx}\bar{u}(k', s')\,[\gamma_\mu(1-\gamma_5)]\,u(k, s)$$

hadron

$$\langle p', s'|h^\mu_+|p, s\rangle \;=\; e^{iqx}\bar{u}(p', s')\,[F_1(t)\gamma^\mu + F_2(t)\sigma^{\mu\nu}\frac{iq_\nu}{2M_N} + G_A(t)\gamma^\mu\gamma_5 + G_P(t)\gamma_5\frac{q^\mu}{2M_N}]\,\tau_+ u(p, s)$$

Vector Axial

Cross section:

$$\frac{\partial^2\sigma}{\partial\Omega_{k'}\partial k'} = \frac{G_F^2\cos^2\theta_C \boldsymbol{k}'^2}{2\pi^2}\cos^2\frac{\theta}{2}\Big[\underline{G_E^2}(1-\frac{\omega^2}{\boldsymbol{q}^2})^2 R_C + \underline{G_A^2}\frac{(M_\Delta - M_N)^2}{\boldsymbol{q}^2} R_L$$

$$+(\underline{G_M^2}\frac{\omega^2}{\boldsymbol{q}^2} + \underline{G_A^2})(1-\frac{\omega^2}{\boldsymbol{q}^2} + 2\tan^2\frac{\theta}{2}) R_T \pm \underline{G_A}\,\underline{G_M}\, 2\frac{k+k'}{M_N}\tan^2\frac{\theta}{2} R_T\Big]$$

Nucleon properties → Form factors: Electric G_E, Magnetic G_M, Axial G_A

Nuclear dynamics → Nuclear Response Functions:

Charge R_c (τ), Isospin Spin-Longitudinal R_L(τ $\sigma\cdot$q), Isospin Spin Transverse R_T (τ σxq)

Form Factors

Standard dipole parameterization

Vector

$$G_E(Q^2) = G_M(Q^2)/(\mu_p - \mu_n) = (1 + Q^2/M_V^2)^{-2}$$

$$Q^2 = q^2 - \omega^2$$

$$M_V = 0.84\,\mathrm{GeV}/c^2$$

Axial

$$G_A(Q^2) = g_A(1 + Q^2/M_A^2)^{-2}$$

$g_A = 1.26$ from neutron β decay

$$\boxed{M_A = (1.026 \pm 0.021)\ GeV/c^2}$$

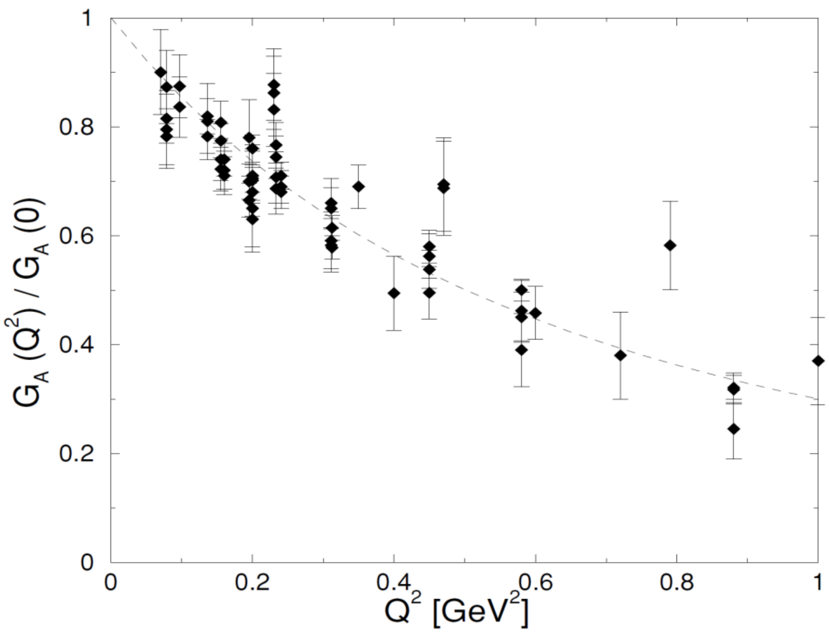

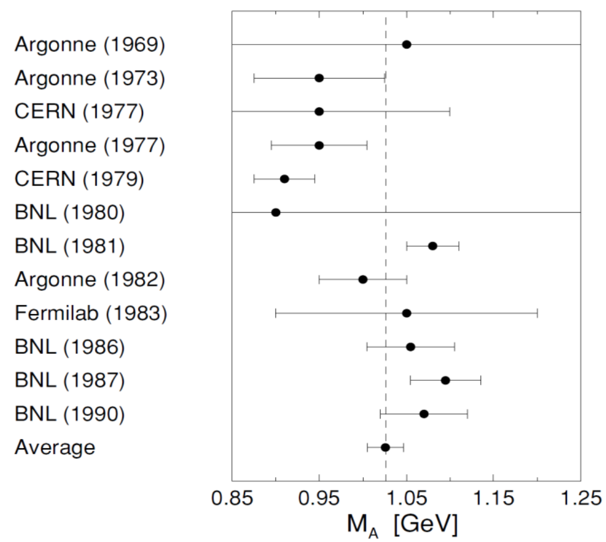

from ν-deuterium CCQE

and

from π electroproduction

V. Bernard, J.Phys. G28 (2002) R1-R35

MiniBooNE CC Quasielastic neutrino cross section on Carbon

AIP Conf. Proc. 1189: 139-144 (2009); Phys. Rev. D 81, 092005 (2010)

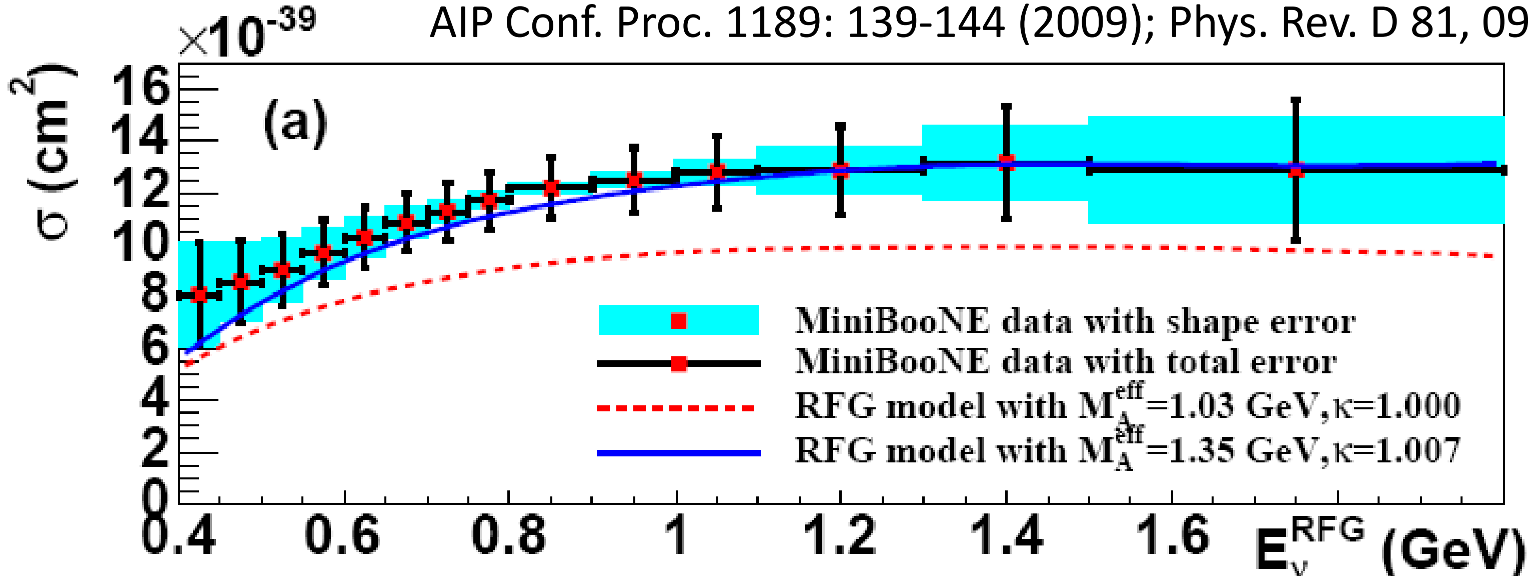

Comparison with predictions using M_A=1.03 GeV (standard value) reveals a discrepancy

In the Relativistic Fermi Gas (RFG) model an axial mass of 1.35 GeV is needed to account for data

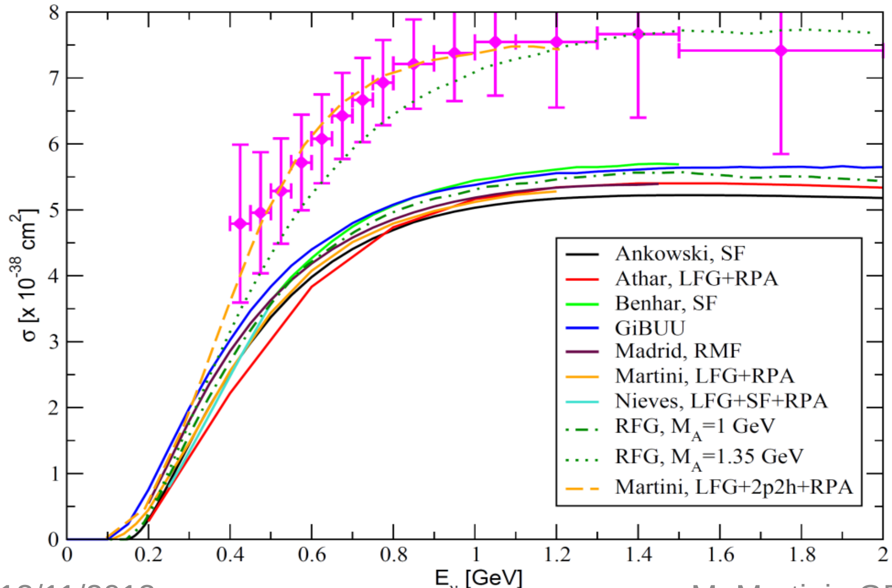

L. Alvarez-Ruso
arXiv:1012.3871
(Neutrino 2010)

puzzle??

An explanation of this puzzle

Inclusion of the multinucleon emission channel (np-nh)

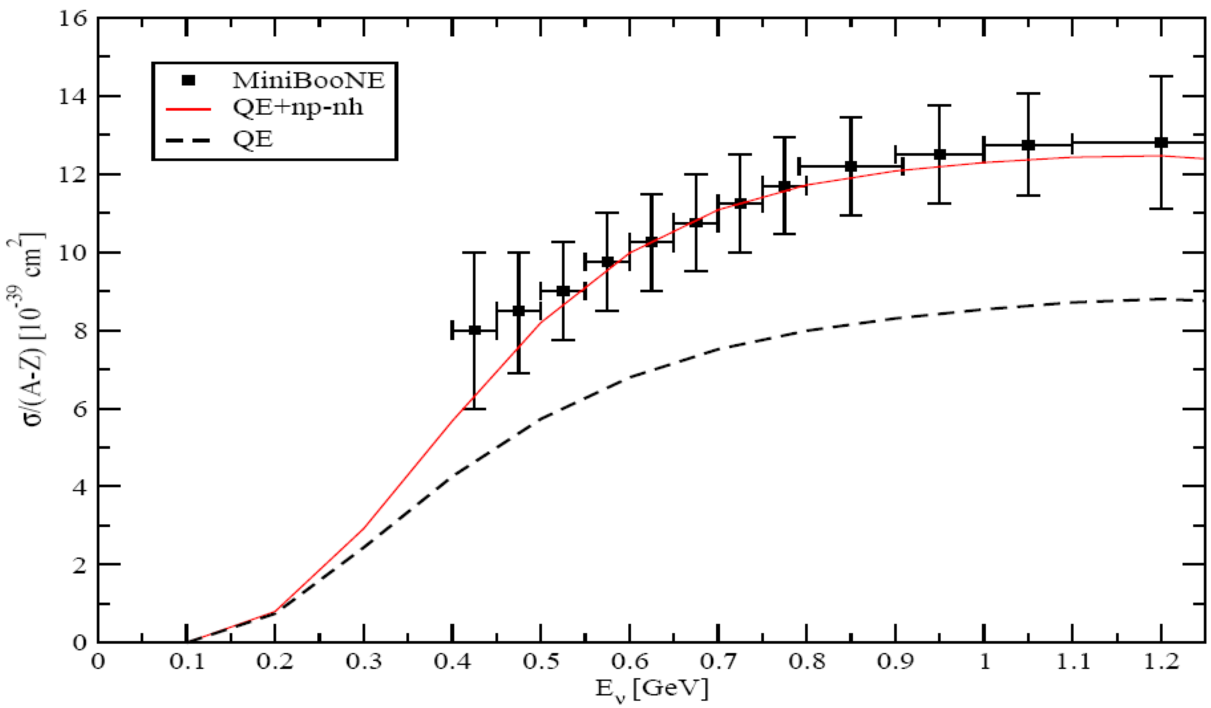

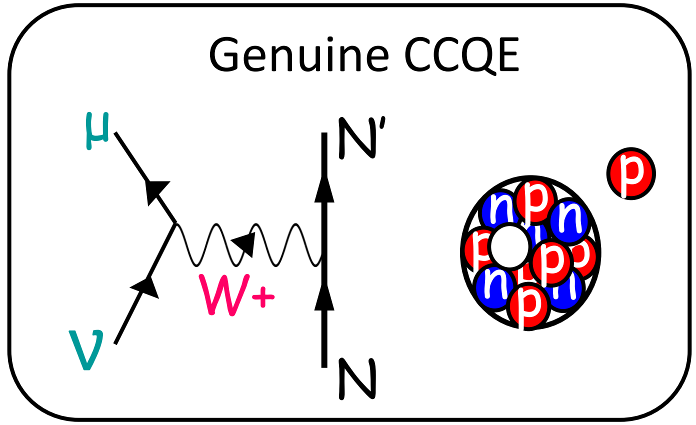

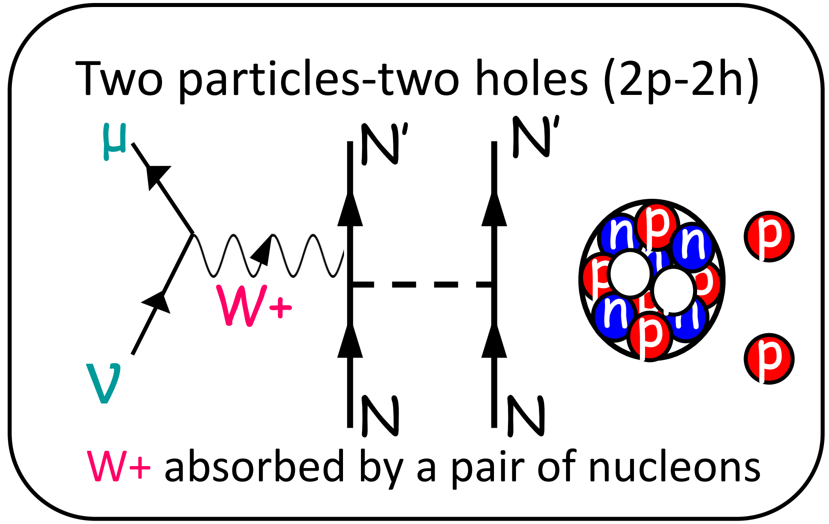

M. Martini, M. Ericson, G. Chanfray, J. Marteau   Phys. Rev. C 80 065501 (2009)

Agreement with MiniBooNE without increasing M_A

CCQE and CCQE-like

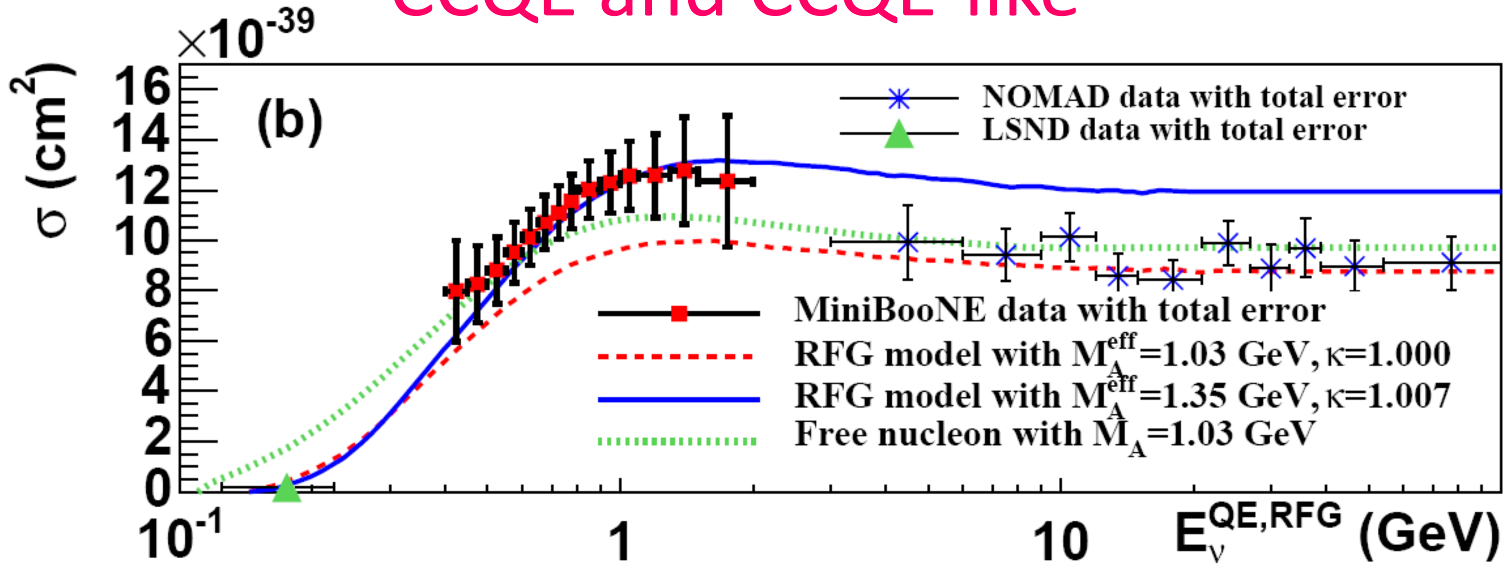

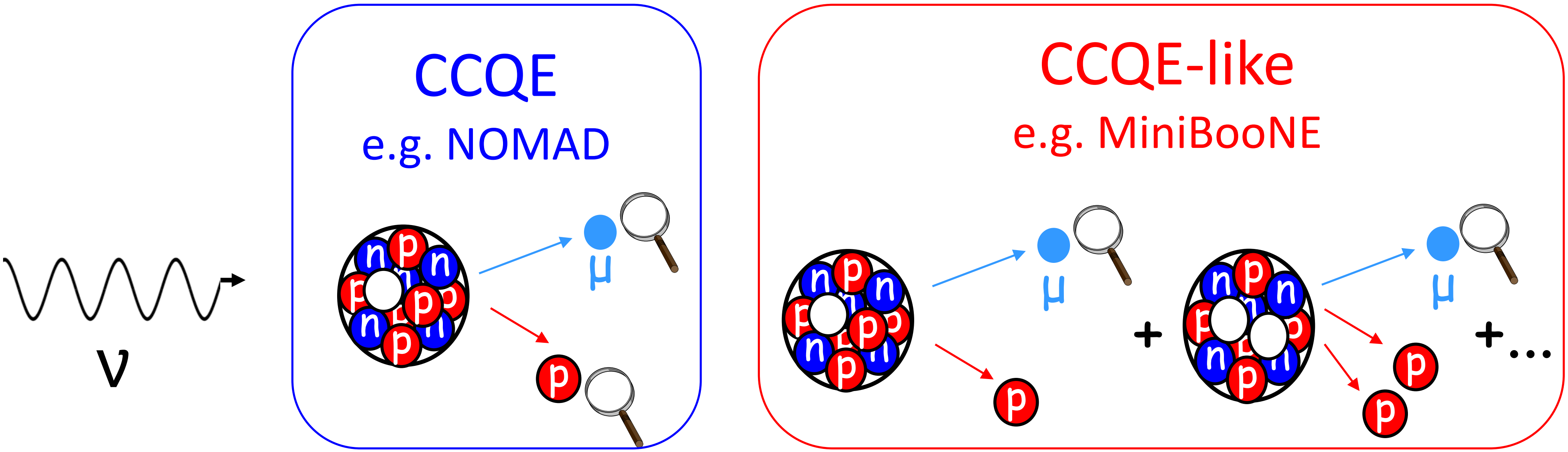

Cherenkov detectors measure CCQE-like which includes np-nh contributions

MiniBooNE CCQE-like flux-integrated double diff. X section

$$\frac{d^2\sigma}{dE_\mu d\cos\theta} = \int dE_\nu \left[\frac{d^2\sigma}{d\omega d\cos\theta}\right]_{\omega=E_\nu-E_\mu} \Phi(E_\nu)$$

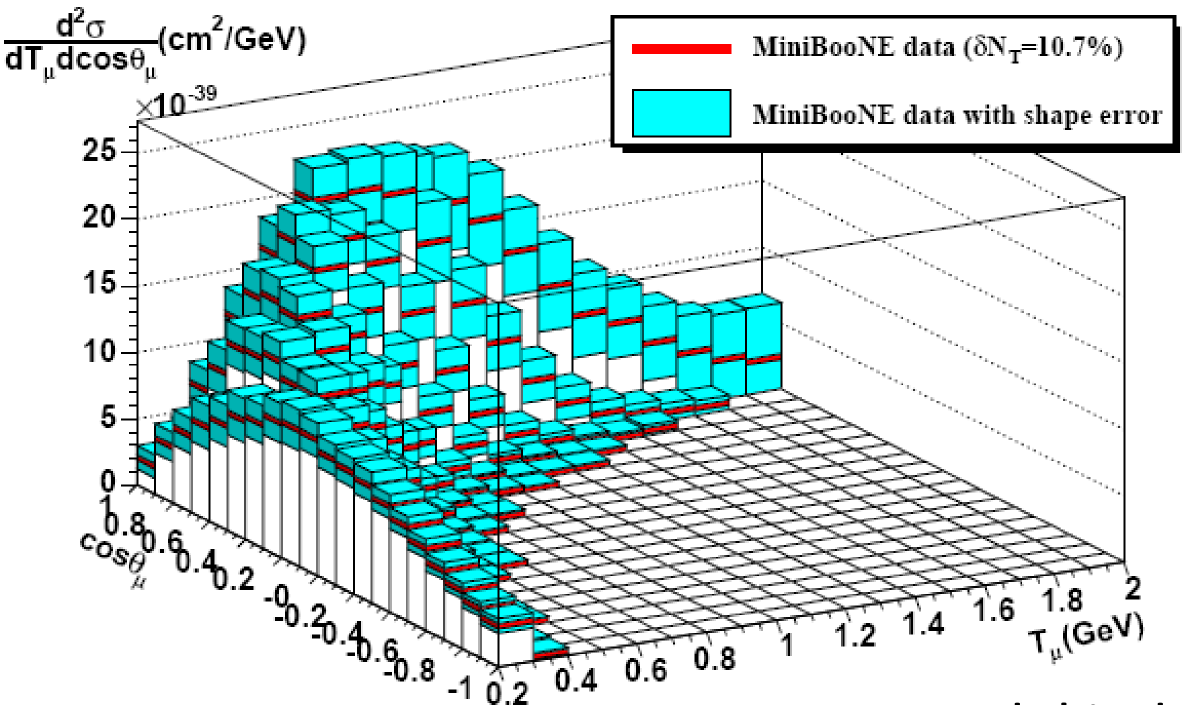

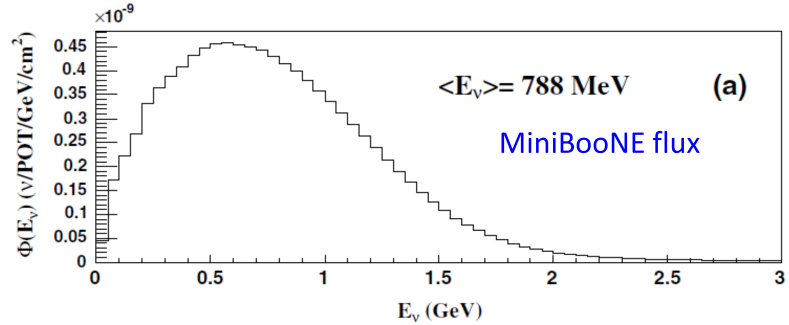

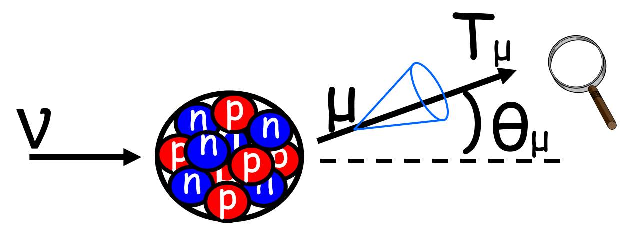

Model independent measurement

MiniBooNE, Phys. Rev. D 81, 092005 (2010)

Flux-integrated double differential cross section

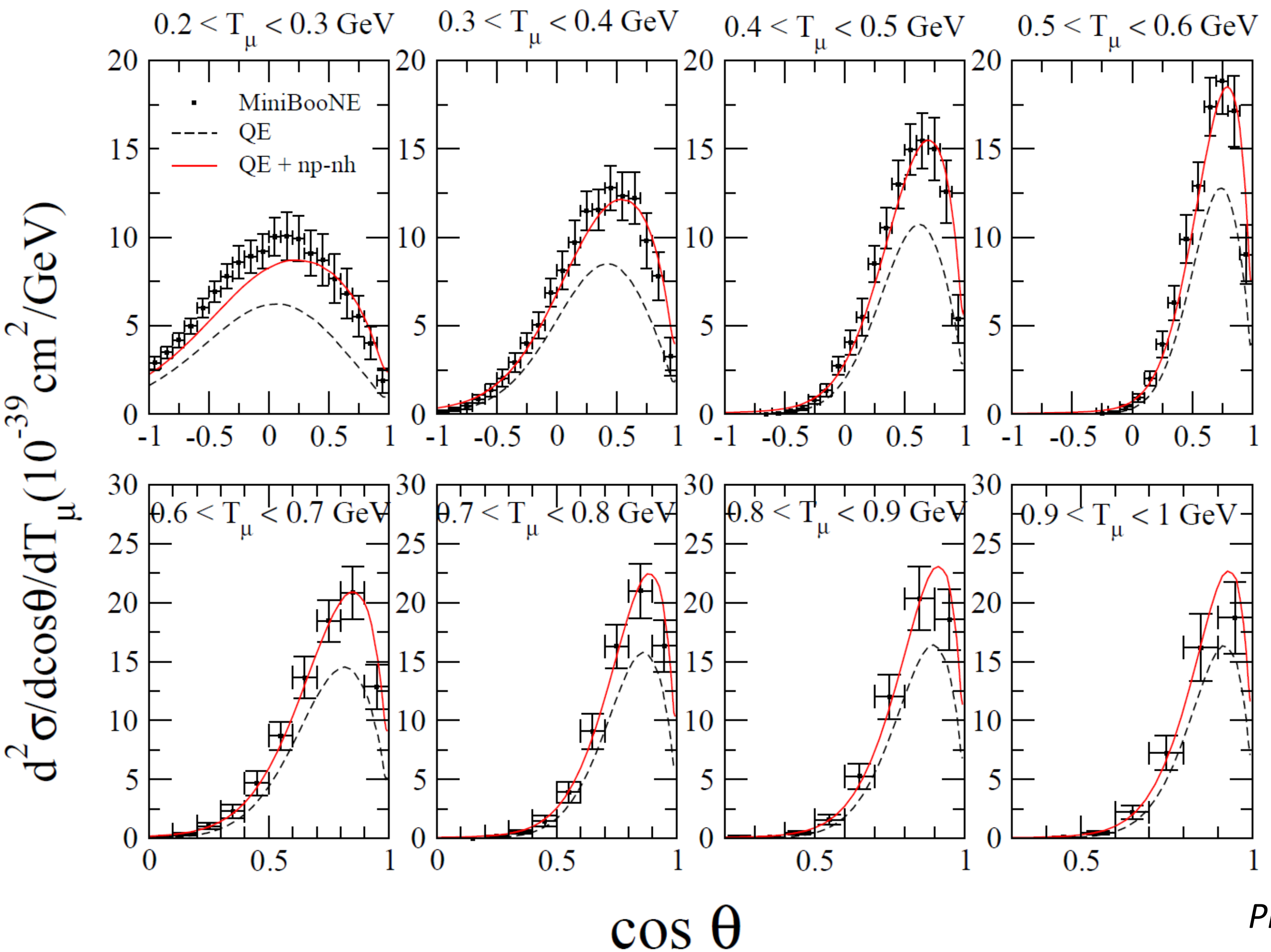

red: including np-nh

black: genuine QE

Martini, Ericson, Chanfray, Phys. Rev. C 84 055502 (2011)

Agreement with MiniBooNE without increasing M_A once np-nh is included

Similar conclusions in *Nieves et al. PLB 707, 72 (2012)*

Theoretical studies on np-nh excitations in CCQE-like

M. Martini, M. Ericson, G. Chanfray, J. Marteau (Lyon, IPNL)

Phys. Rev. C 80 065501 (2009) ν σtotal
Phys. Rev. C 81 045502 (2010) ν vs antiν (σtotal)
Phys. Rev. C 84 055502 (2011) ν $d^2\sigma$, $d\sigma/dQ^2$
Phys. Rev. D 85 093012 (2012) impact of np-nh on ν energy recostruction
Phys. Rev. D 87 013009 (2013) impact of np-nh on ν energy recostruction and ν oscillation
Phys. Rev. C 87 065501 (2013) antiν $d^2\sigma$, $d\sigma/dQ^2$

J. Nieves, I. Ruiz Simo, M.J. Vicente Vacas, F. Sanchez, R. Gran (Valencia, IFIC)

Phys. Rev. C 83 045501 (2011) ν, antiν σtotal
Phys. Lett. B 707 72-75 (2012) ν $d^2\sigma$
Phys. Rev. D 85 113008 (2012) impact of np-nh on ν energy recostruction
Phys. Lett. B 721 90-93 (2013) antiν $d^2\sigma$
arXiv 1307.8105 (2013) extension of np-nh up to 10 GeV

J.E. Amaro, M.B. Barbaro, J.A. Caballero, T.W. Donnelly , J.M. Udias, C. F. Williamson (Superscaling)

Phys. Lett. B 696 151-155 (2011) ν $d^2\sigma$
Phys. Rev. D 84 033004 (2011) ν $d^2\sigma$, σtotal
Phys. Rev. Lett. 108 152501 (2012) antiν $d^2\sigma$, σtotal

Effective models taking into account np-nh excitations

O. Lalakulich, K. Gallmeister and U. Mosel (GiBUU)

Phys. Rev. C 86 014614 (2012) ν σtotal, $d^2\sigma$, $d\sigma/dQ^2$
Phys. Rev. C 86 054606 (2012) impact of np-nh on ν energy recostruction and ν oscillation

A. Bodek, H.S. Budd, M.E. Christy (Transverse Enancement Model)

EPJ C 71 1726 (2011) ν and antiν σtotal, $d\sigma/dQ^2$

In the neutrino interaction generators corresponding to experimental studies on ν cross sections and oscillations published up to now the np-nh channel was not included

Today there is an effort to include this np-nh channel in several Monte Carlo (GENIE, NuWro,…)

Theoretical models

Response picture

Response functions $$R(\omega, q) = -\frac{\mathcal{V}}{\pi}\,\mathrm{Im}[\Pi(\omega, q, q)]$$

easy to separate the several channels

1p-1h
QE

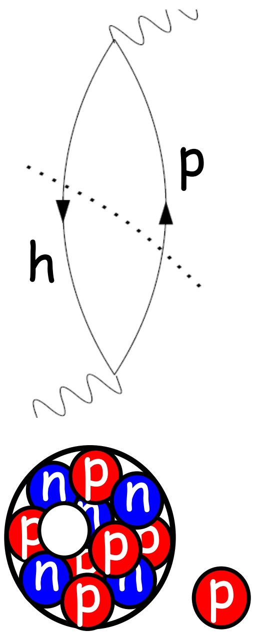

1p-1h
1π production

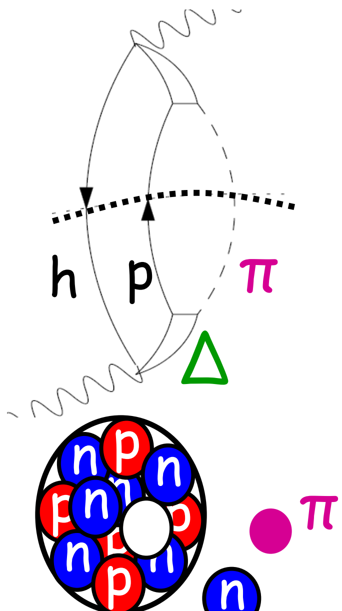

2p-2h:
two examples

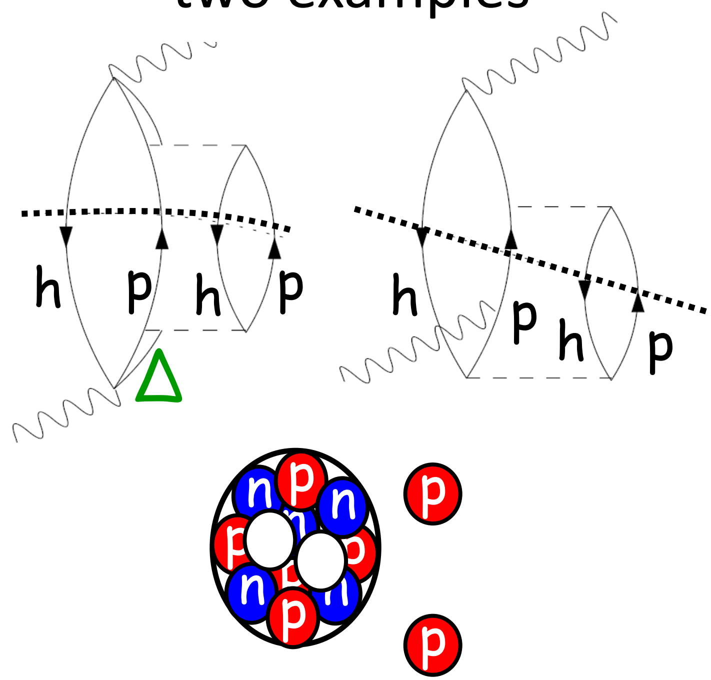

Genuine Quasielastic Scattering

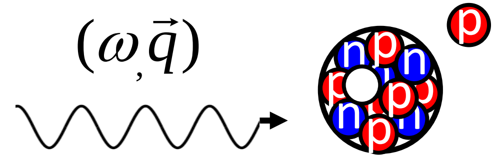

Nucleon-Nucleon interaction switched off

Nucleons respond individually

Nucleon at rest:

$$R \alpha\ \delta\left(\omega - \left(\sqrt{q^2 + M^2} - M\right)\right)$$

Nucleon inside the nucleus:

Fermi motion spreads δ distribution (Fermi Gas)

Pauli blocking cuts part of the low momentum Resp.

$q < 2\,k_F$

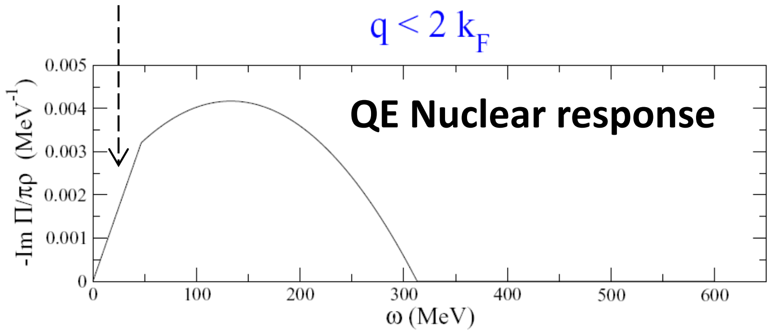

$q > 2\,k_F$

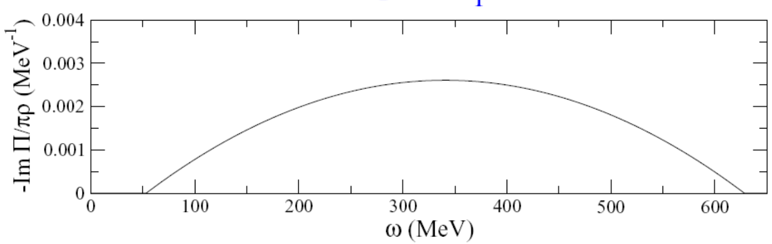

Nucleon-Nucleon interaction switched on

The nuclear response becomes collective

Random Phase Approximation

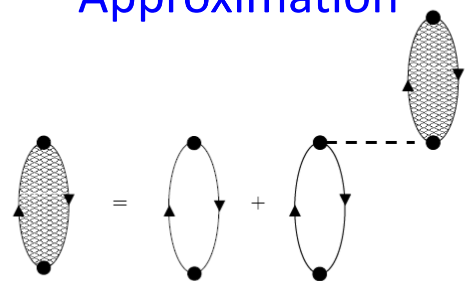

$$\Pi = \Pi^0 + \Pi^0 V \Pi$$

*Force acting on one nucleon is transmitted by the interaction

*Shift of the peak with respect to Fermi Gas, decrease, increase,…

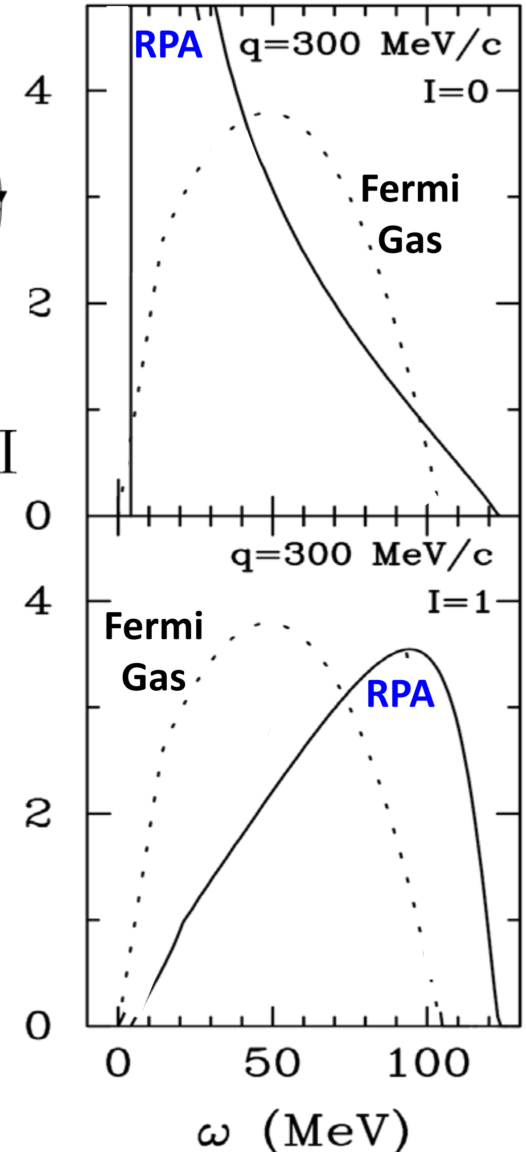

Effects of the RPA in the ν genuine quasielastic scattering

QE totally dominated by isospin spin-transverse response $R_{\sigma\tau(T)}$

RPA reduction

- expected from the repulsive character of p-h interaction in T channel
- mostly due to interference term $R^{N\Delta} < 0$
(Lorentz-Lorenz or Ericson-Ericson effect)

Lowest order contribution to QE

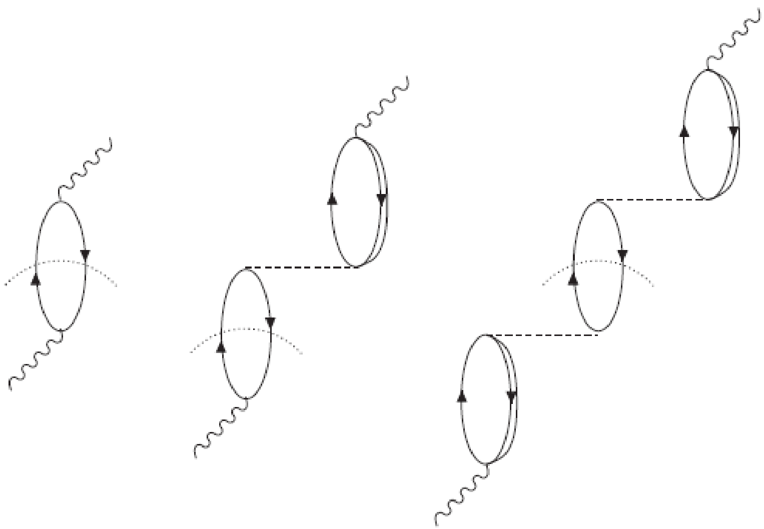

R^{NN}_{QE} $R^{N\Delta}_{QE}$ $R^{\Delta\Delta}_{QE}$

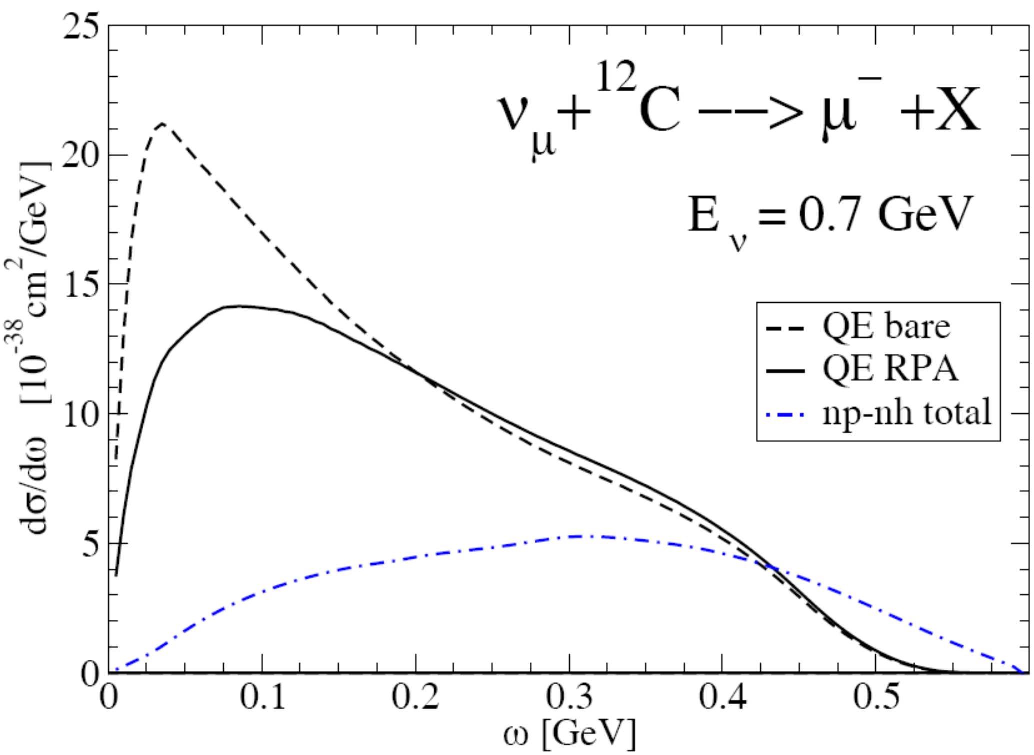

Two particle-two hole sector (2p-2h)

Three equivalent representations of the same process

2 body current

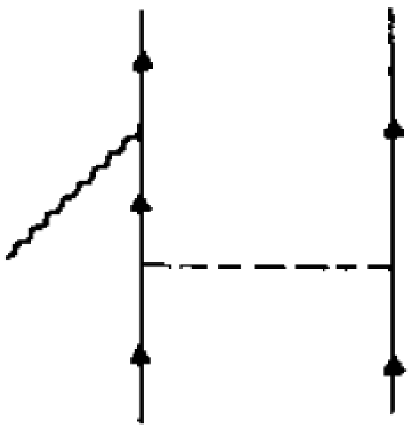

2p-2h matrix element

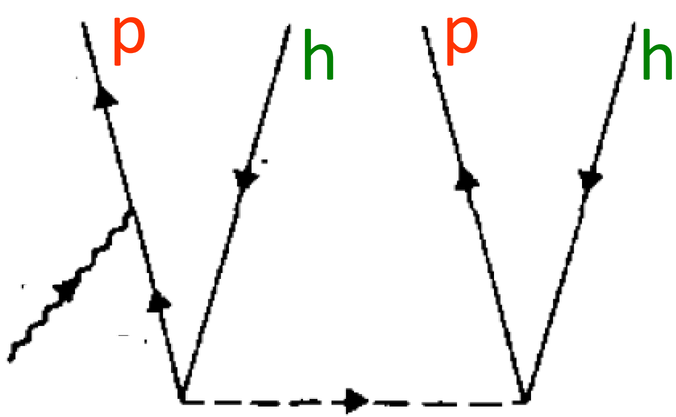

2p-2h response

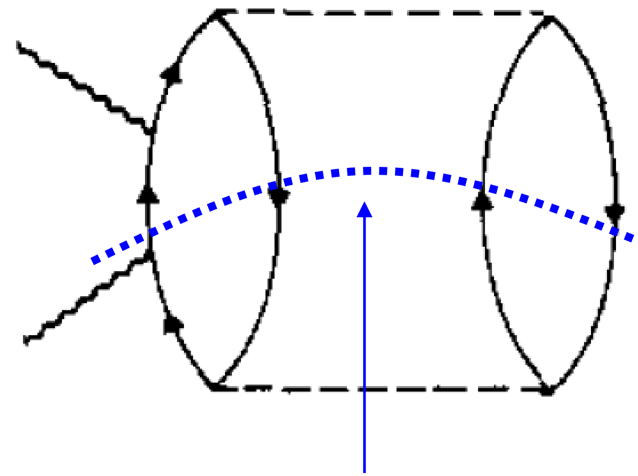

Cut
(optical theorem)

Final state: two particles-two holes

Some diagrams for 2 body currents

Nucleon-Nucleon correlations

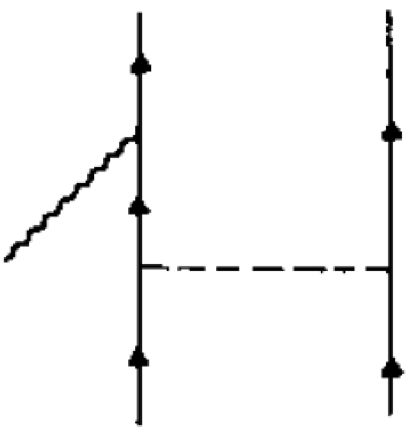

Meson Exchange Currents (MEC)

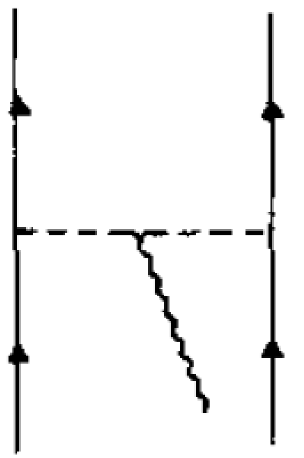

Pion in flight

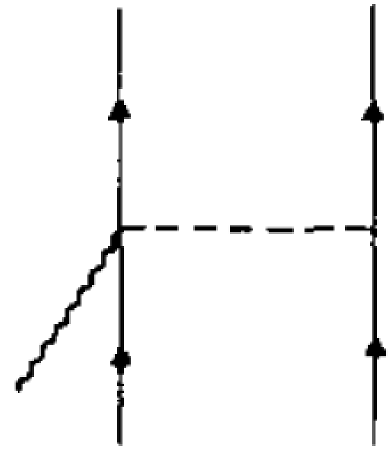

Contact

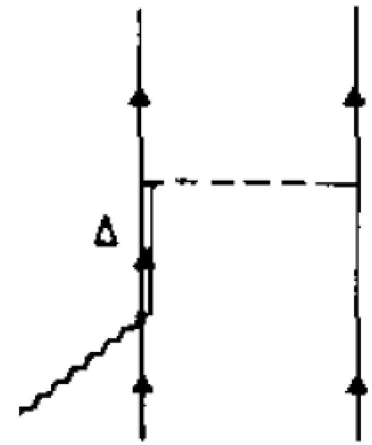

Delta

Some diagrams for 2p-2h responses

NN correlations

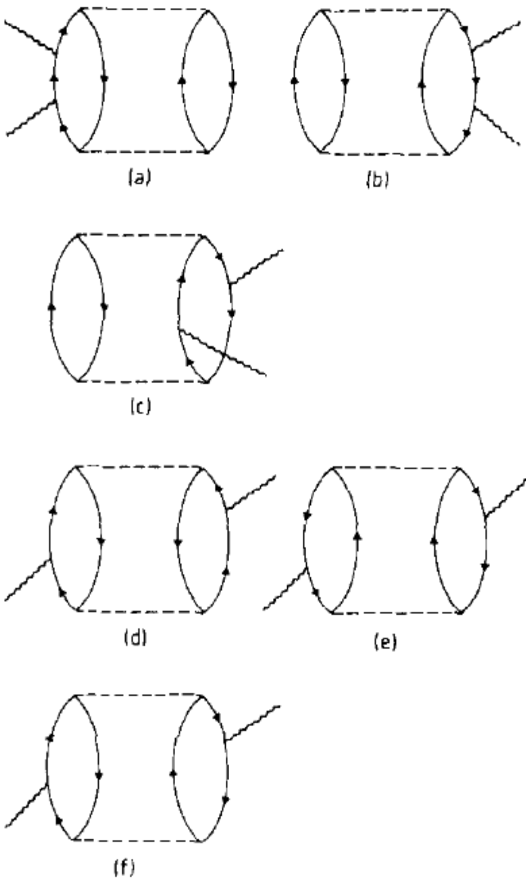

16 diagrams

MEC

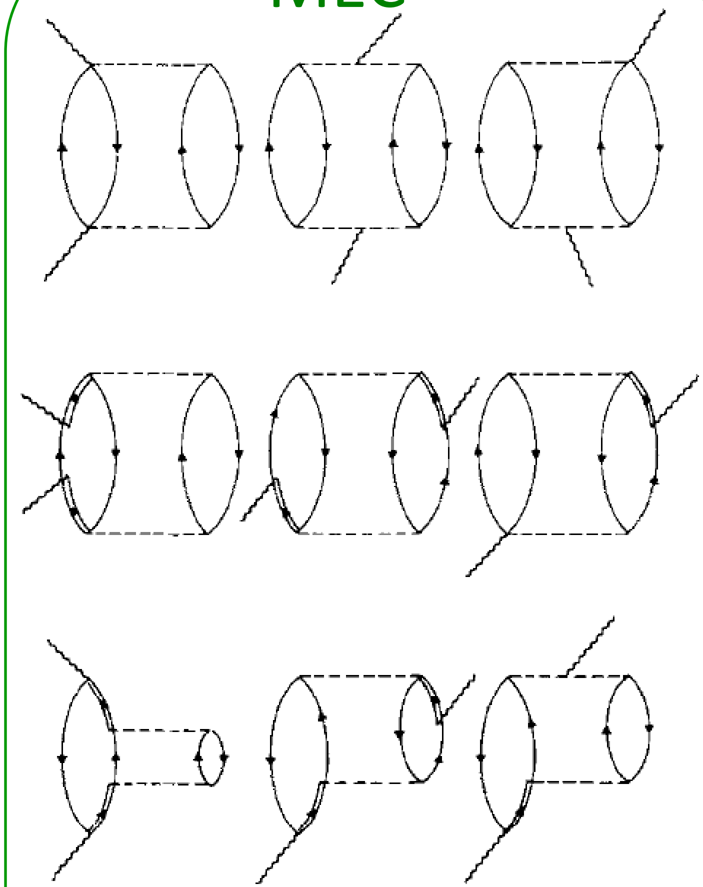

49 diagrams

NN correlation-MEC interference

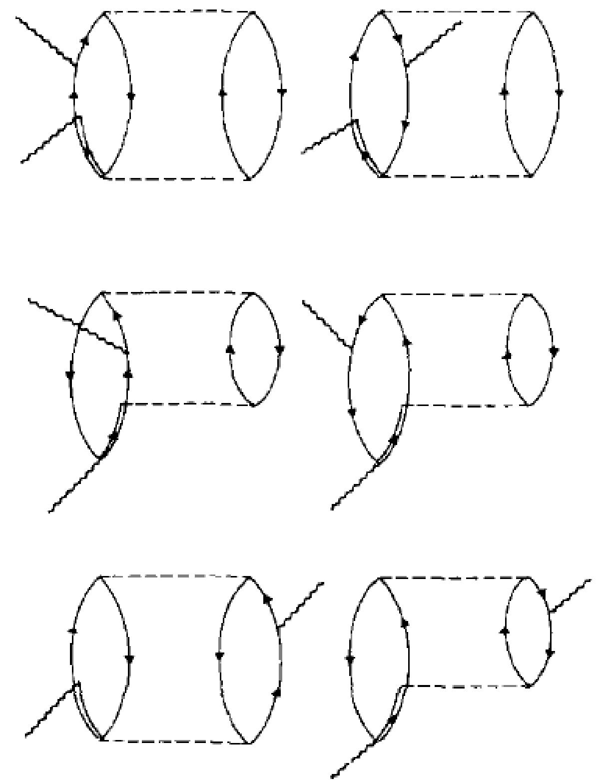

56 diagrams

Main difficulties in the 2p-2h sector

- Huge number of diagrams and terms

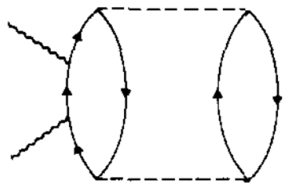
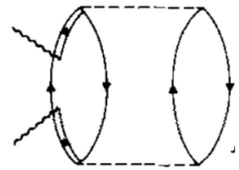
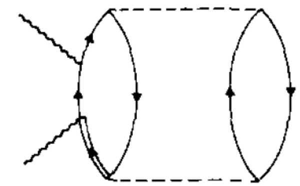

16 from NN correlations   **49** from MEC   **56** from interference

Alberico, Ericson, Molinari, Ann. Phys. 154, 356 (1984)

fully relativistic calculation (just of MEC !):

3000 direct terms   More than **100 000** exchange terms

De Pace, Nardi, Alberico, Donnelly, Molinari, Nucl. Phys. A741, 249 (2004)

- Divergences in NN correlations

prescriptions:

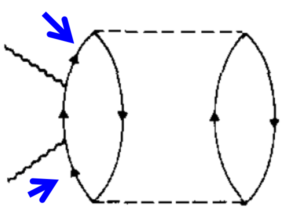

-nucleon propagator only off the mass shell (*Alberico et al. Ann. Phys. 1984*)

-kinematical constraints + nucleon self energy in the medium (*Nieves et al PRC 83*)

- regularization parameter taking into account the finite size of the nucleus to be fitted to data (*Amaro et al. PRC 82 044601 2010*)

Analogies and differences of 2p-2h

M. Martini, M. Ericson, G. Chanfray, J. Marteau

Axial and Vector | NN corr. | Δ-MEC | NΔ interf.

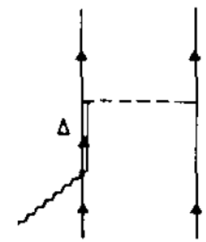

[Genuine CCQE (1p-1h): LRFG+RPA]

J. Nieves, I. Ruiz Simo, M.J. Vicente Vacas et al.

Axial and Vector | NN corr. | MEC | N-MEC interf.

[Genuine CCQE (1p-1h): LRFG+SF+RPA]

J.E. Amaro, M.B. Barbaro, J.A. Caballero, T.W. Donnelly et al.

Only Vector | MEC

[Genuine CCQE (1p-1h): Superscaling]

Where 2p-2h enter in ν-nucleus cross-section?

$$\frac{\partial^2\sigma}{\partial\Omega\,\partial k'} = \frac{G_F^2\,\cos^2\theta_c\,(\boldsymbol{k}')^2}{2\,\pi^2}\,\cos^2\frac{\theta}{2}\,\Big[G_E^2\,(\frac{q_\mu^2}{\boldsymbol{q}^2})^2\,R_\tau^{NN}$$

isovector nuclear response

$$+\quad G_A^2\,\frac{(M_\Delta - M_N)^2}{2\,\boldsymbol{q}^2}\,R_{\sigma\tau(L)}$$

isospin spin-longitudinal

$$+\quad \left(G_M^2\,\frac{\omega^2}{\boldsymbol{q}^2} + G_A^2\right)\left(-\frac{q_\mu^2}{\boldsymbol{q}^2} + 2\tan^2\frac{\theta}{2}\right)R_{\sigma\tau(T)}$$

isospin spin-transverse

$$\pm\quad 2\,G_A\,G_M\,\frac{k+k'}{M_N}\,\tan^2\frac{\theta}{2}\,R_{\sigma\tau(T)}\Big]$$

interference V-A

The 2p-2h term affects the magnetic and axial responses (terms in G_M, G_A) (spin-isospin, στ excitation operator)

Other processes, with the same excitation operator (στ), where 2p-2h are relevant

- Transverse response in electron scattering

$$\frac{d^2\sigma}{d\theta\, d\omega} = \sigma_M \left\{ \frac{(\omega^2 - q^2)^2}{q^4} R_L(\omega, q) + \left[\tan^2\left(\frac{\theta}{2}\right) - \frac{\omega^2 - q^2}{2q^2} \right] \boxed{R_T(\omega, q)} \right\}$$

- Photon absorption

$$\sigma_\gamma^{tot} = 2\pi^2 \frac{\alpha}{\omega} \boxed{R_T(q, q)}$$

- Pion absorption

Two-nucleon mechanism: πNN --> NN (πN --> N strongly suppressed)

Dominated by p-n initial pairs

ν scattering

Ejected pairs will be predominantly:

p-p for ν CC

n-n for antiν CC

p-n for NC

First results of MINERνA seem to confirm this prediction (PRL 111 022501; 022502 2013)

Sources and References of 2p-2h

M. Martini, M. Ericson, G. Chanfray, J. Marteau

Alberico, Ericson, Molinari, Ann. Phys. 154, 356 (1984) (e,e') γ π

**Oset and Salcedo, Nucl. Phys. A 468, 631 (1987)* π γ

Shimizu, Faessler, Nucl. Phys. A 333,495 (1980) π

Delorme, Ericson, Phys.Lett. B156 263 (1985)
Marteau, Eur.Phys.J. A5 183-190 (1999); PhD thesis
Marteau, Delorme, Ericson, NIM A 451 76 (2000)
} ν *pioneer works*

J. Nieves, I. Ruiz Simo, M.J. Vicente Vacas et al.

Gil, Nieves, Oset, Nucl. Phys. A 627, 543 (1997) (e,e') γ

**Oset and Salcedo, Nucl. Phys. A 468, 631 (1987)* π γ

J.E. Amaro, M.B. Barbaro, J.A. Caballero, T.W. Donnelly et al.

De Pace, Nardi, Alberico, Donnelly, Molinari, Nucl. Phys. A741, 249 (2004) (e,e') γ

Electron scattering

$$\frac{d^2\sigma}{d\theta\, d\omega} = \sigma_M \left\{ \frac{(\omega^2 - q^2)^2}{q^4} R_L(\omega, q) + \left[\tan^2\left(\frac{\theta}{2}\right) - \frac{\omega^2 - q^2}{2q^2} \right] \boxed{R_T(\omega, q)} \right\}$$

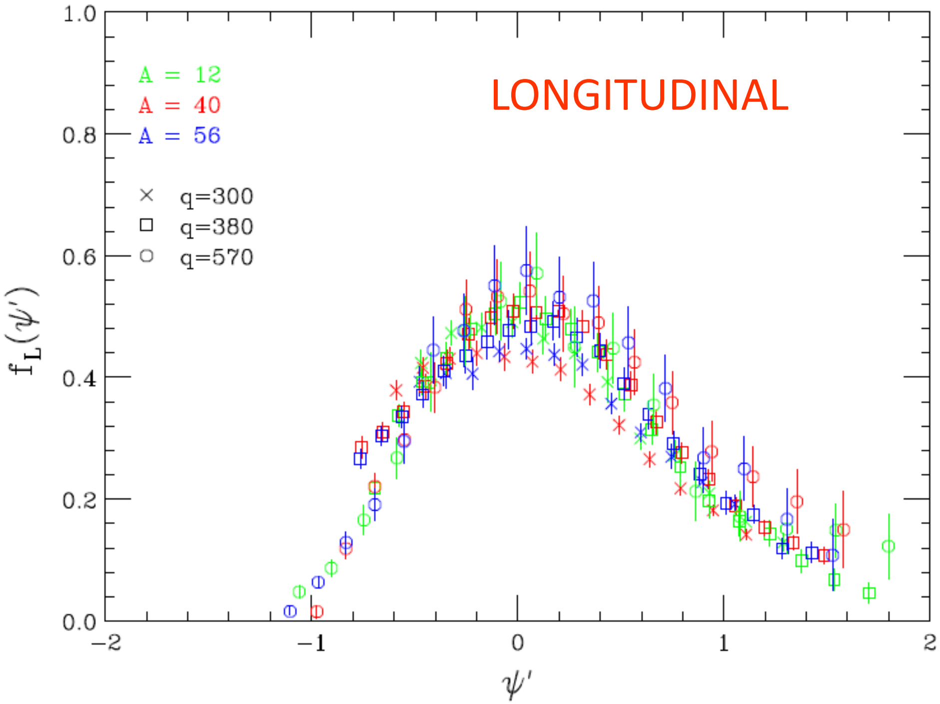

$$f_L(\Psi) = k_F \frac{q^2 - \omega^2}{q\, m} \frac{R_L(\omega, q)}{Z(G_E^p)^2 + N(G_E^n)^2}$$

Donnelly et al. PRC 60 '99,...

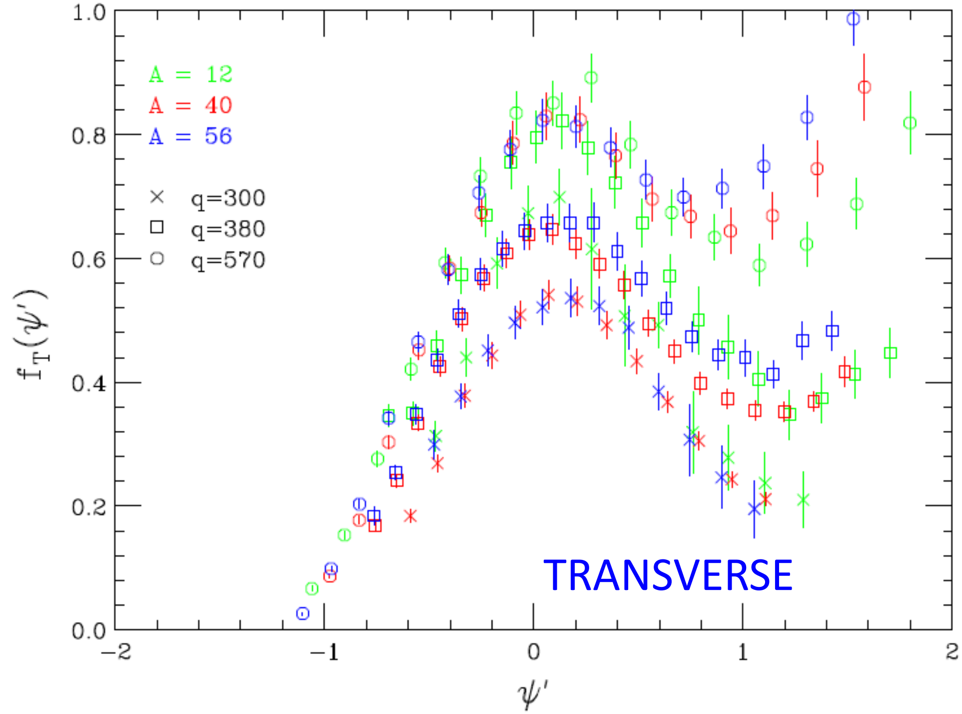

$$f_T(\Psi) = 2\, k_F \frac{q\, m}{q^2 - \omega^2} \frac{R_T(\omega, q)}{Z(G_M^p)^2 + N(G_M^n)^2}$$

Excess in the transverse channel likely due to 2-body currents (MEC and correlations)

A.Bodek et al. Eur.Phys.J. C71 (2011) : parametrization of the enhancement in T channel in terms of correction to $G_M(Q^2)$

Transverse response in electron scattering

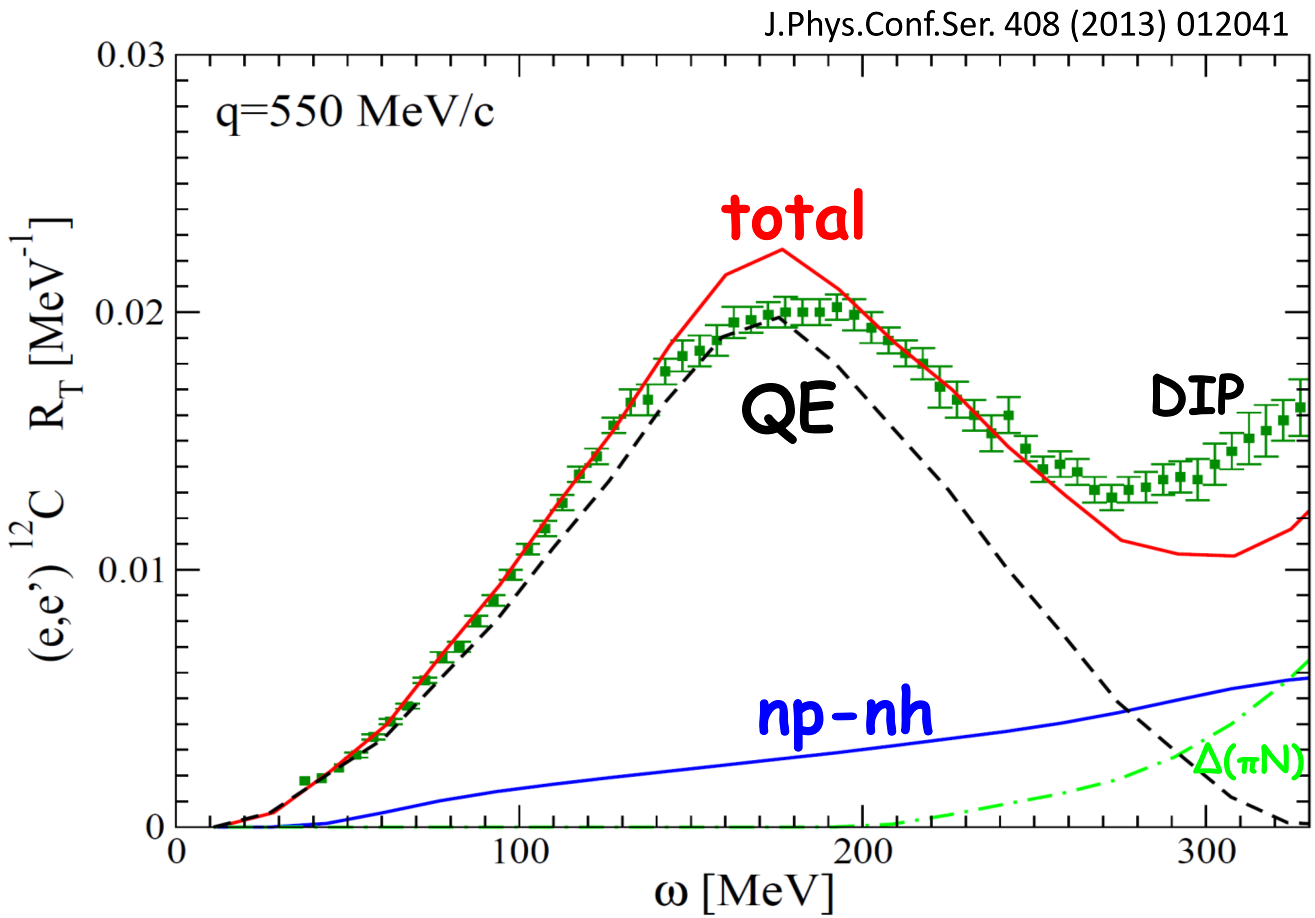

np-nh creates a high energy tail in the nuclear response above the QE peak

R_T of ^{12}C: comparison with data and with calculations of Gil et al.

Our calculation J.Phys.Conf.Ser. 408 (2013) 012041

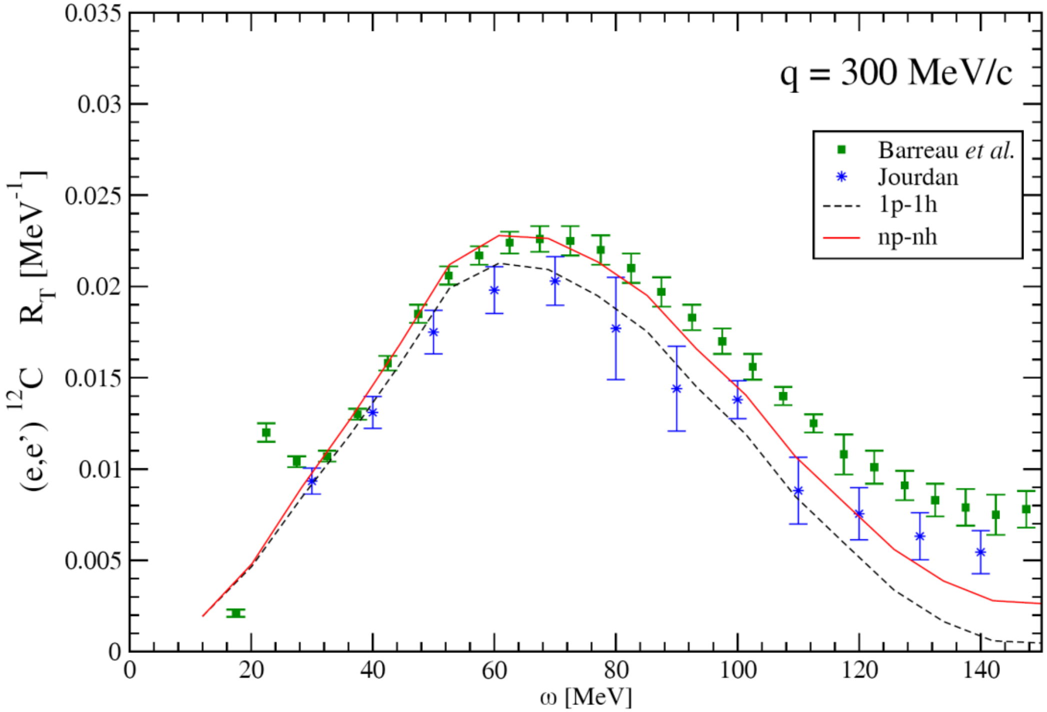

Gil, Nieves, Oset NPA 627, 543 (1997)

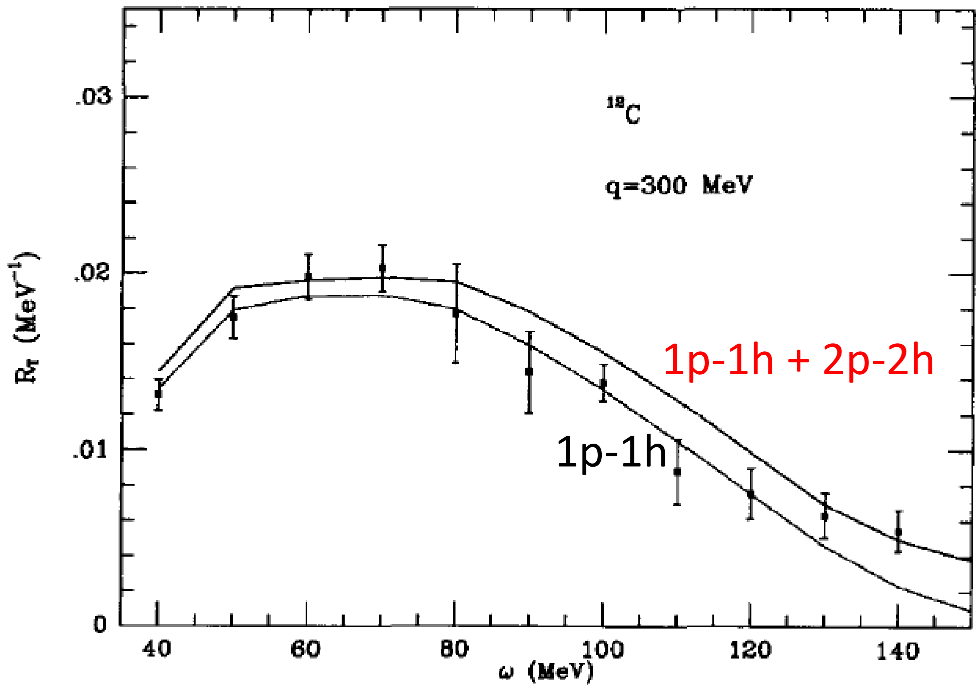

The evaluations of 2p-2h contributions to R_T are compatible among them and with data.

This test is important for ν cross section which is dominated by R_T

Getting back to
ν cross sections

Flux-integrated ν CCQE double differential X section versus Tμ

Martini, Ericson, Chanfray, Phys. Rev. C 84 055502 (2011)

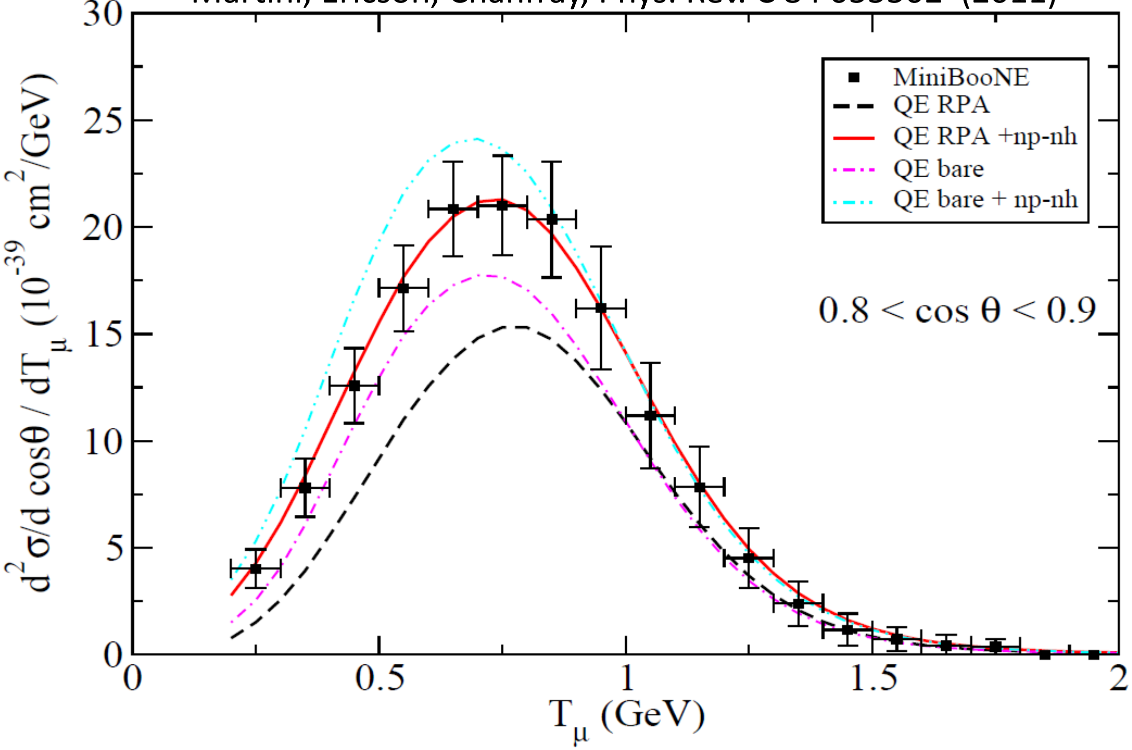

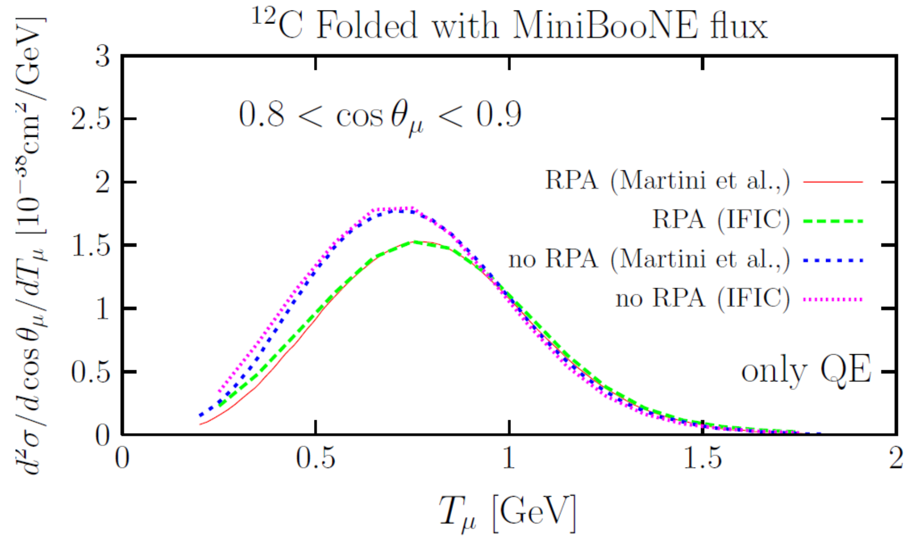

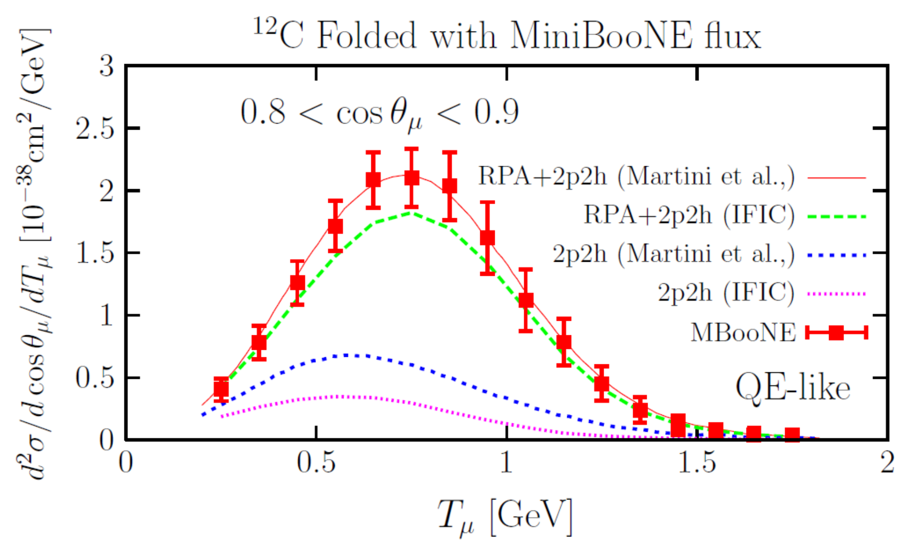

Morfin, Nieves, Sobczyk
Adv.High Energy Phys. 2012 (2012) 934597

Delicate balance between
RPA quenching and np-nh enhancement

- Genuine QE bare and RPA very similar in Martini et al. and Nieves et al.
- Factor ~2 for the np-nh contribution
- Both models compatible with MiniBooNE

(additional normalization uncertainty of 10% in the MB data not shown here)

Charged current Q^2 distribution

Historically of interest for the determination of the axial form factor

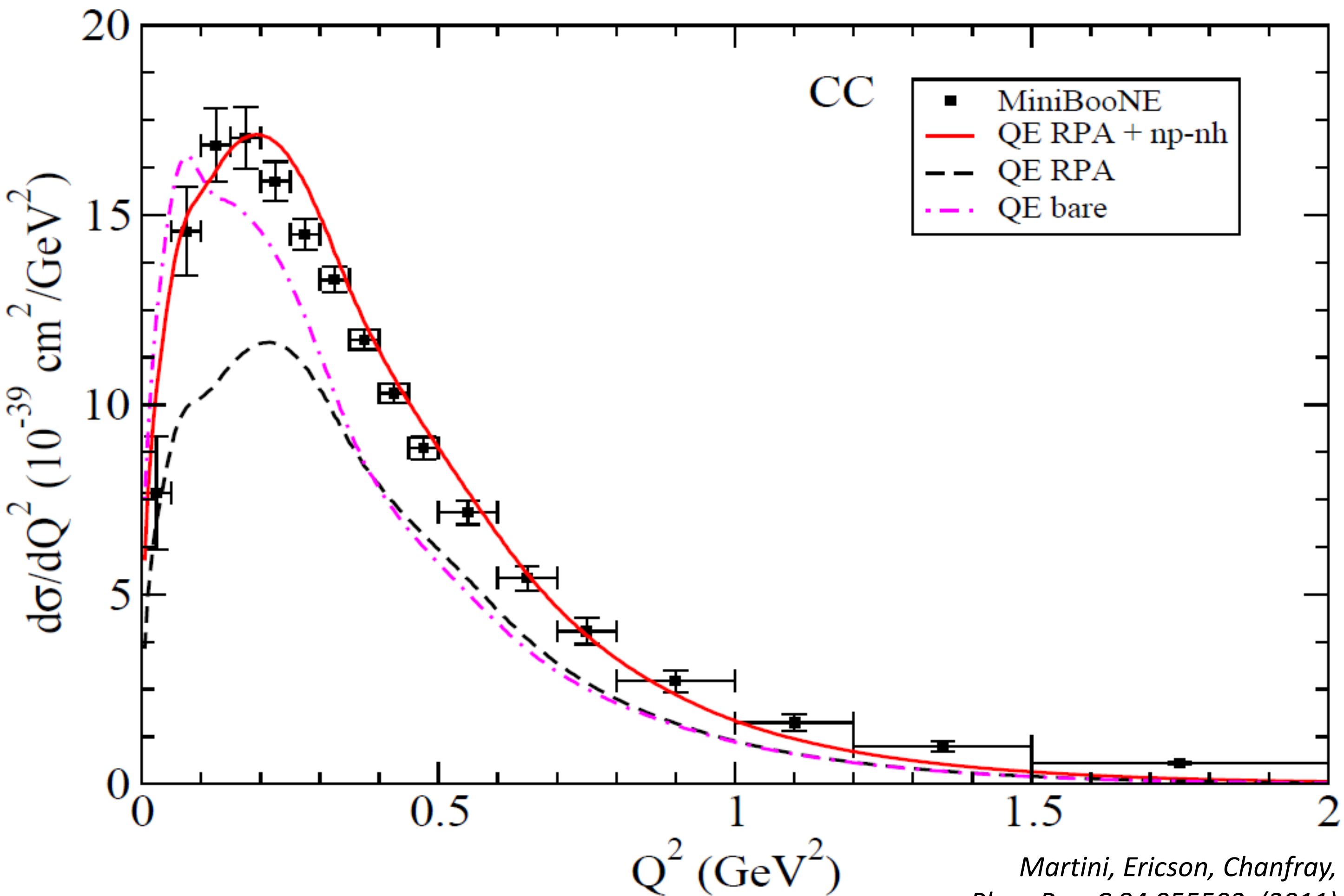

Martini, Ericson, Chanfray, Phys. Rev. C 84 055502 (2011)

low Q^2:
opposite actions of RPA quenching and np-nh enhancement

$Q^2 > 0.2$ GeV^2:
np-nh contribution singled out

Neutral current Q^2 distribution

Exp. Data: MiniBooNE, Phys. Rev. D 82, 092005 (2010)

obtained indirectly from the energy of ejected nucleons

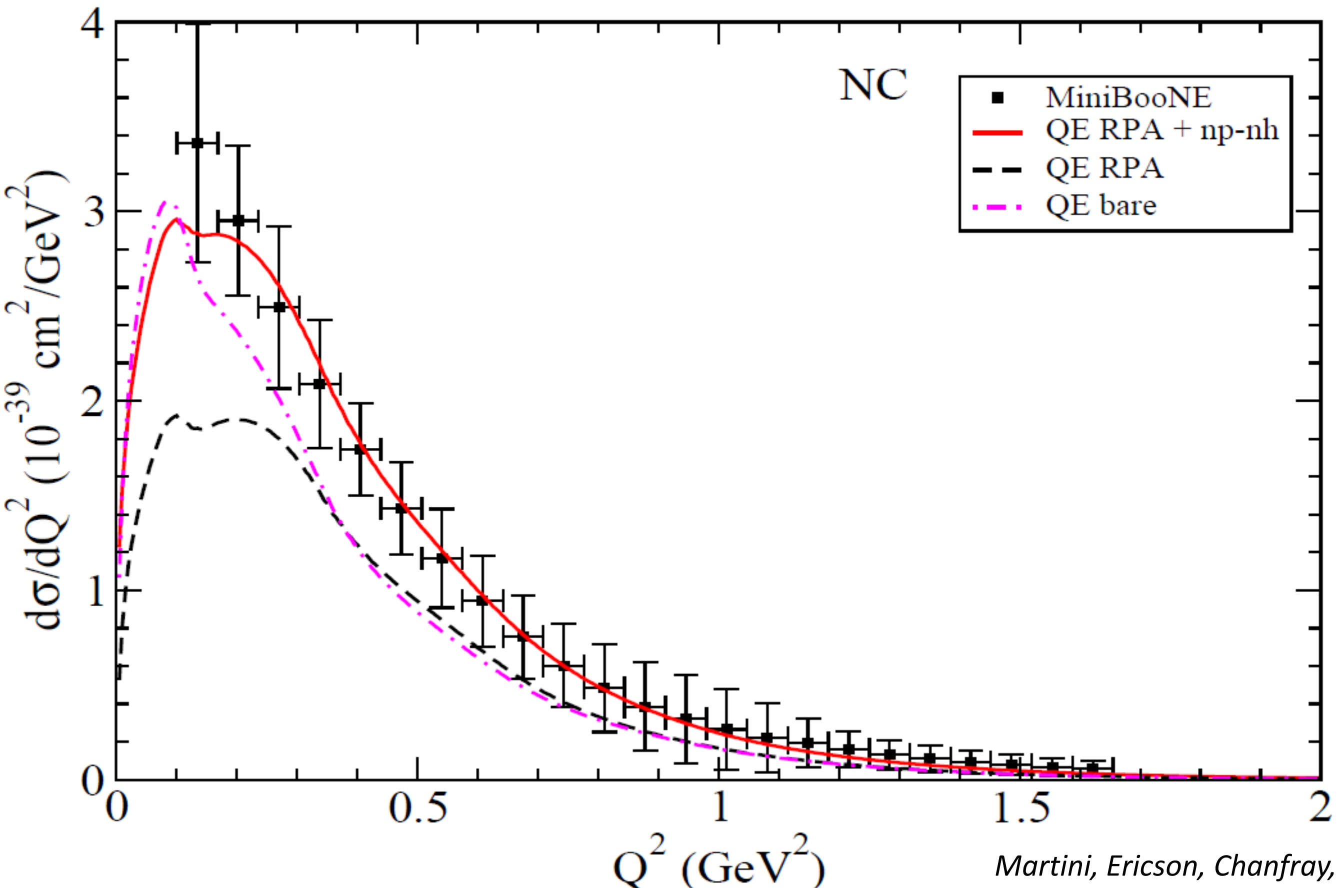

Martini, Ericson, Chanfray, Phys. Rev. C 84 055502 (2011)

is not clear how multinucleon component shows up in the data

low Q^2:
opposite actions of RPA quenching and np-nh enhancement

$Q^2 > 0.3$ GeV^2:
np-nh contribution singled out

Neutrino *vs* Antieutrino-nucleus cross-section

The asymmetry between neutrinos and antineutrinos interactions is important for the investigation of CP violation effects.

Nuclear effects generate an additional asymmetry due to **interference term**

$$
\begin{aligned}
\frac{\partial^2\sigma}{\partial\Omega\,\partial k'} \;=\;& \frac{G_F^2\,\cos^2\theta_c\,(\boldsymbol{k}')^2}{2\,\pi^2}\,\cos^2\frac{\theta}{2}\,\Bigg[G_E^2\,\Big(\frac{q_\mu^2}{\boldsymbol{q}^2}\Big)^2\boxed{R_\tau^{NN}} \quad \text{isovector nuclear response}\\
&+\; G_A^2\,\frac{(M_\Delta-M_N)^2}{2\,\boldsymbol{q}^2}\,\boxed{R_{\sigma\tau(L)}} \quad \text{isospin spin-longitudinal}\\
&+\; \Big(G_M^2\,\frac{\omega^2}{\boldsymbol{q}^2}+G_A^2\Big)\Big(-\frac{q_\mu^2}{\boldsymbol{q}^2}+2\tan^2\frac{\theta}{2}\Big)\,\boxed{R_{\sigma\tau(T)}} \quad \text{isospin spin-transverse}\\
\begin{cases} + & (\nu)\\ - & (\bar{\nu})\end{cases}\;& \boxed{\pm}\;2\,G_A\,G_M\,\frac{k+k'}{M_N}\,\tan^2\frac{\theta}{2}\,\boxed{R_{\sigma\tau(T)}}\Bigg] \quad \textbf{interference V-A}
\end{aligned}
$$

In the model of M. Martini, M. Ericson, G. Chanfray, J. Marteau:

- The 2p-2h term affects the magnetic and axial responses (terms in G_A, G_M)
- The isovector response R_τ (term in G_E) is not affected
  (remember the Superscaling analysis of the electron scattering data)

Various response contributions to the ν and $\bar{\nu}$ CCQE

The role of interference term (in $G_A G_M$) is crucial: it enhances the contribution of Rστ(T) for neutrinos. For antineutrinos instead the destructive interference partially suppresses this contribution leaving a larger role for isovector Rτ which is insensitive to 2p-2h.

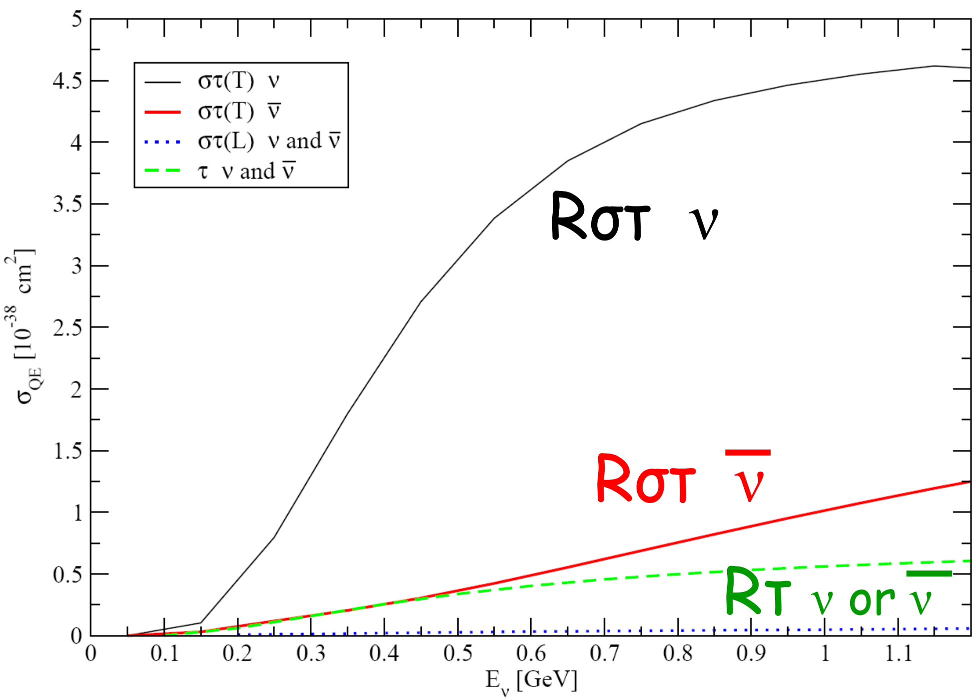

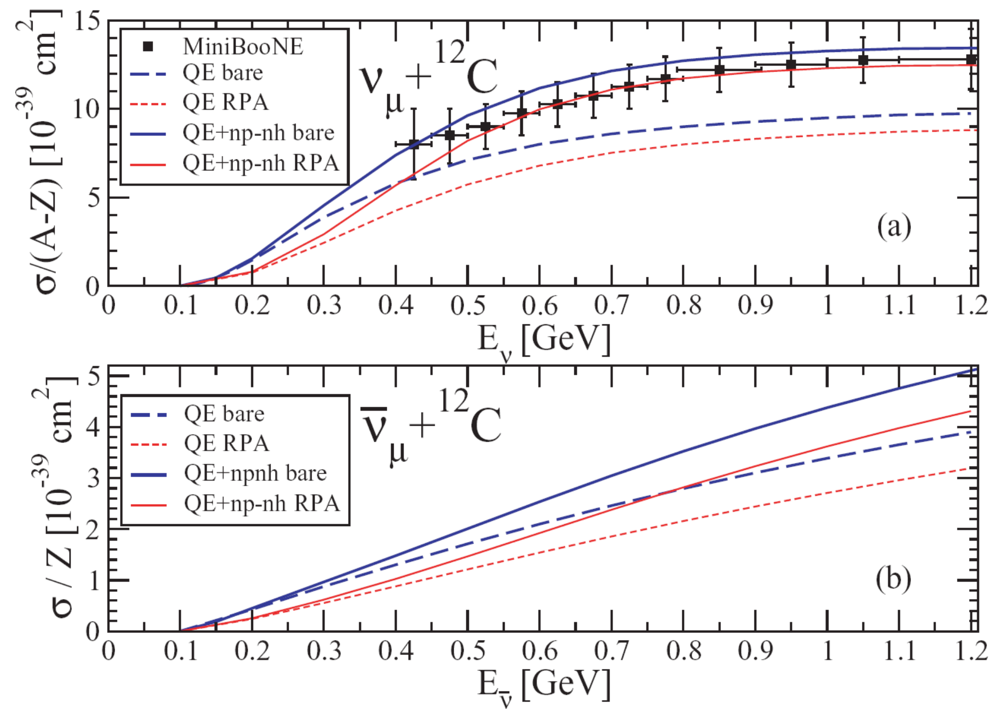

Relative role of 2p-2h smaller for antineutrinos

Antineutrino X section very sensitive to RPA

M. Martini, M. Ericson, G. Chanfray, J. Marteau, Phys. Rev. C 81 045502 (2010)

2p-2h contributions in the different approaches

$$\begin{aligned}\frac{\partial^2\sigma}{\partial\Omega\,\partial k'} &= \frac{G_F^2\,\cos^2\theta_c\,(\boldsymbol{k}')^2}{2\,\pi^2}\,\cos^2\frac{\theta}{2}\,\Big[G_E^2\,(\frac{q_\mu^2}{\boldsymbol{q}^2})^2\,\boxed{R_\tau^{NN}}\\ &+ G_A^2\,\frac{(M_\Delta - M_N)^2}{2\,\boldsymbol{q}^2}\,\boxed{R_{\sigma\tau(L)}}\\ &+ \left(G_M^2\,\frac{\omega^2}{\boldsymbol{q}^2} + G_A^2\right)\left(-\frac{q_\mu^2}{\boldsymbol{q}^2} + 2\tan^2\frac{\theta}{2}\right)\boxed{R_{\sigma\tau(T)}}\\ &\pm 2\,G_A\,G_M\,\frac{k+k'}{M_N}\,\tan^2\frac{\theta}{2}\,\boxed{R_{\sigma\tau(T)}}\Big]\end{aligned}$$

M. Martini, M. Ericson, G. Chanfray, J. Marteau — terms in G_M and G_A

J. Nieves, I. Ruiz Simo, M.J. Vicente Vacas et al. — all the terms

J.E. Amaro, M.B. Barbaro, J.A. Caballero, T.W. Donnelly et al. — only in the G_M^2 term

Relative role of 2p-2h for neutrinos and antineutrinos is different

Antineutrino MiniBooNE CCQE-like $d^2\sigma$

Recent Measurement

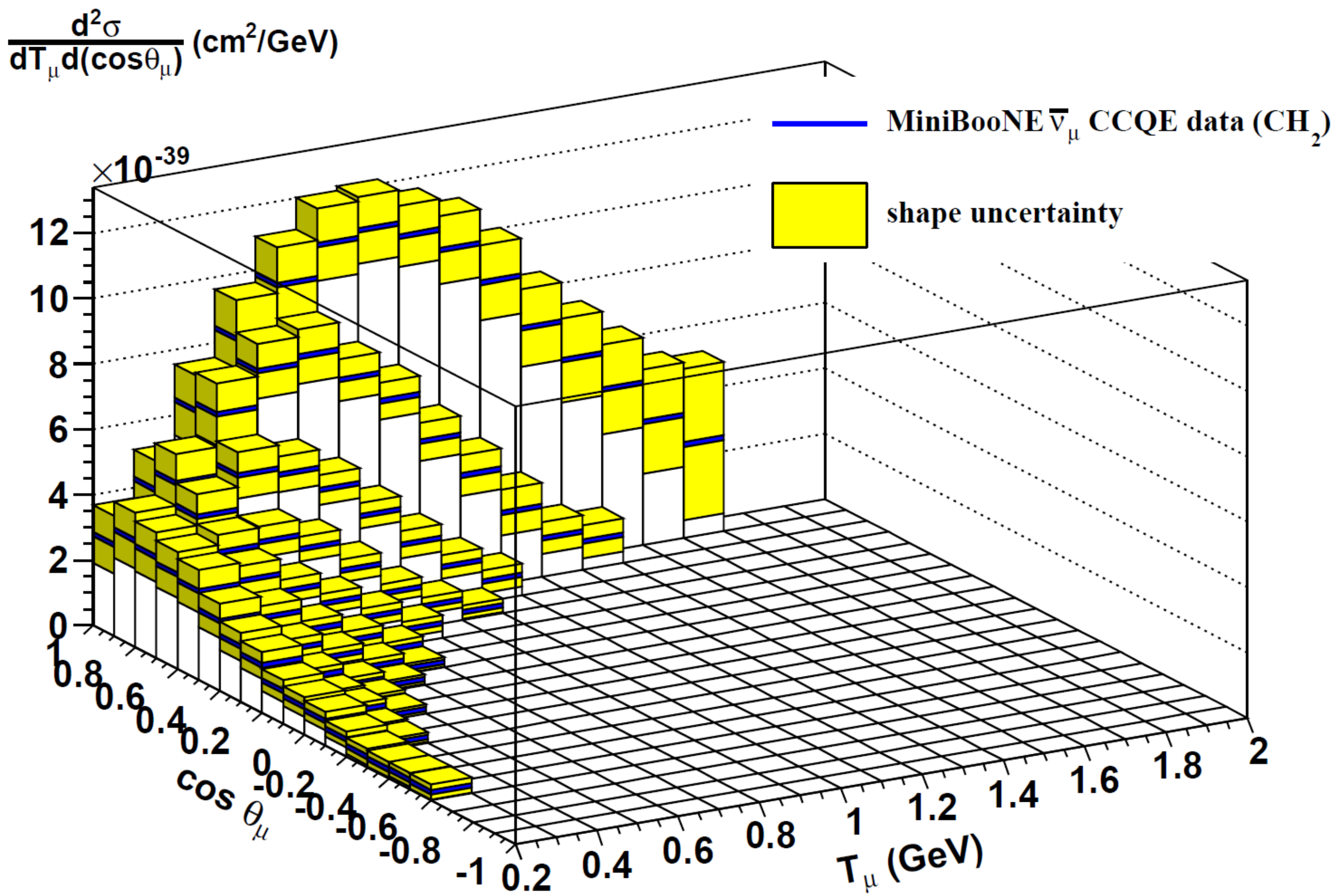

MiniBooNE, Phys. Rev. D 88 (2013) 032001

CH_2 and Carbon

ν $\bar{\nu}$

Martini et al.

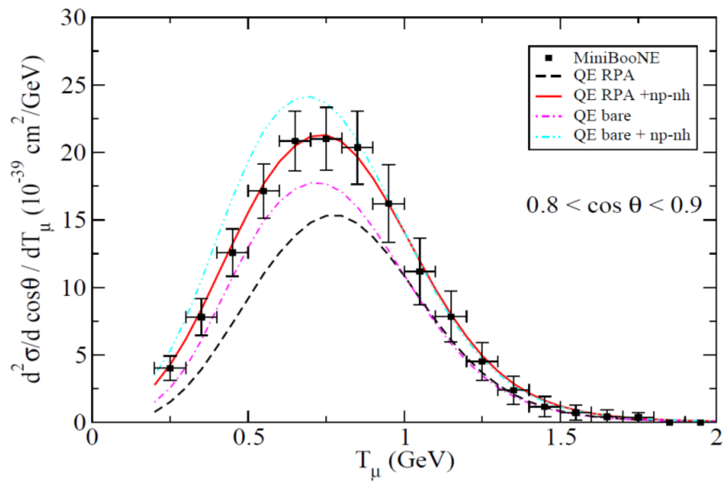

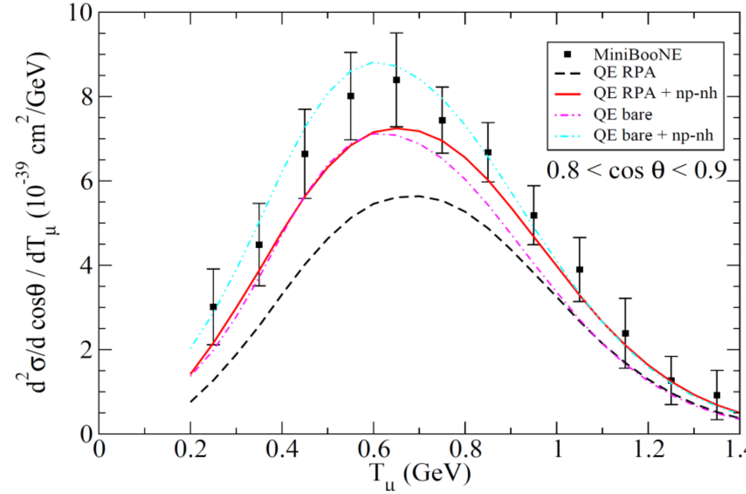

Nieves et al.

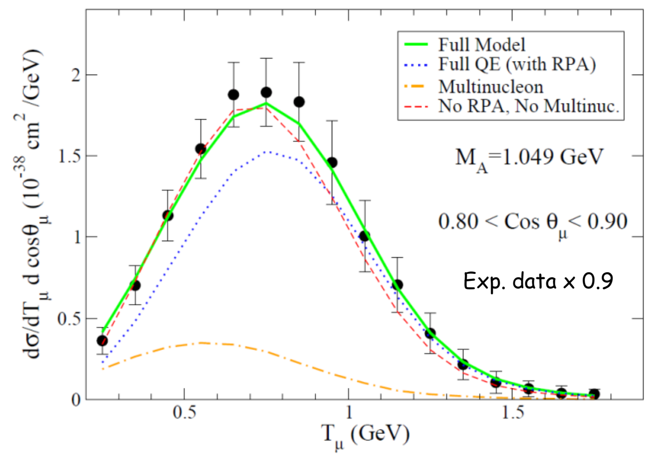

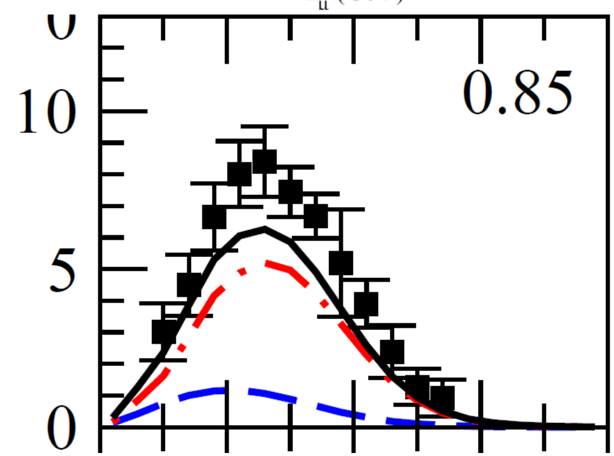

black: QE RPA+2p2h

red: QE RPA

Amaro et al.

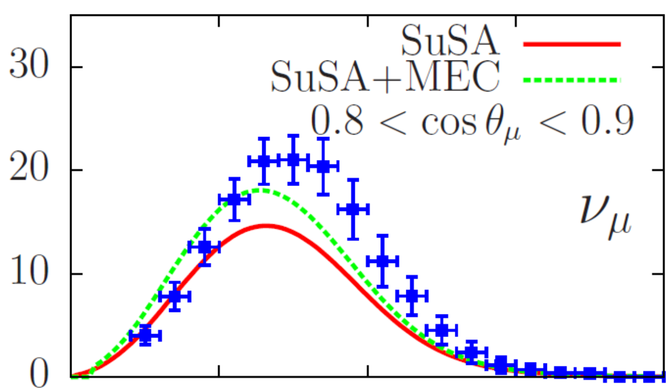

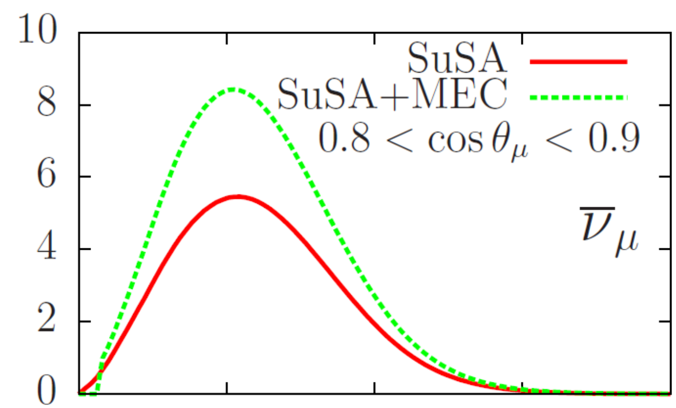

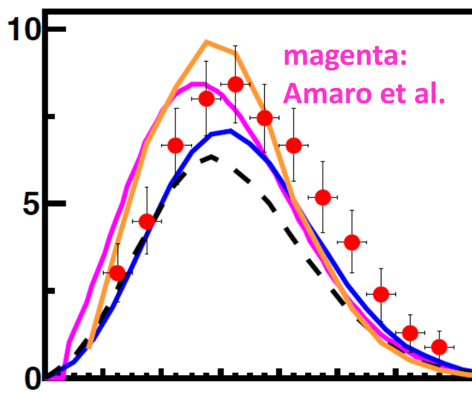

Our results for $\overline{\nu}$

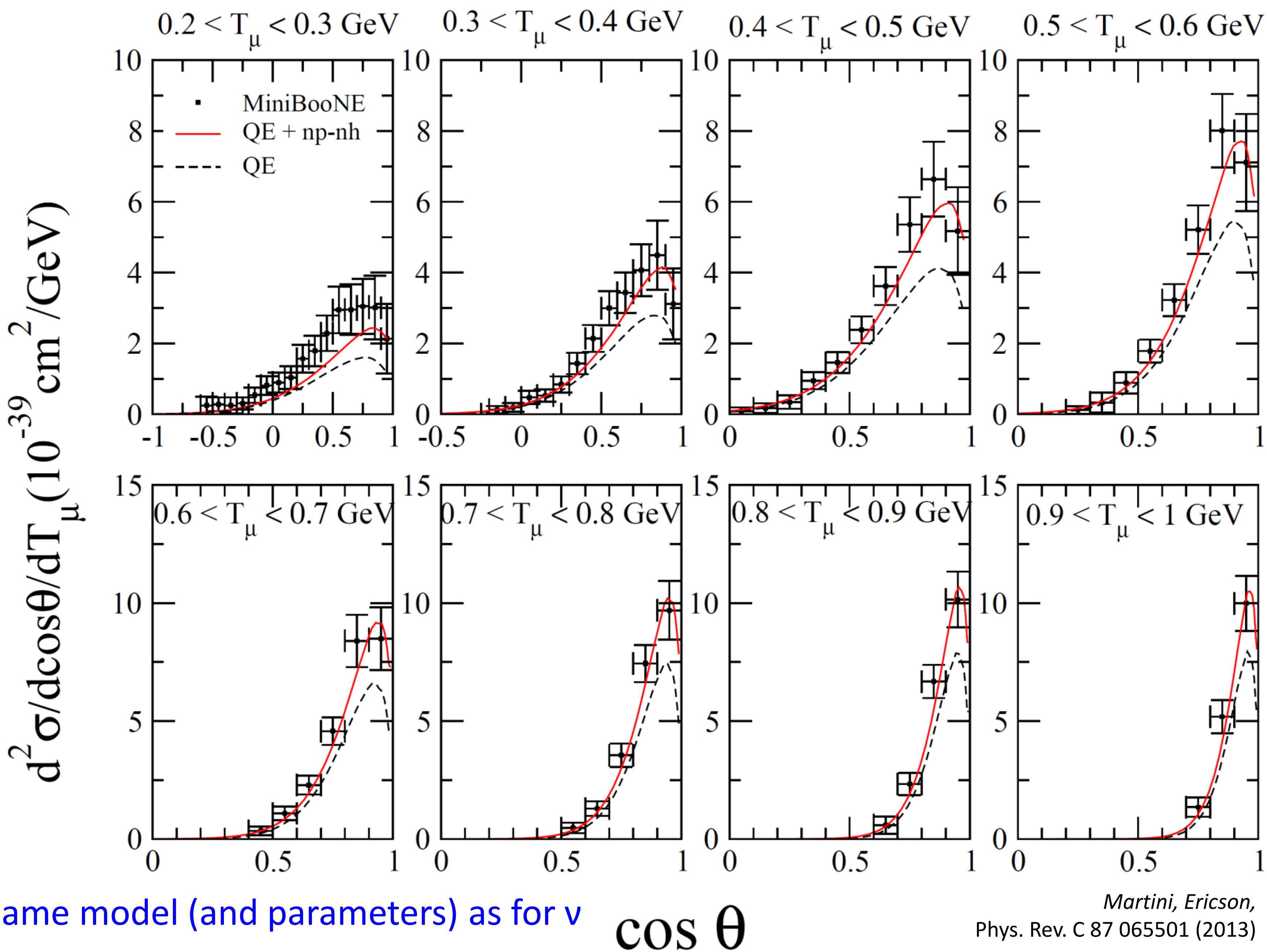

same model (and parameters) as for ν

Martini, Ericson,
Phys. Rev. C 87 065501 (2013)

Antineutrino $d\sigma/dT_\mu$

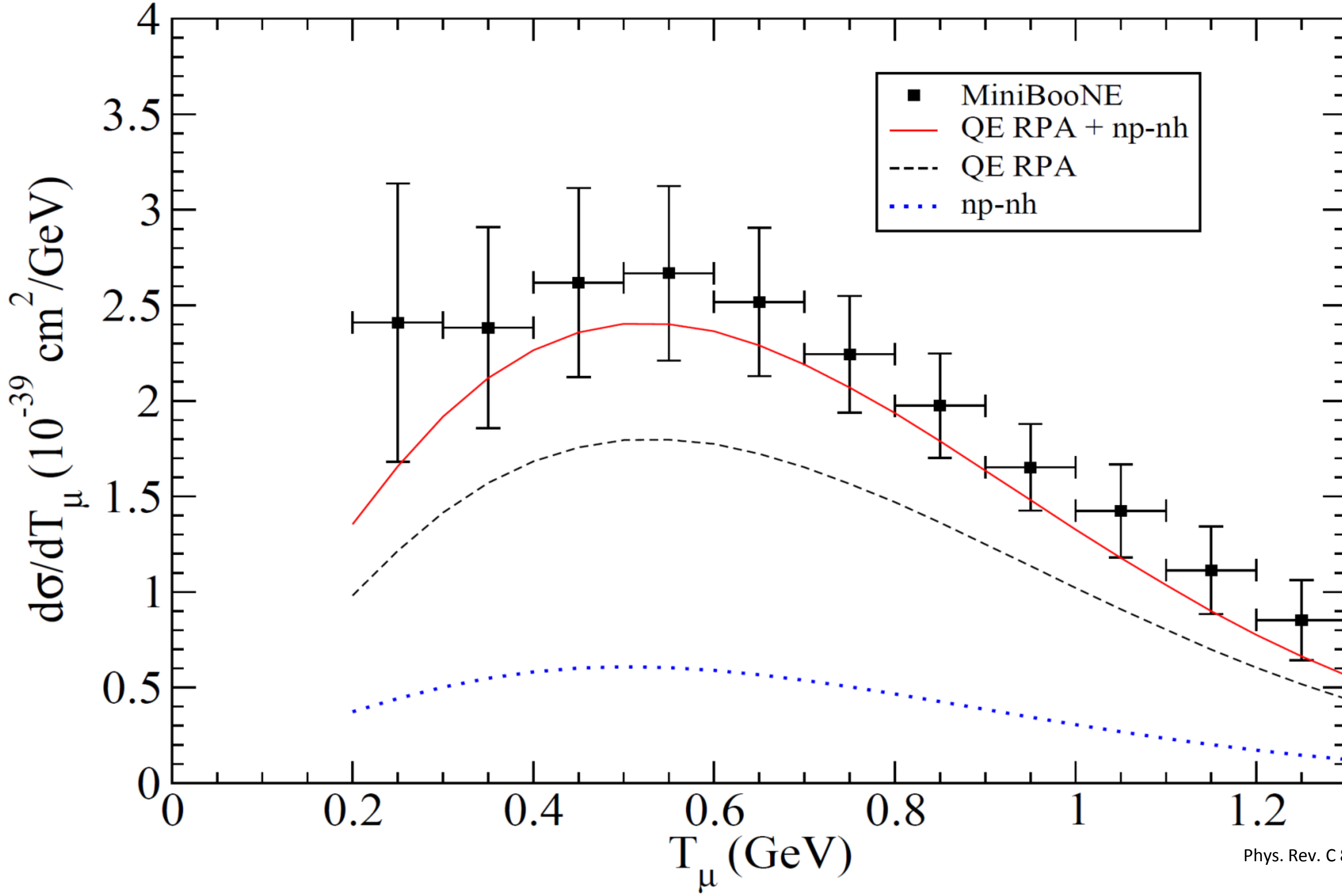

Martini, Ericson,
Phys. Rev. C 87 065501 (2013)

Our results are fully compatible with experimental data.
Nevertheless a small but systematic underestimation shows up.
We remind the additional normalization uncertainty of 17.2% in the MiniBooNE data not shown here.

dσ/dcosθ

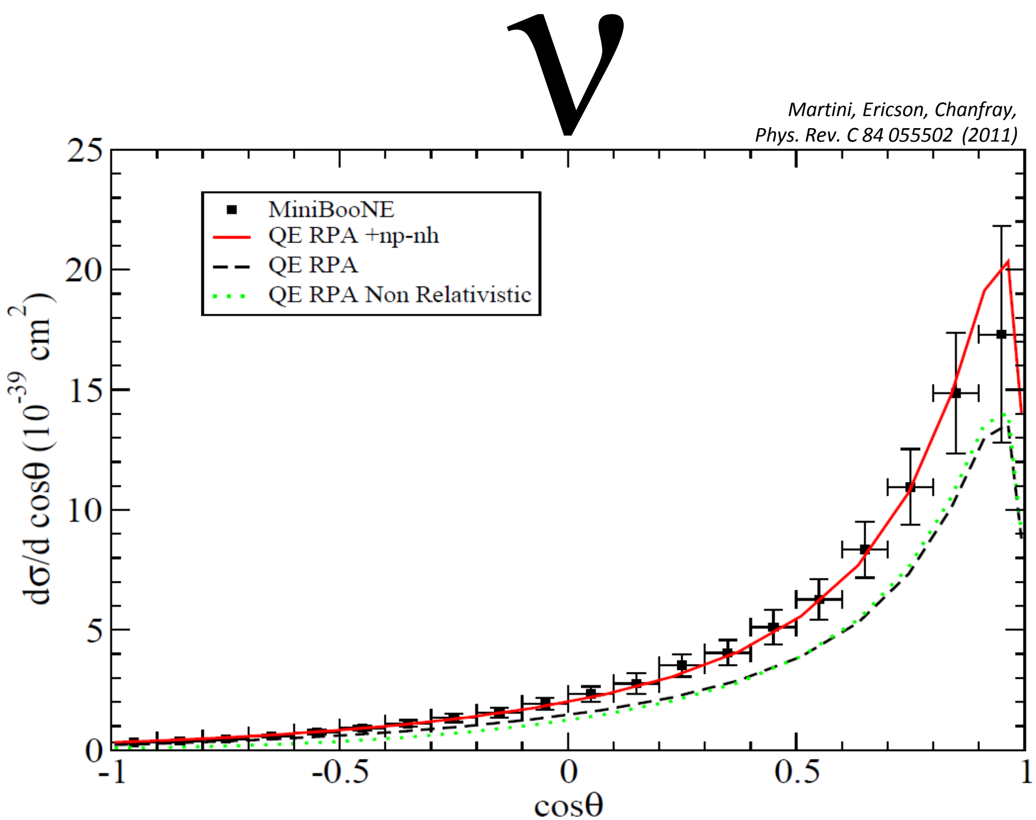

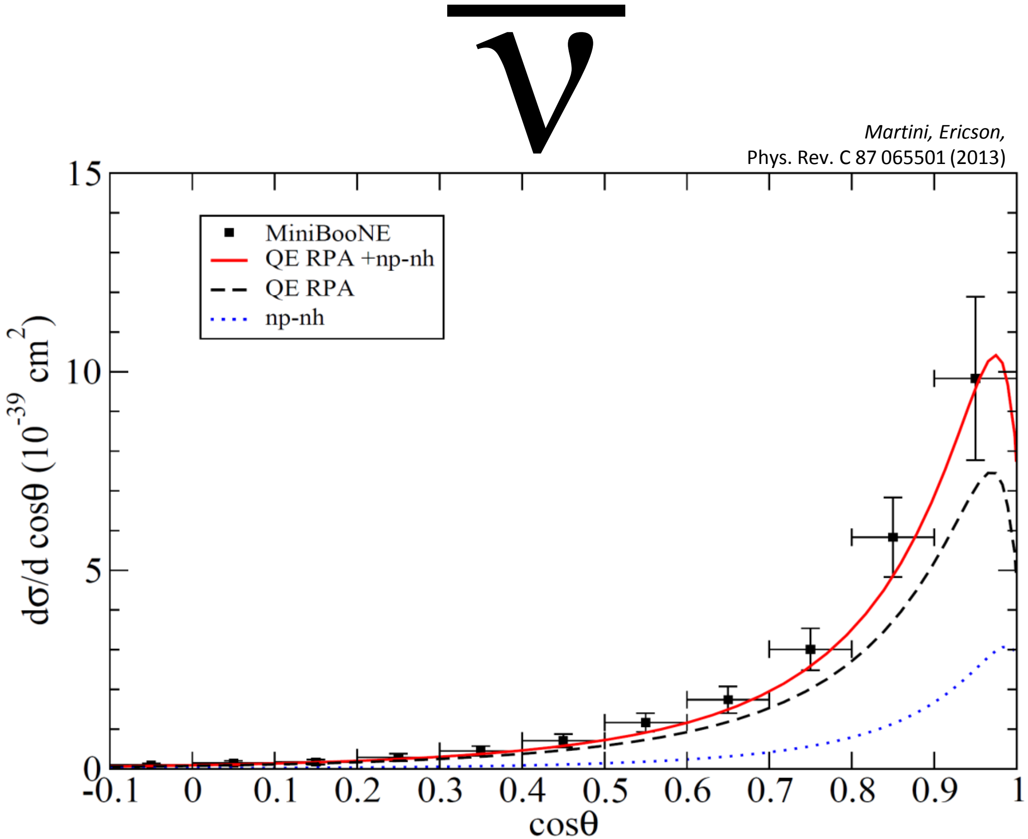

Antineutrino cross section falls more rapidly with angle than the neutrino one

CC Q^2 distribution

$\bar{\nu}$

Martini, Ericson,
Phys. Rev. C 87 065501 (2013)

ν

Martini, Ericson, Chanfray,
Phys. Rev. C 84 055502 (2011)

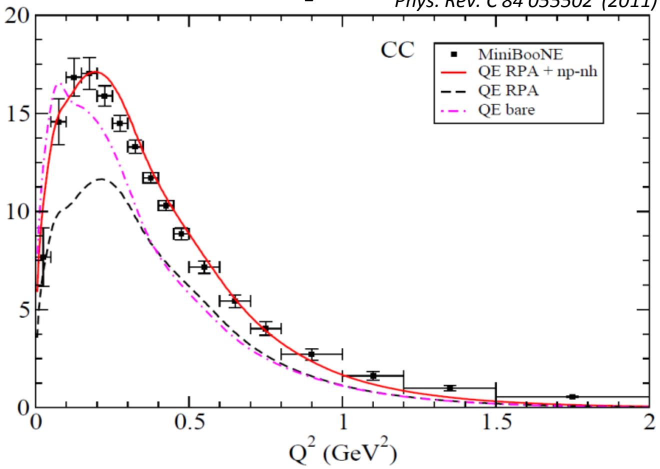

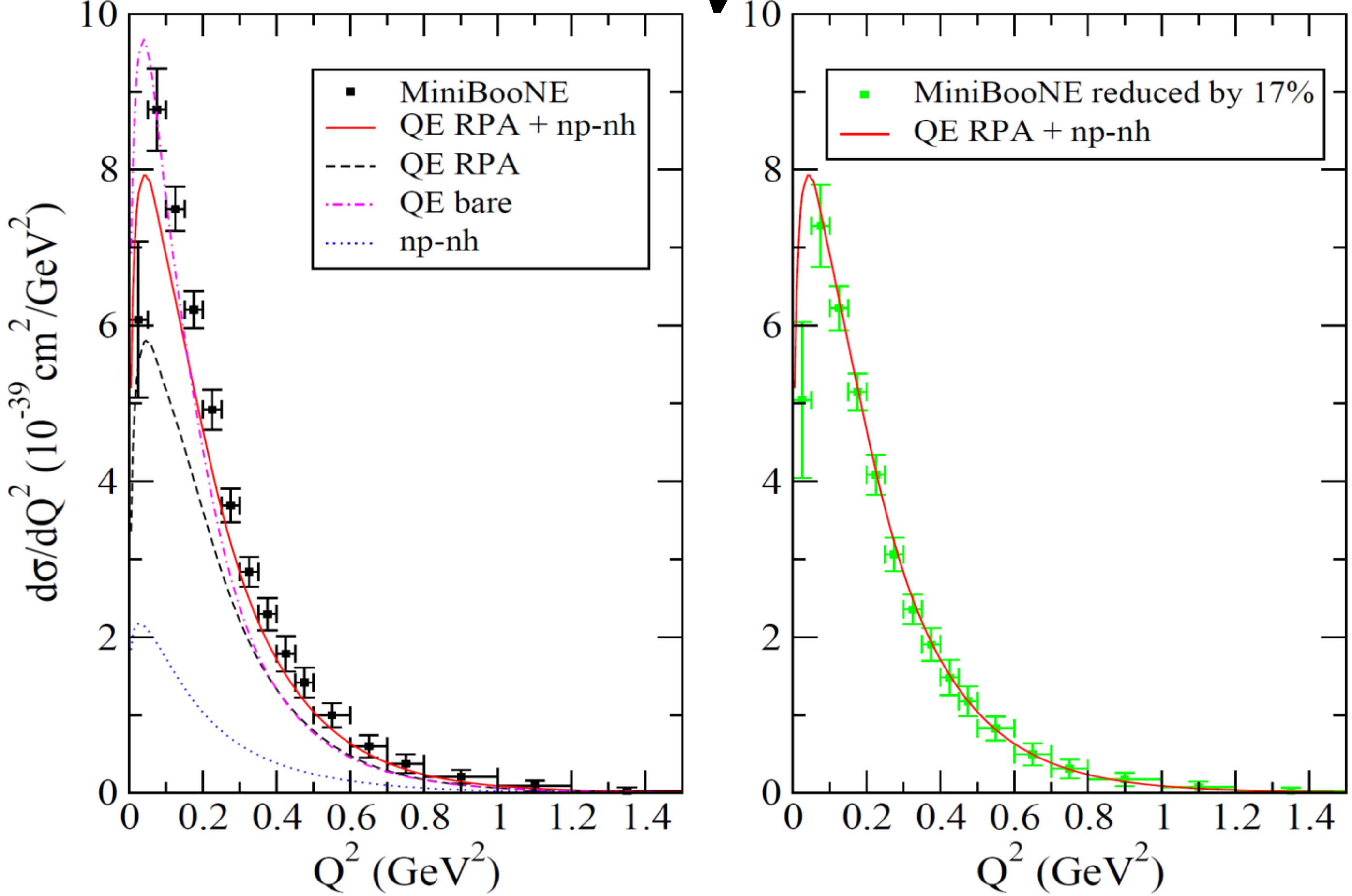

- Antineutrino Q^2 distribution peaks at smaller Q^2 values than the neutrino one
- RPA effects disappears beyond $Q^2 \geq 0.3$ GeV^2 where the np-nh contribution is required

Inclusive CC cross section on Carbon

Less affected by background subtraction with respect to exclusive channels

SciBooNE, *Phys. Rev. D. 83, 012005 (2011)*

T2K, *Phys. Rev. D 87, 092003 (2013)*

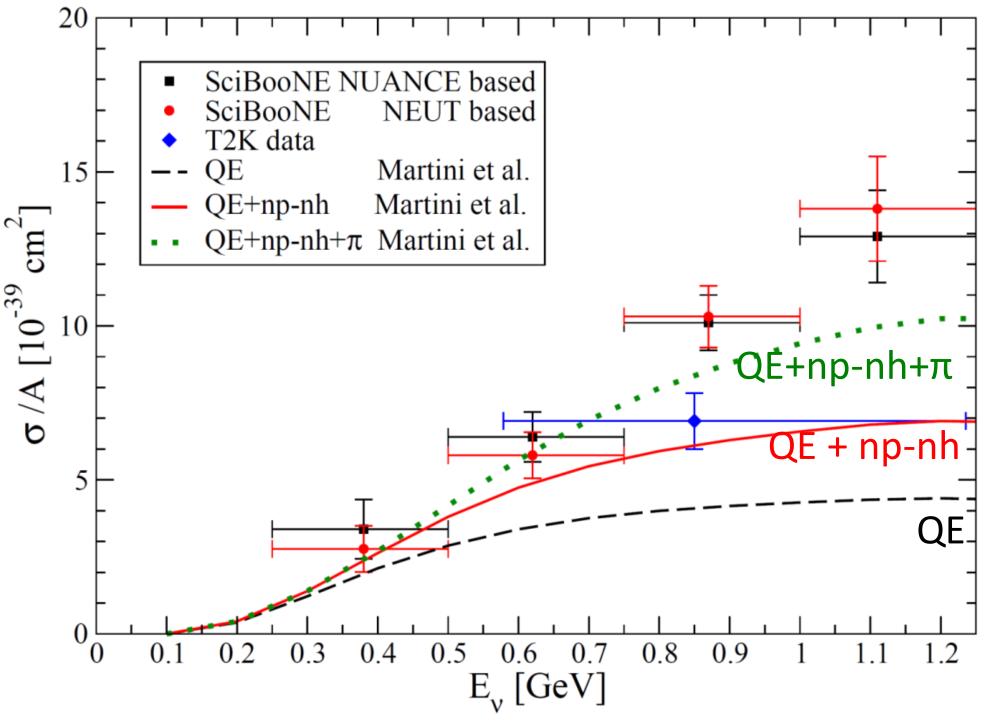

M. Martini, M. Ericson, G. Chanfray, J. Marteau
Phys. Rev. C 80 065501 (2009)

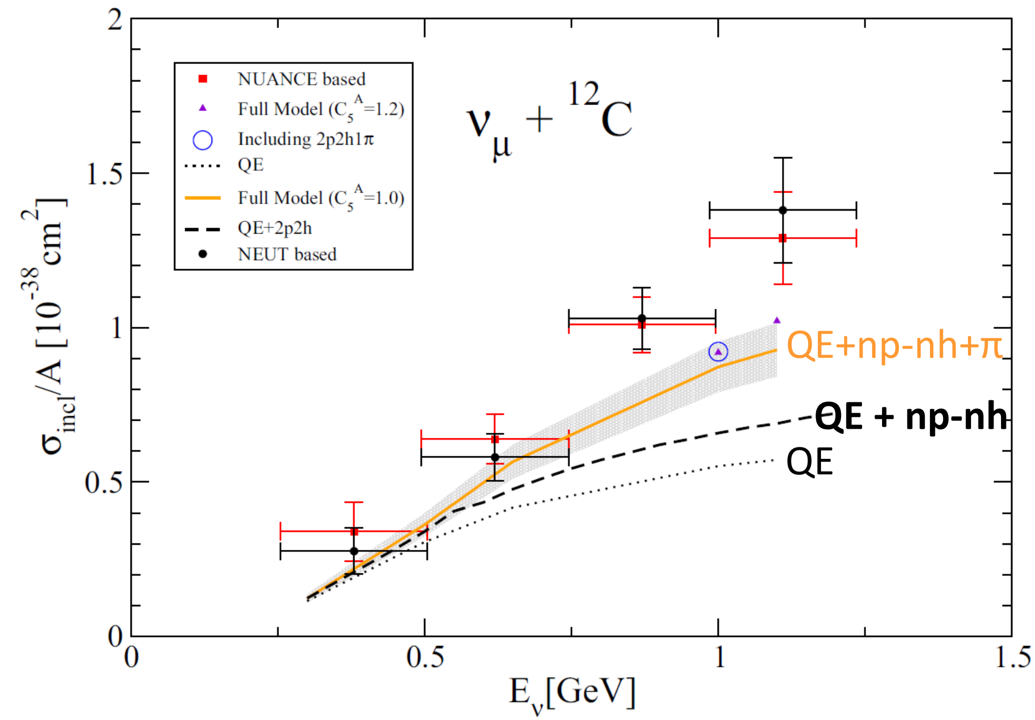

J. Nieves, I. Ruiz Simo, M.J. Vicente Vacas
Phys. Rev. C 83 045501 (2011)

Neutrino energy reconstruction problems and neutrino oscillations

Towards the neutrino oscillation physics

Neutrino oscillation experiments require the determination of the neutrino energy which enters the expression of the oscillation probability.
The neutrino energy is unknown. We know only broad fluxes.
The determination of the neutrino energy is done through
Charged Current QuasiElastic events.

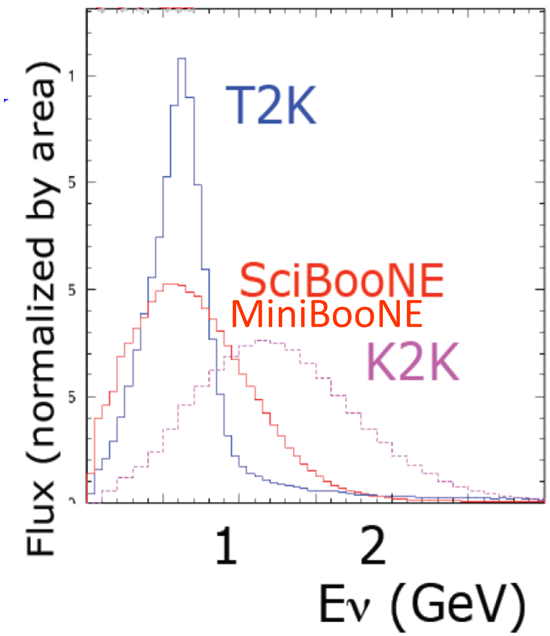

$\nu_\mu\, n \rightarrow \mu^- p$ CCQE

e.g. for μ

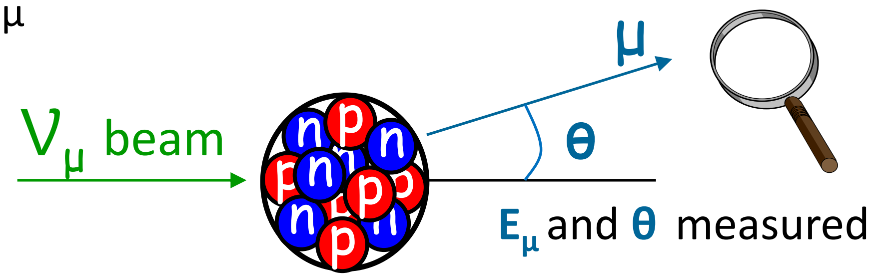

Reconstructed neutrino energy

$$\overline{E_\nu} = \frac{E_\mu - m_\mu^2/(2M)}{1-(E_\mu - P_\mu \cos\theta)/M}$$

via two-body kinematics

$\overline{E_\nu} = E_\nu$ is exact only for CCQE with free nucleon

reconstructed neutrino energy $\overline{E_\nu} \overset{?}{\longleftrightarrow} E_\nu$ true neutrino energy

From true neutrino energy to reconstructed neutrino energy

Probability energy distribution $(E_\nu, \bar{E}_\nu)$

$$D_{rec}(\overline{E_\nu}) = \int dE_\nu \Phi(E_\nu) \int_{E_l^{min}}^{E_l^{max}} dE_l \frac{ME_l - m_l^2/2}{\overline{E}_\nu^2 P_l} \left[\frac{d^2\sigma}{d\omega\ d\cos\theta}\right]_{\omega=E_\nu-E_l,\ \cos\theta=\cos\theta(E_l,\overline{E_\nu})}$$

The quantity $D_{rec}(\overline{E_\nu})$ corresponds to the product $\sigma(E_\nu)\Phi(E_\nu)$ but in terms of reconstructed neutrino energy

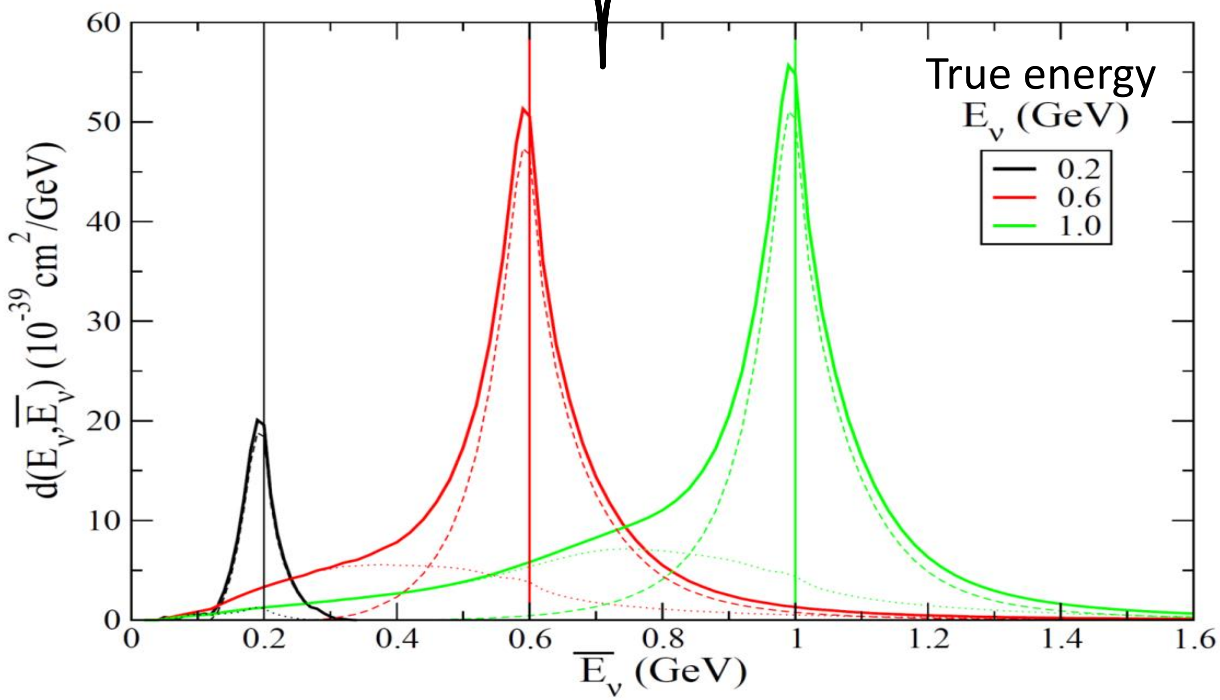

M. Martini, M. Ericson, G. Chanfray
- Phys. Rev. D 85 093012 (2012)
- Phys. Rev. D 87 013009 (2013)

Crucial role of np-nh: low energy tail

Viceversa: distributions in terms of true E_ν for fixed values of reconstructed E_ν

Martini, Ericson, Chanfray, PRD 85 093012 (2012)

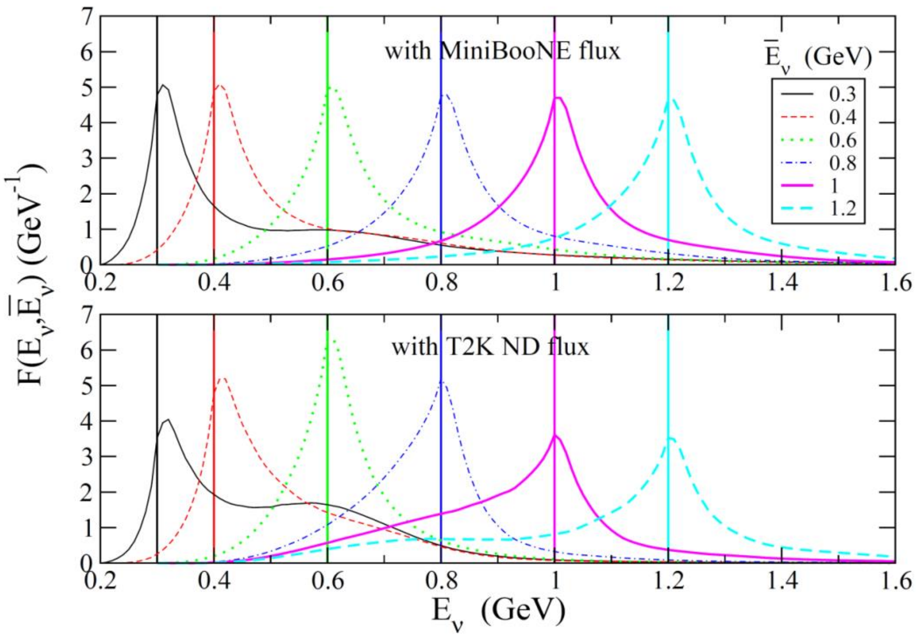

O. Lalakulich, U. Mosel, K. Gallmeister PRC 86 054606 (2012)

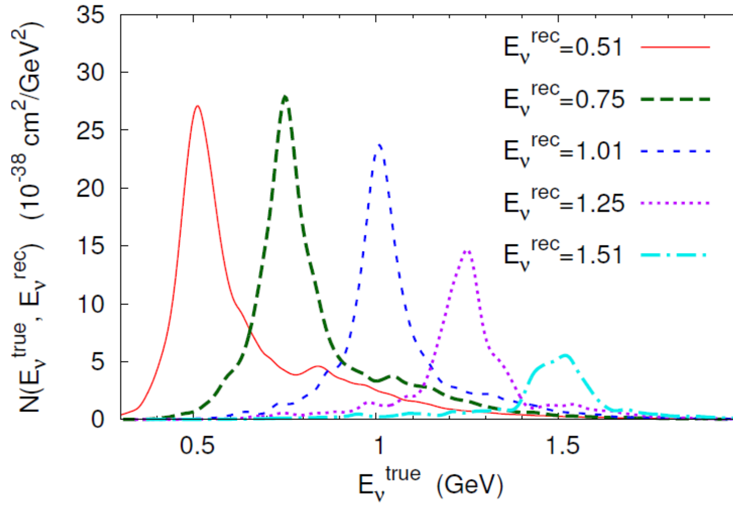

- The distributions are not symmetrical around Ēv.
- The asymmetry favors higher energies at low Ēv and smaller energies for large Ēv.
- Crucial role of neutrino flux.

J. Nieves, F. Sanches, I. Ruiz Simo, M.J. Vicente Vacas
PRD 85 113008 (2012)

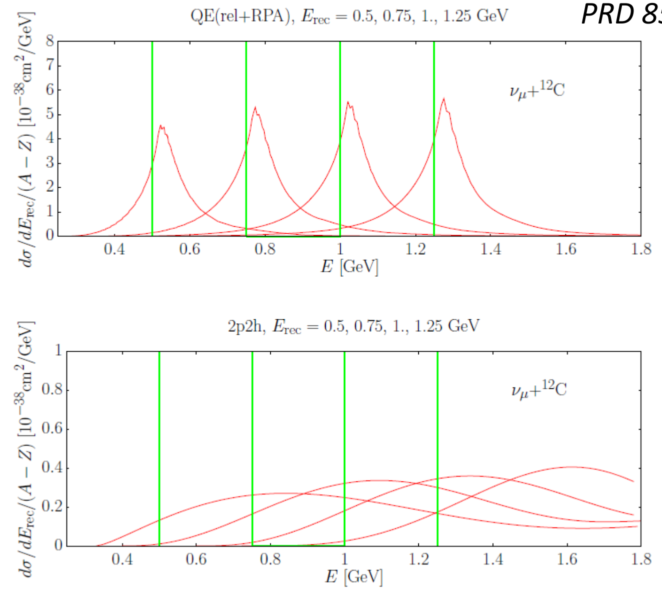

Real and effective cross sections for ν_μ and ν_e

Let's define the effective cross section through $D_{\mathrm{rec}}(\bar{E}_\nu) = \sigma_\nu^{\mathrm{eff}}(\bar{E}_\nu)\Phi(\bar{E}_\nu)$

Let's then ignore the difference between the true and reconstructed neutrino energies

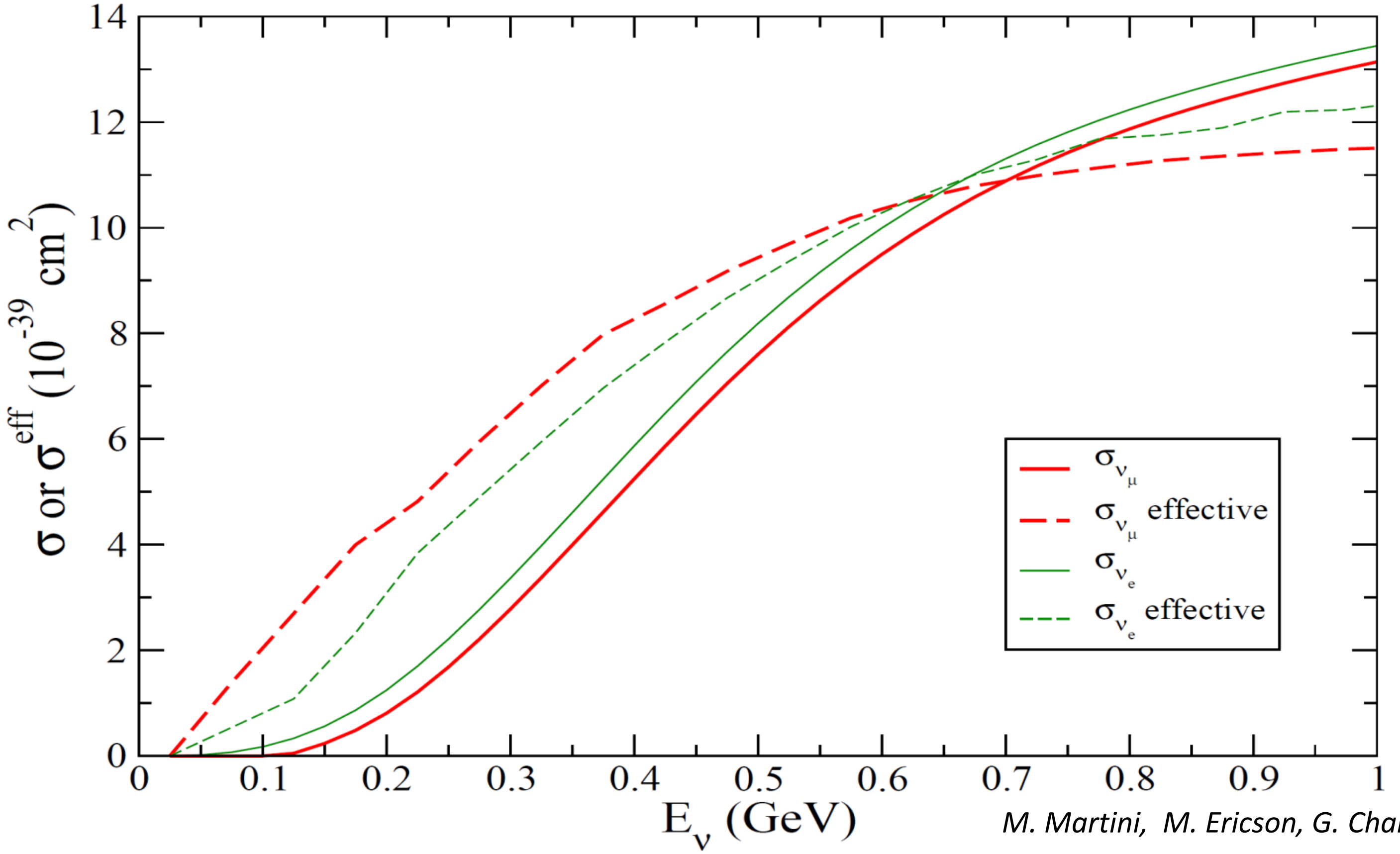

M. Martini, M. Ericson, G. Chanfray, PRD 87 013009 (2013)

The effective cross section is not universal but it depends on the particular beam energy distribution

(here we used ν_μ and ν_e MiniBooNE fluxes)

Application to ν oscillation analysis

$\nu_\mu \rightarrow \nu_e$ T2K

PRL 107 (2011), PRD 88 (2013)

2013: 28 events

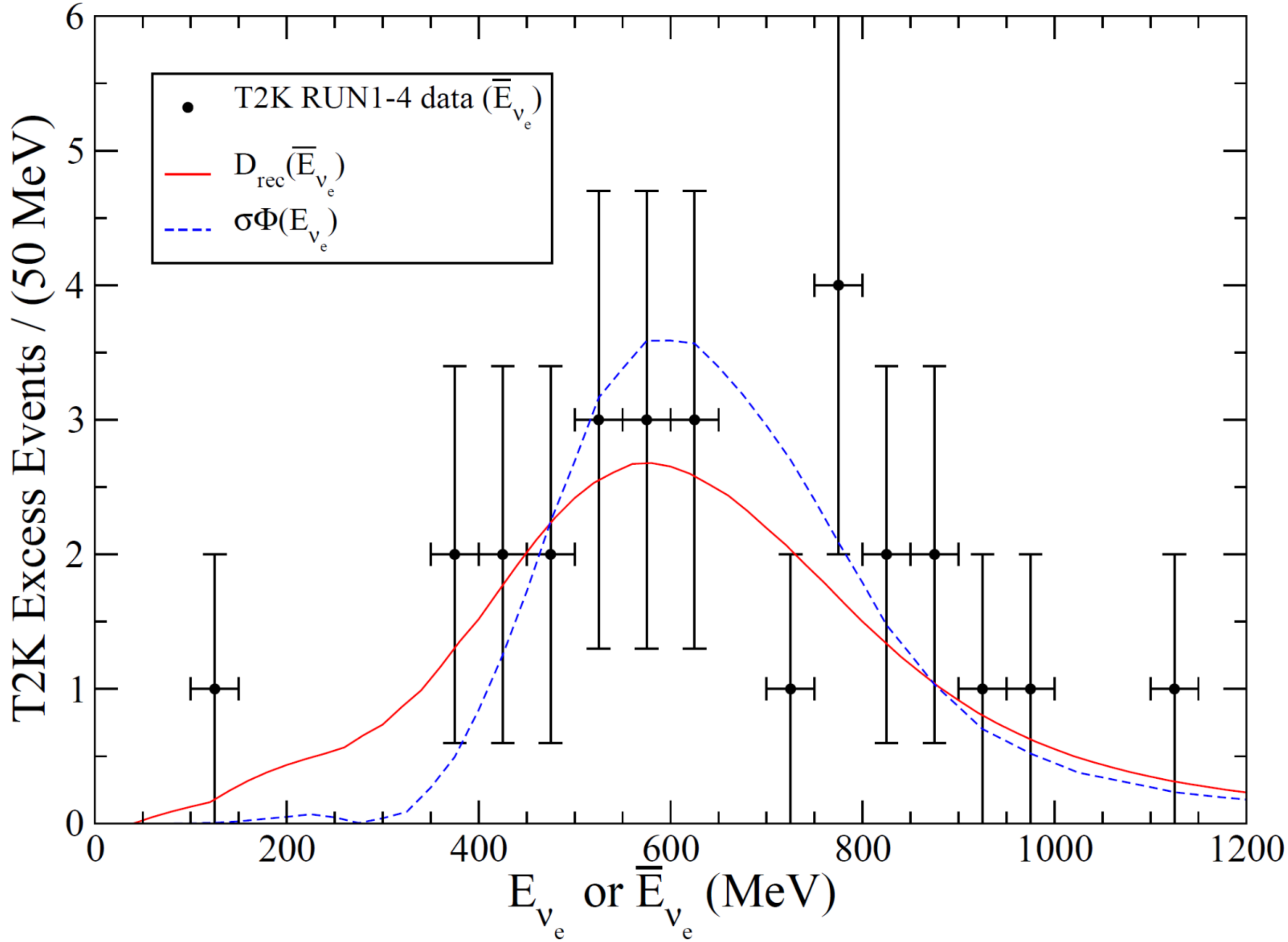

The reconstruction correction tends to make events leak outside the high flux region especially towards the low energy side, in agreement with the observed trend

νμ disappearance T2K

PRD85 (2012); 1308.0465 (2013)

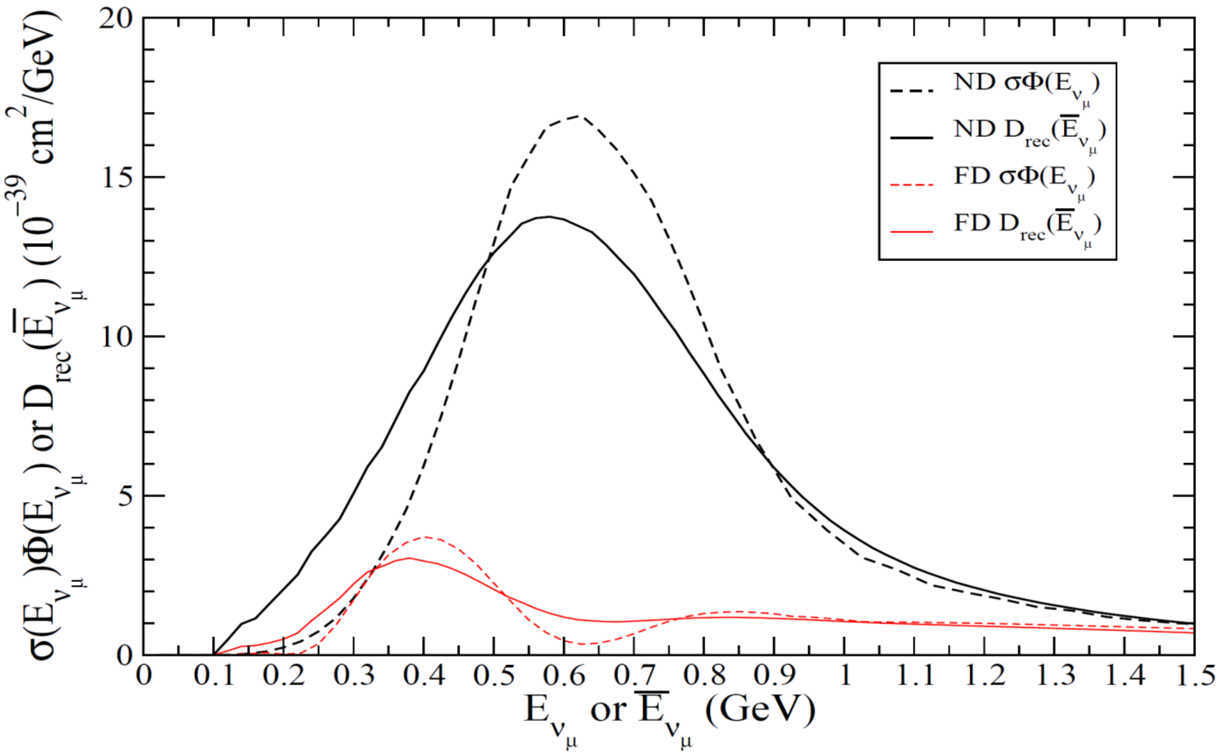

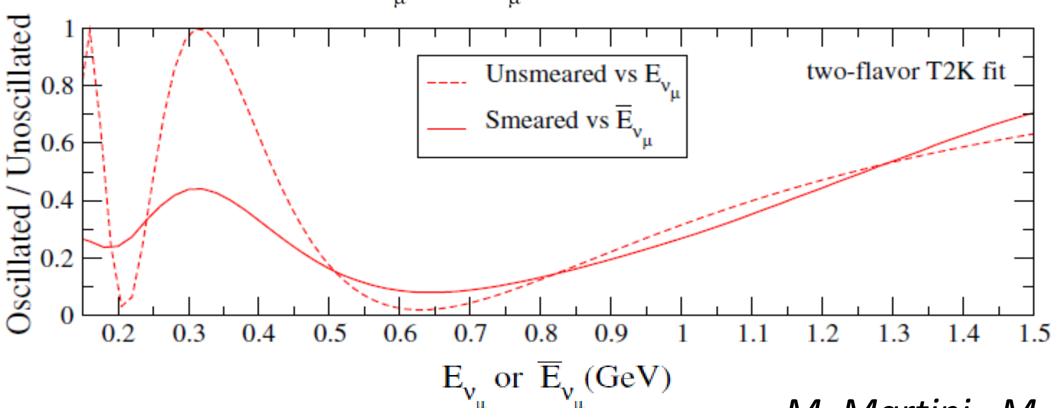

After reconstruction:

- Near Detector:
  clear low energy enhancement
- Far Detector:
  low energy tail and
  the middle hole is largely filled

Effects largely due to np-nh

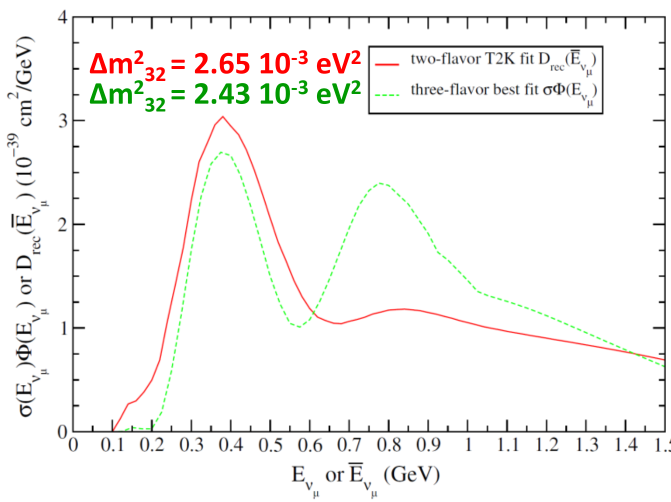

E_ν reconstruction leads to an increase of oscillation mass parameters

M. Martini, M. Ericson, G. Chanfray, PRD 87 013009 (2013)

Similar results in: O. Lalakulich, U. Mosel, K. Gallmeister, PRC 86 054606 (2012)

$\nu_\mu \longrightarrow \nu_e$ MiniBooNE

PRL 98 (2007), PRL 102 (2009), PRL 105 (2010), PRL 110 (2013)

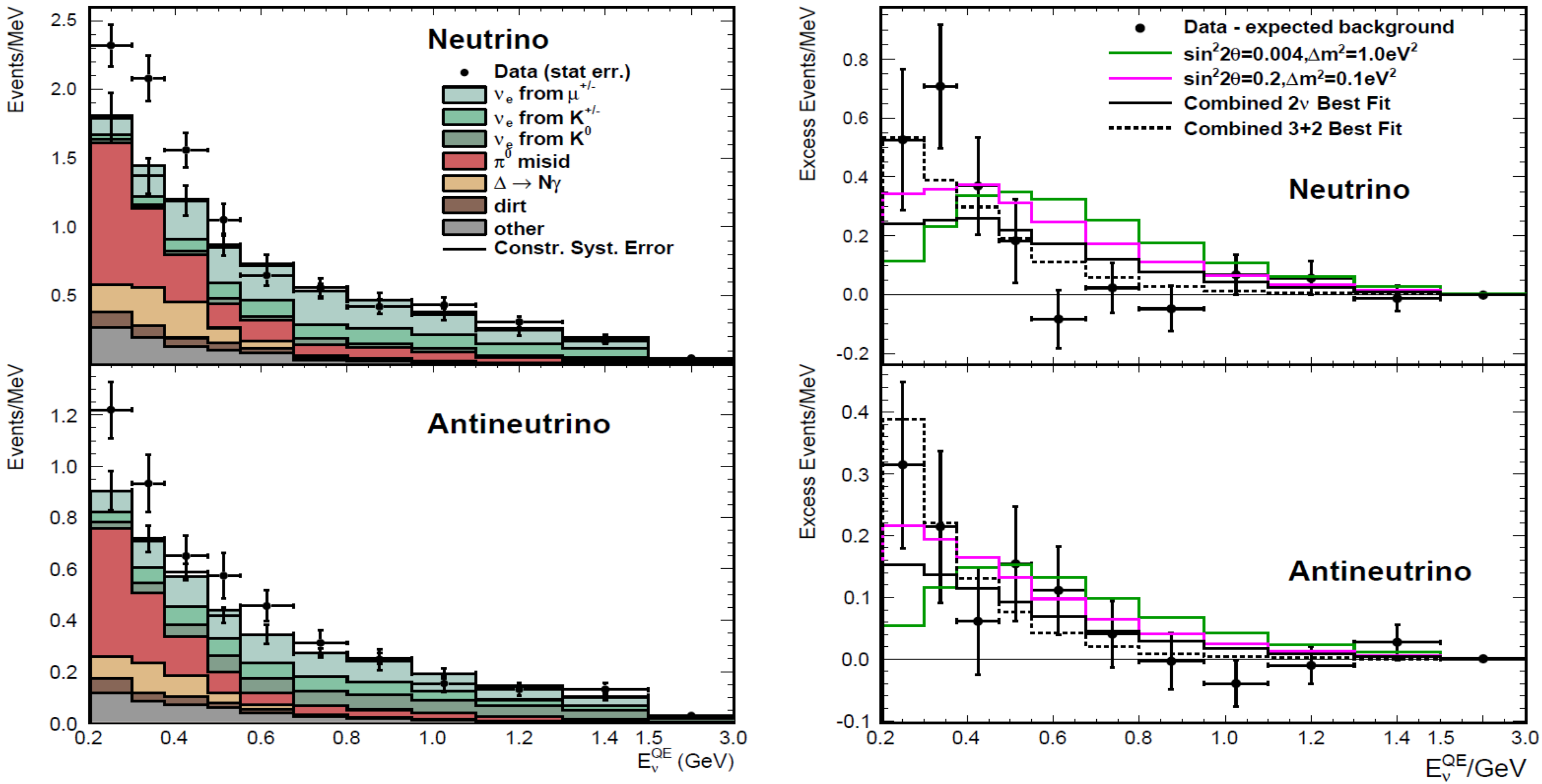

MiniBooNE Anomaly: Excess of events at low energies

Sterile neutrino??

Taking now into account the smearing procedure

M. Martini, M. Ericson, G. Chanfray, PRD 87 013009 (2013)

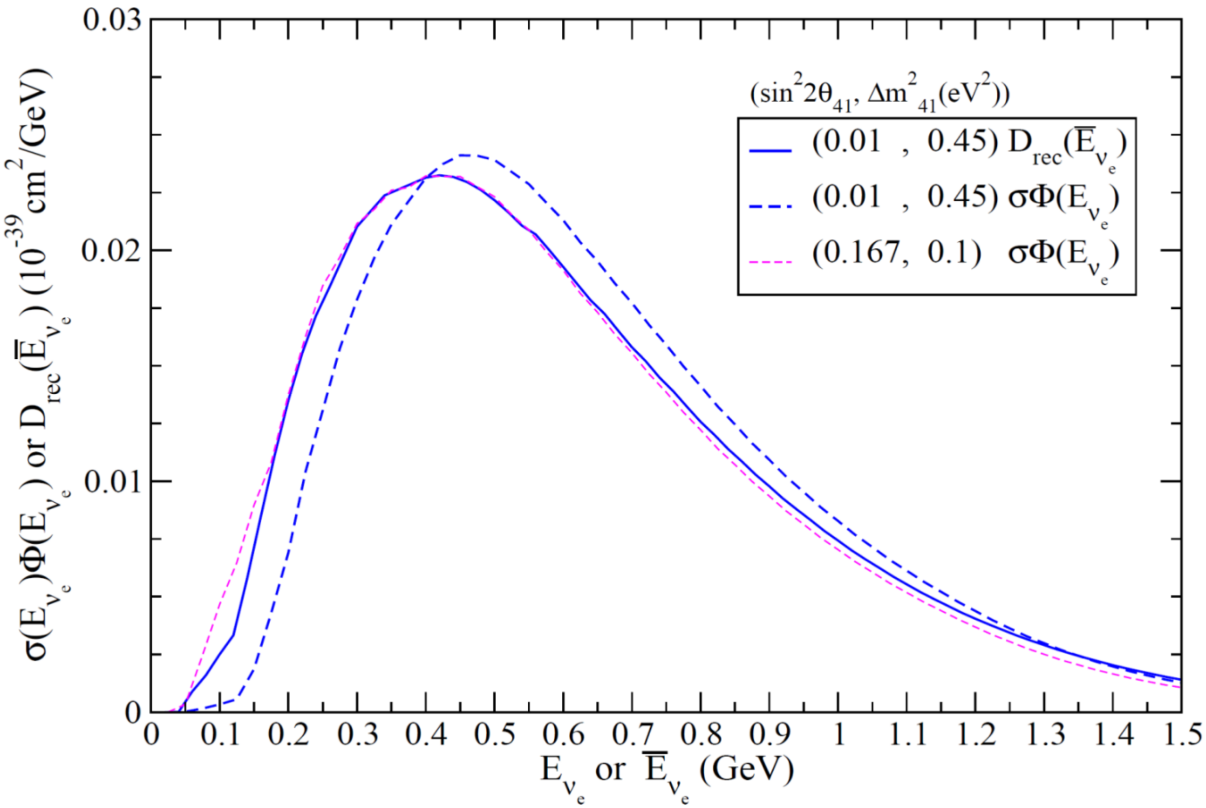

OPERA, JHEP 1307 (2013) 004,
Addendum-ibid. 1307 (2013) 085

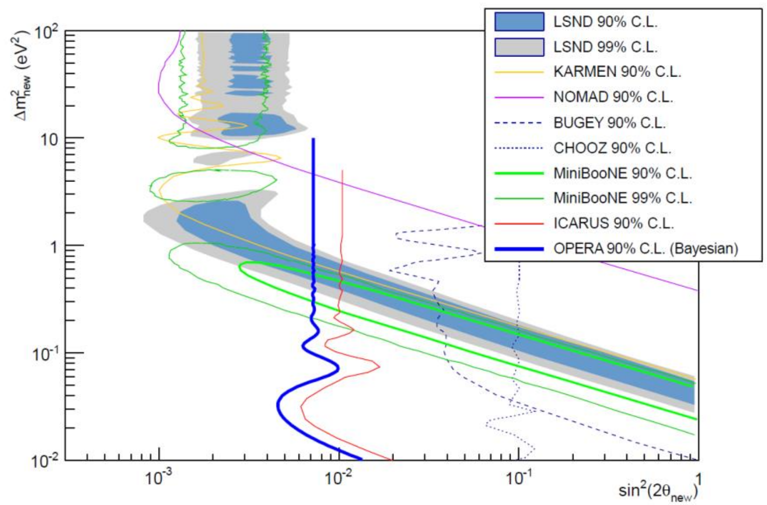

A large mass value allows the same quality of fit of data than is obtained in the unsmeared case with a much smaller mass.

The energy reconstruction leads to an increase of the oscillation mass parameters

⇨ **Gain for the compatibility with the existing constraints**

Nuclear effects in neutrino interactions

Summary

- Quasielastic σ , $d^2\sigma/(dT_\mu \, d\cos\theta)$, $d\sigma/dQ^2$ measured by MiniBooNE can be explained without any modification of M_A including the np-nh channel

- Several theoretical calculations agree on the crucial role of the multinucleon channel in order to explain data but there are some differences on the way to treat this channel

- Nuclear effects generate an asymmetry between ν and antiν interaction: important for the investigation of CP violation effects

- Neutrino energy reconstruction and neutrino oscillations $\overline{E_\nu} \Longleftrightarrow E_\nu$
  - **T2K**: agreement with $\nu_\mu \text{-->} \nu_e$ data
  - **T2K** ν_μ and **MiniBooNE**: the energy reconstruction correction is expected to lead to an increase of the best fit oscillation mass parameters
  - **MiniBooNE**: the smearing procedure improve the compatibility with existing constraints

Spares

Neutrino - nucleus cross sections

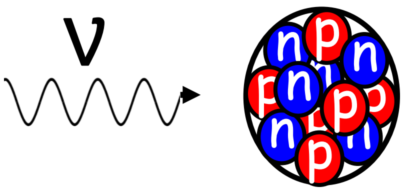

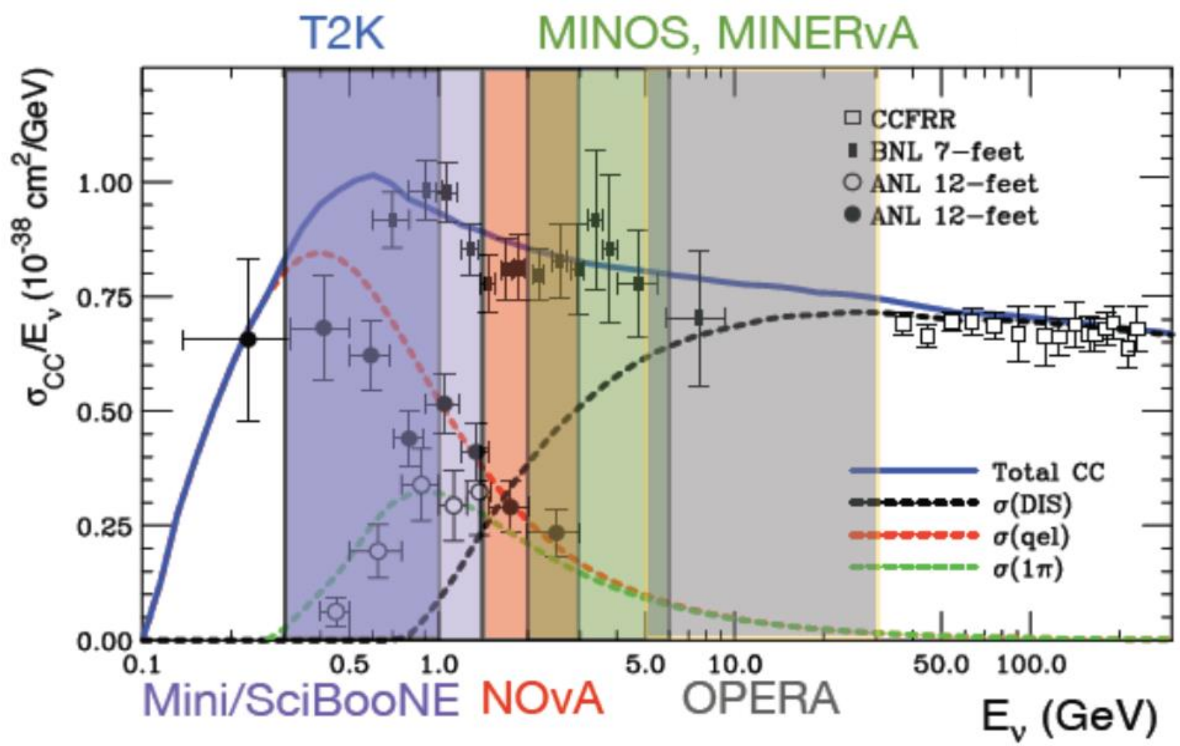

- Relatively precise measurements at high neutrino energies, where deep inelastic scattering is important
- Less precise measurements in **few-GeV** region, where **many processes** contribute
- Nuclear effects important at all energies, especially low energies
- Large uncertainties, some puzzles

Bare nuclear responses

Several partial components
(final state channels)

- QE (1 nucleon knock-out)
- Pion production
- Multinucleon emission

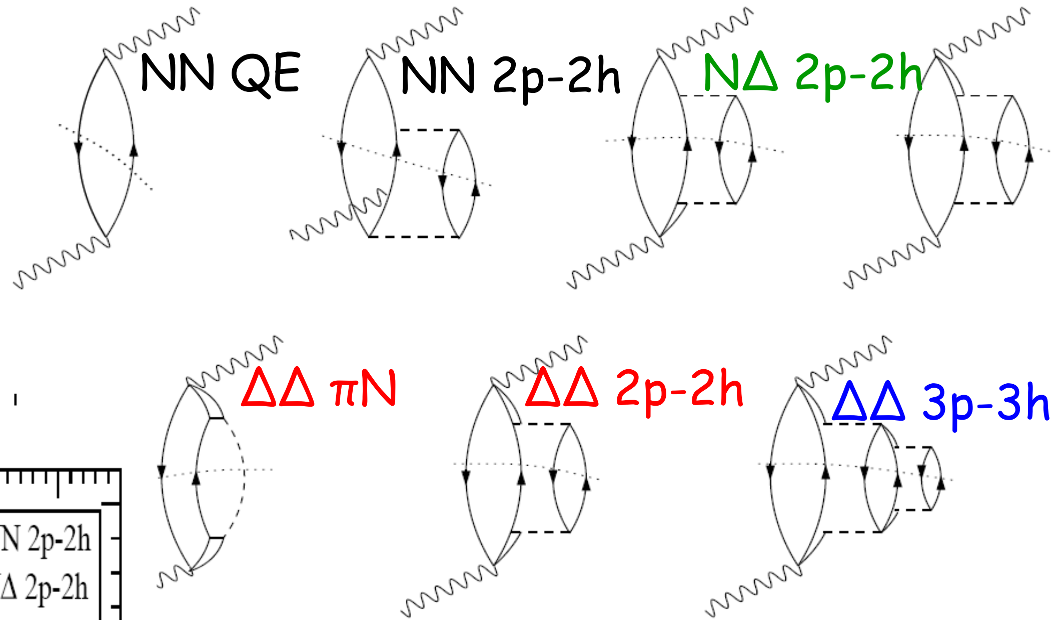

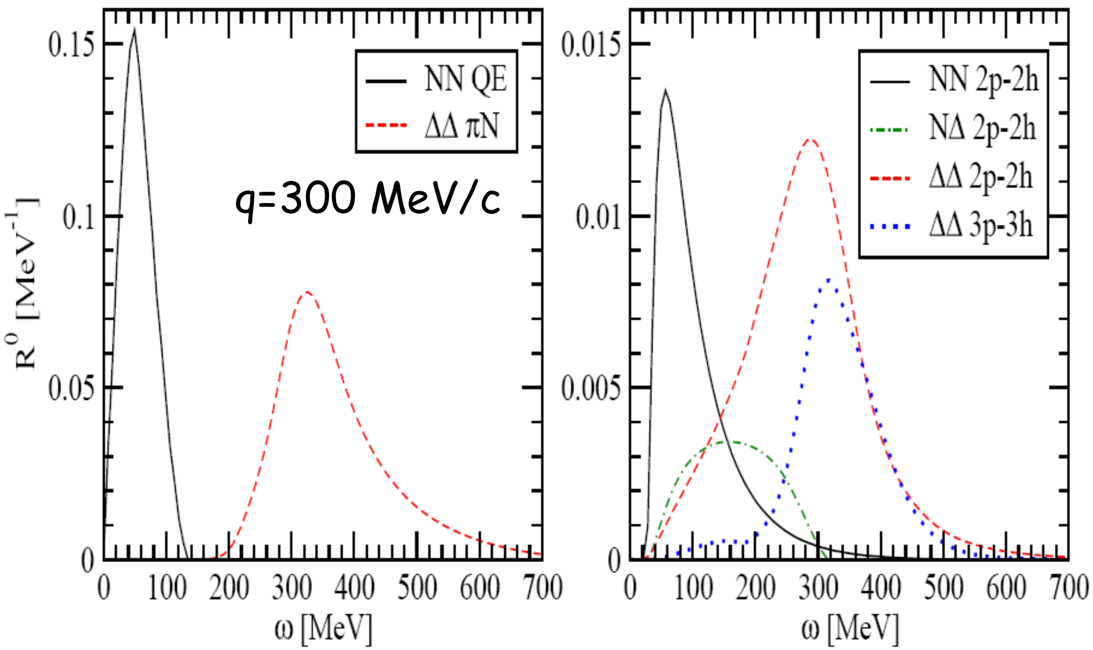

Bare polarization propagators

Quasielastic

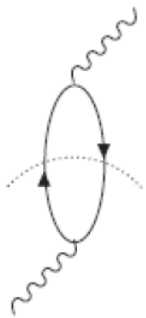

$$\Pi^0(\vec{q},\omega) = g\int \frac{\mathrm{d}\vec{k}}{(2\pi)^3}\left[\frac{\theta(|\vec{k}+\vec{q}|-k_F)\theta(k_F-k)}{\omega-(\omega_{\vec{k}+\vec{q}}-\omega_{\vec{k}})+i\eta}-\frac{\theta(k_F-|\vec{k}+\vec{q}|)\theta(k-k_F)}{\omega+(\omega_{\vec{k}}-\omega_{\vec{k}+\vec{q}})-i\eta}\right]$$

Nucleon-hole

Pion production

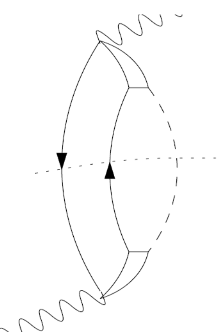

$$\Pi_{\Delta-h}(q) = \frac{32\tilde{M}_\Delta}{9}\int \frac{d^3k}{(2\pi)^3}\theta(k_F-k)\left[\frac{1}{s-\tilde{M}_\Delta^2+i\tilde{M}_\Delta\Gamma_\Delta}-\frac{1}{u-\tilde{M}_\Delta^2}\right]$$

Delta-hole

Delta in the medium

Mass

$$\tilde{M}_\Delta = M_\Delta + 40(MeV)\frac{\rho}{\rho_0}$$

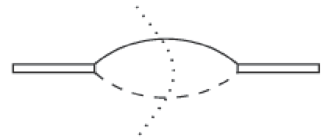

$\Delta \rightarrow \pi N$

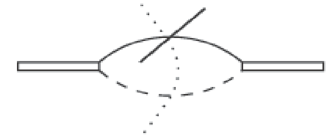

Pauli correction (F_P)

Width

$$\widetilde{\Gamma_\Delta} = \Gamma_\Delta\ F_P - 2\mathrm{Im}(\Sigma_\Delta)$$

Pion distortion (C_Q)

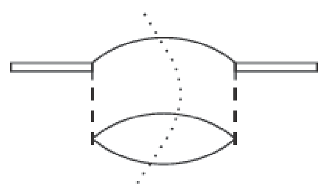

2p-2h

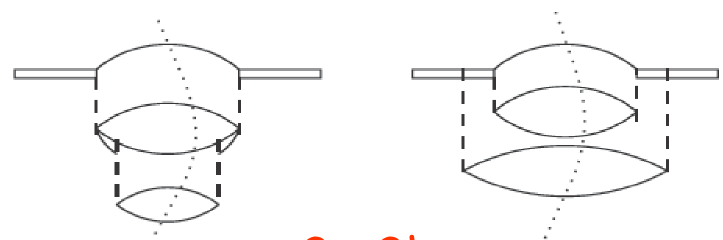

3p-3h

Self energy

$$\mathrm{Im}(\Sigma_\Delta(\omega)) = -\left[C_Q(\frac{\rho}{\rho_0})^\alpha + C_{2p2h}(\frac{\rho}{\rho_0})^\beta + C_{3p3h}(\frac{\rho}{\rho_0})^\gamma\right]$$

E. Oset and L. L. Salcedo, Nucl. Phys. A 468, 631 (1987)

Switching on the interaction: random phase approximation

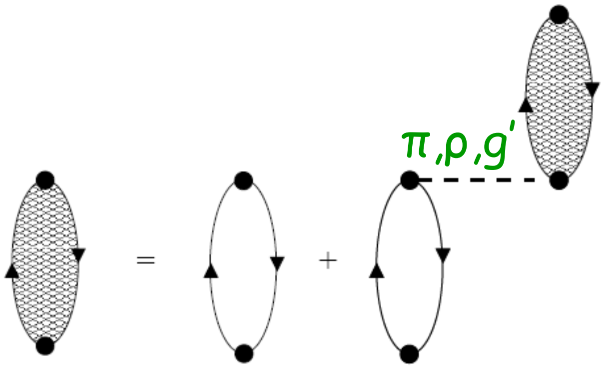

RPA $$\Pi = \Pi^0 + \Pi^0 V \Pi$$

$$\mathrm{Im}\Pi = |\Pi|^2\ \mathrm{Im}V + |1 + \Pi\, V|^2\ \mathrm{Im}\Pi^0$$

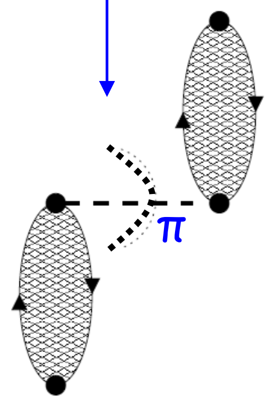

coherent π production

$$\Pi^0 = \sum_{k=1}^{N_k} \Pi^0_{(k)}$$

exclusive channels:
QE, 2p-2h, $\Delta \rightarrow \pi N$ ...

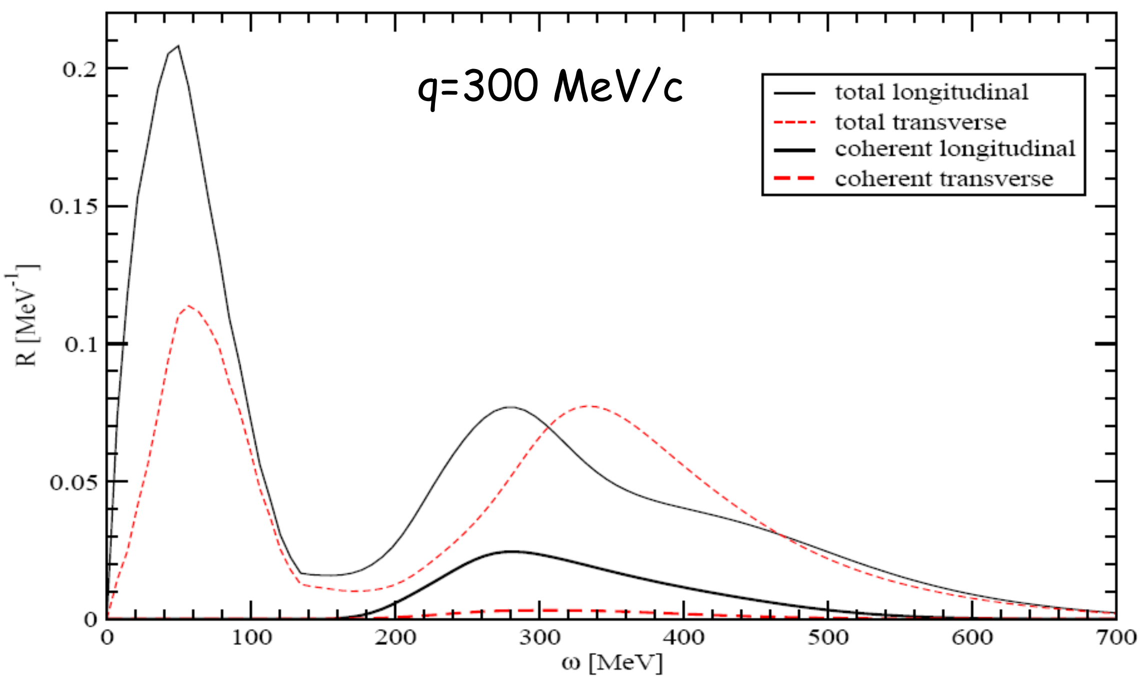

Several partial components treated in self-consistent, coupled and coherent way

From nuclear matter to finite nuclei

Semi-classical approximation

$$\Pi^0(\omega,\boldsymbol{q},\boldsymbol{q}') = \int d\boldsymbol{r}\, e^{-i(\boldsymbol{q}-\boldsymbol{q}')\cdot\boldsymbol{r}}\, \Pi^0\left(\omega, \frac{1}{2}\left(\boldsymbol{q}+\boldsymbol{q}'\right), \boldsymbol{r}\right)$$

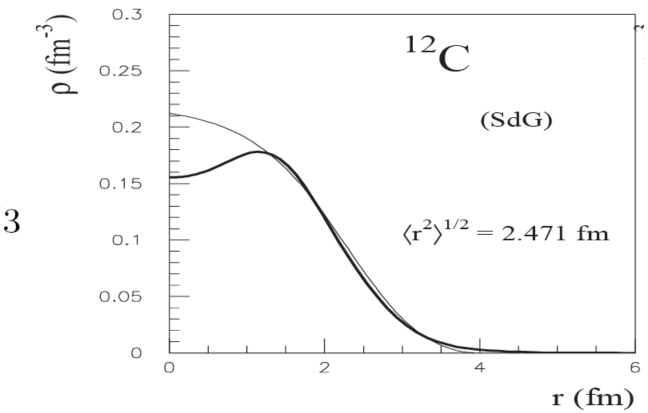

Local density approximation $k_F(r) = (3/2\,\pi^2\,\rho(r))^{1/3}$

$$\Pi^0\left(\omega, \frac{\boldsymbol{q}+\boldsymbol{q}'}{2}, \boldsymbol{r}\right) = \Pi^0_{k_F(r)}\left(\omega, \frac{\boldsymbol{q}+\boldsymbol{q}'}{2}\right)$$

e.g. Lindhard funct. for QE

$$\Pi^{0(L)}_{k_F(R)}(\omega,q,q') \quad = \quad 2\pi \int du\, P_L(u)\Pi^0_{k_F(R)}(\omega, \frac{\boldsymbol{q}+\boldsymbol{q}'}{2})$$

$$\Pi^{0(L)}(\omega,q,q') \quad = \quad 4\pi \sum_{l_1,l_2}(2l_1+1)(2l_2+1)\begin{pmatrix} l_1 & l_2 & L \\ 0 & 0 & 0 \end{pmatrix}^2 \times \int dR R^2\, j_{l_1}(qR)\, j_{l_1}(q'R)\Pi^{0(l_2)}_{k_F(R)}(\omega,q,q')$$

N, Δ

$$R^{0PP'}_{(k)\,xy}(\omega,q) = -\frac{\mathcal{V}}{\pi}\sum_J \frac{2J+1}{4\pi}\,\mathrm{Im}[\Pi^{0(J)}_{(k)xy_{PP'}}(\omega,q,q)]$$

QE,2p-2h,... Longit., Transv., Charge

Details: p-h effective interaction

$$
\begin{aligned}
V_{NN} &= (f' + V_\pi + V_\rho + V_{g'})\, \boldsymbol{\tau}_1.\boldsymbol{\tau}_2 \\
V_{N\Delta} &= (V_\pi + V_\rho + V_{g'})\, \boldsymbol{\tau}_1.\boldsymbol{T}_2^\dagger \\
V_{\Delta N} &= (V_\pi + V_\rho + V_{g'})\, \boldsymbol{T}_1.\boldsymbol{\tau}_2 \\
V_{\Delta\Delta} &= (V_\pi + V_\rho + V_{g'})\, \boldsymbol{T}_1.\boldsymbol{T}_2^\dagger.
\end{aligned}
$$

$f' = 0.6 \quad g'_{NN} = 0.7 \quad g'_{N\Delta} = g'_{\Delta\Delta} = 0.5$

$G^*_M/G_M = G^*_A/G_A = f^*/f = 2.2$

$$
\begin{aligned}
V_\pi &= \left(\frac{g_r}{2M_N}\right)^2 F_\pi^2 \frac{\boldsymbol{q}^2}{\omega^2 - \boldsymbol{q}^2 - m_\pi^2}\, \boldsymbol{\sigma}_1.\widehat{q}\; \boldsymbol{\sigma}_2.\widehat{q} \\
V_\rho &= \left(\frac{g_r}{2M_N}\right)^2 C_\rho F_\rho^2 \frac{\boldsymbol{q}^2}{\omega^2 - \boldsymbol{q}^2 - m_\rho^2}\, \boldsymbol{\sigma}_1 \times \widehat{q}\; \boldsymbol{\sigma}_2 \times \widehat{q} \\
V_{g'} &= \left(\frac{g_r}{2M_N}\right)^2 F_\pi^2\; g'\; \boldsymbol{\sigma}_1.\boldsymbol{\sigma}_2
\end{aligned}
$$

$C_\rho = 1.5 \quad F_\pi(q) = (\Lambda_\pi^2 - m_\pi^2)/(\Lambda_\pi^2 - q^2)$

$\Lambda_\pi = 1\ \text{GeV} \quad \Lambda_\rho = 1.5\ \text{GeV}$

RPA

$$\Pi = \Pi^0 + \Pi^0\, V\, \Pi$$

$$(1 + \Pi\, V)^*\, \Pi = (1 + \Pi\, V)^*\, \Pi^0 + (1 + \Pi\, V)^*\, \Pi^0\, V\, \Pi$$

$$\Pi + \Pi^*\, V^*\, \Pi = (1 + \Pi\, V)^*\, \Pi^0\, (1 + V\, \Pi)$$

$$\mathrm{Im}\,(\Pi) = |\Pi|^2\, \mathrm{Im}\,(V) + |1 + V\,\Pi|^2\, \mathrm{Im}\,(\Pi^0)$$

coherent

exclusive channels:
QE, 2p-2h, Δ→πN …

Relativistic corrections

$$\omega \rightarrow \omega(1 + \frac{\omega}{2M_N})$$

$$\Pi \longrightarrow (1 + \frac{\omega}{M_N})\,\Pi$$

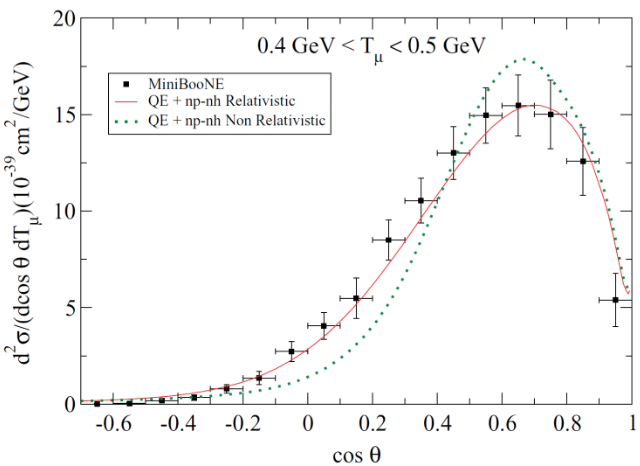

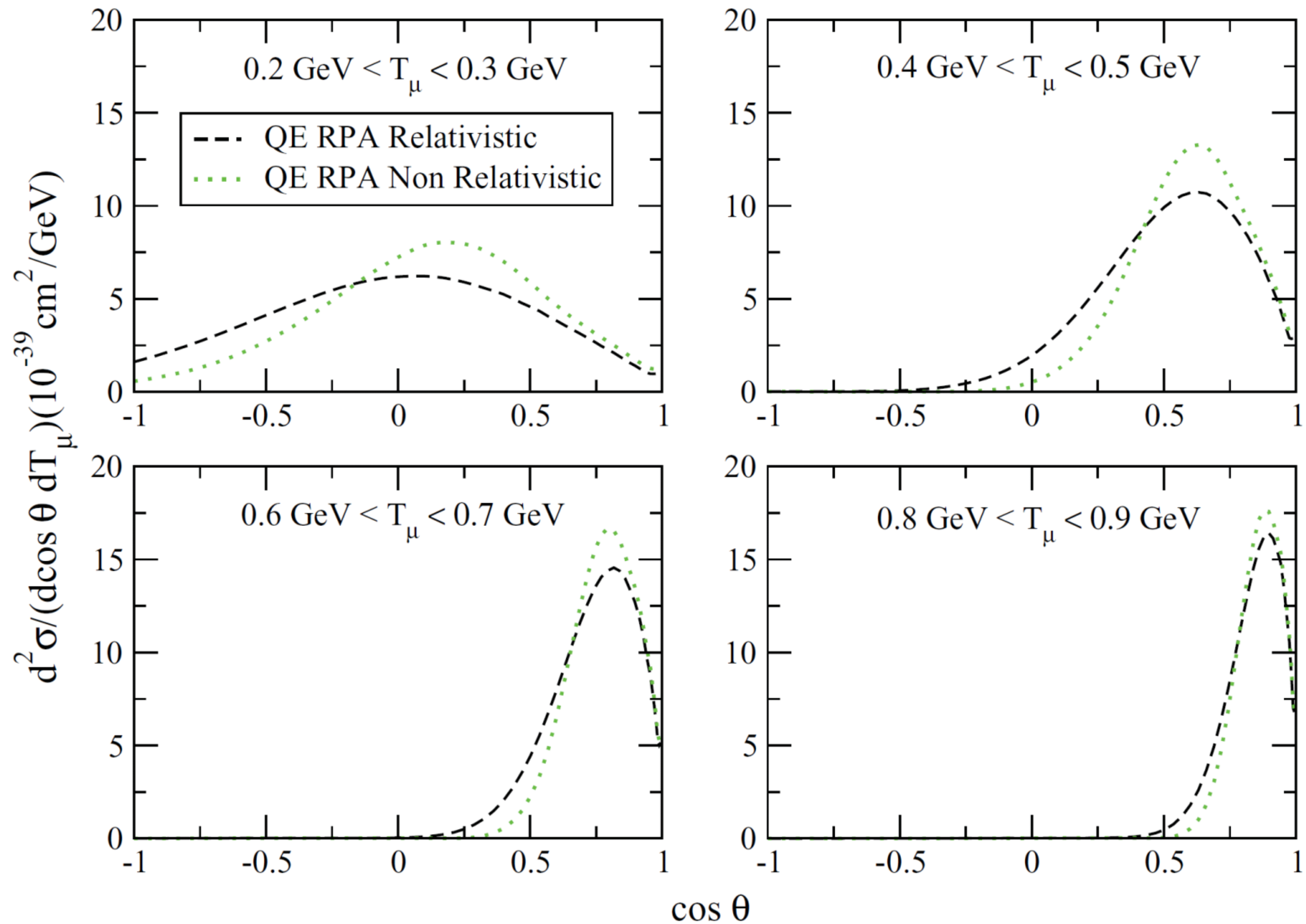

NN correlations and NΔ interference contributions to 2p-2h

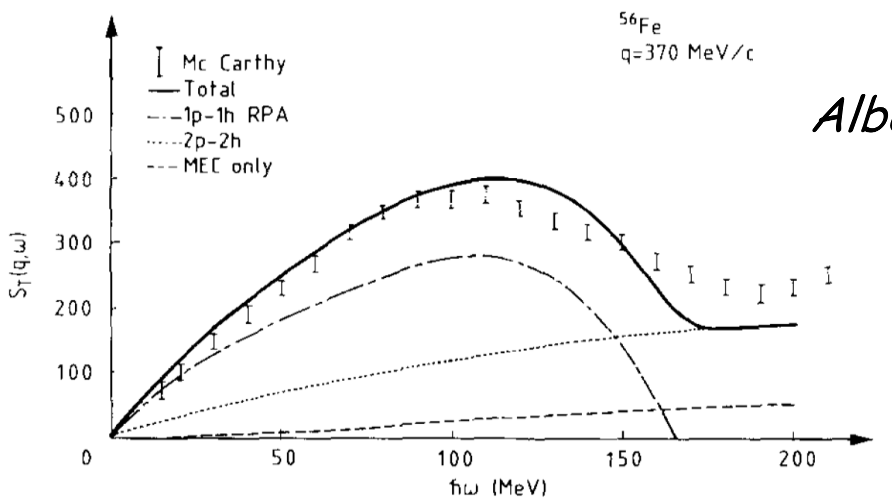

Starting point: a microscopic evaluation of R_T

Alberico, Ericson, Molinari, Ann. Phys. 154, 356 (1984)

Transverse magnetic response of (e,e')

for some values of q and ω,but:

^{56}Fe, few q and ω, too large Im C_0

Our work

•Parameterization of the responses in terms of $x = \frac{q^2-\omega^2}{2M_N\omega}$ $\longrightarrow$ Extrapolation to cover V region

•Global reduction ≈ 0.5 to reproduce the absorptive p-wave π-A optical potential

A comparison between our parameterization of 2p-2h (PRC 2009) and the one of the PRC (2010) paper of Amaro et al. on electron scattering

Alberico et al. Ann. Phys. 154, 356 (1984)

Amaro et al. PRC 82 044601 (2010)
(not yet inserted in neutrino calculations)

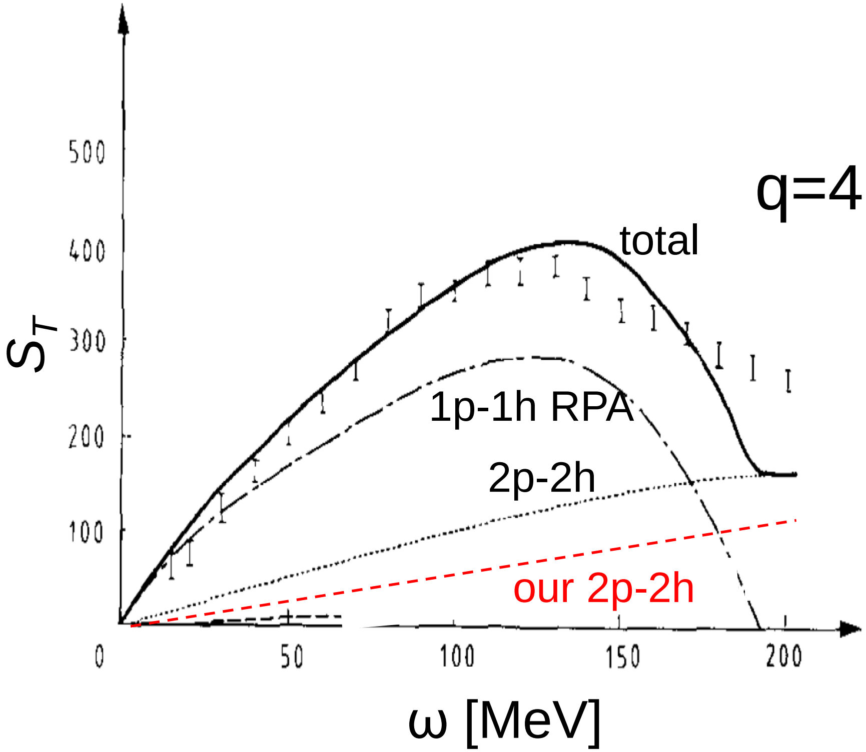

^{56}Fe
q=410 MeV/c

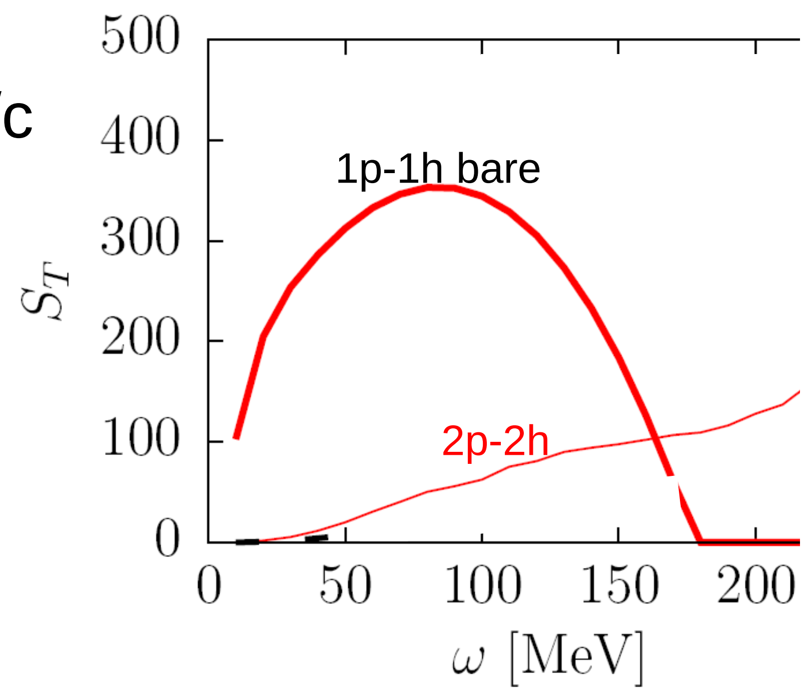

With the reduction factor that we had applied in order to reproduce ImC_0, our parameterization is quite close to the results of Amaro et al.

$\Delta\Delta$ contributions to np-nh in our model

- Reducible to a modification of the Delta width in the medium

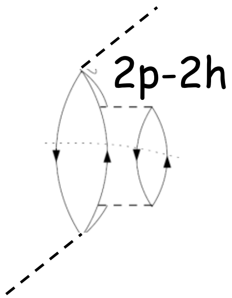

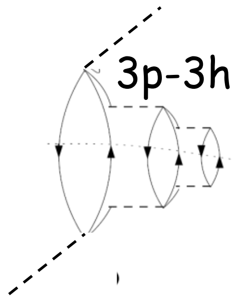

E. Oset and L. L. Salcedo, Nucl. Phys. A 468, 631 (1987):

$$\widetilde{\Gamma_\Delta} = \Gamma_\Delta \; F_P - 2\mathrm{Im}(\Sigma_\Delta)$$

$$\mathrm{Im}(\Sigma_\Delta(\omega)) = -\left[C_Q(\frac{\rho}{\rho_0})^\alpha + C_{2p2h}(\frac{\rho}{\rho_0})^\beta + C_{3p3h}(\frac{\rho}{\rho_0})^\gamma\right]$$

Nieves et al. in PRC 83 (2011) and in 1106.5374 use the same model for these contributions

- Not reducible to a modification of the Delta width

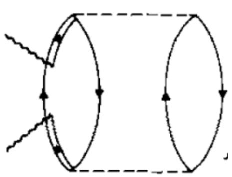

Microscopic calculation of π absorption at threshold: **$\omega = m_\pi$**

Shimizu, Faessler, Nucl. Phys. A 333,495 (1980)

Extrapolation to other energies

$$Im(\Pi^0_{\Delta\Delta}) \quad = \quad -4\pi\rho^2 \frac{(2M_N + m_\pi)^2}{(2M_N+\omega)^2} C_3 \, \Phi_3(\omega) \; \left[\frac{1}{(\omega + M_\Delta - M_N)^2}\right]$$

Further considerations on 2p-2h

e.g. NN correlation

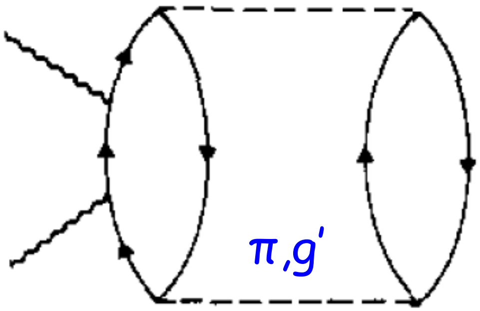

q =410 MeV/c

	central	tensor
$\hbar\omega$	βA_l^C	βA_1^T
50	11.3	20.3
100	12.5	31.8
150	23.6	47.8
200	20.9	53.1
250	17.3	51.1
300	10.9	39.9

Alberico et al.
Ann. Phys. '84

Tensor correlations are dominant in the NN correlation term but 2p-2h contributions involving Δ excitations are also very important. Tensor correlations alone are insufficient to account the overall 2p-2h effect.

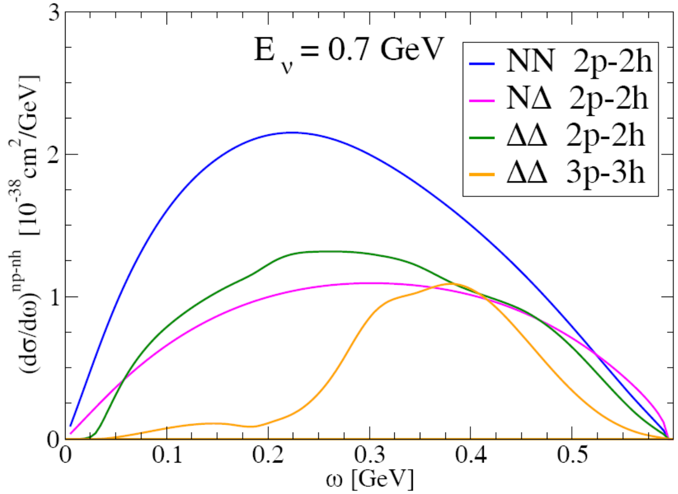

Comparison of the two 2p-2h parameterizations in ν-^{12}C scattering

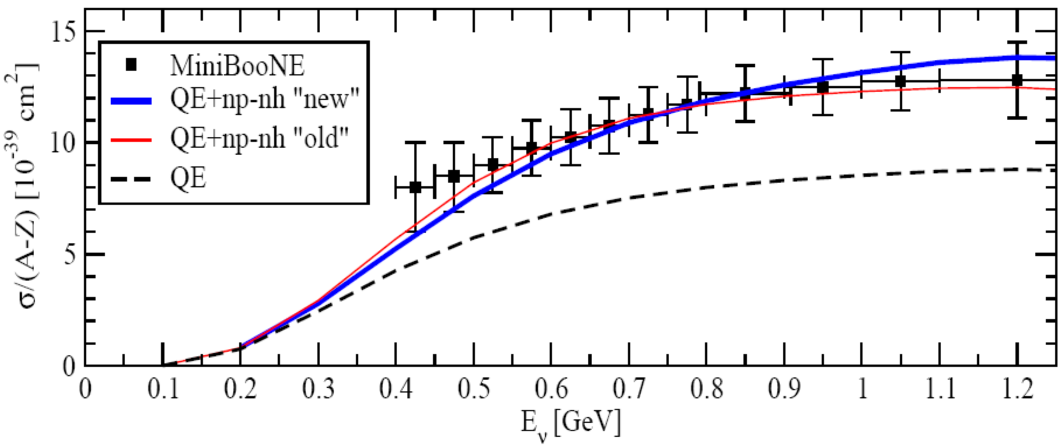

In the paper
Martini, Ericson, Chanfray, Marteau, PRC 80 (2009)
we considered 2 different parameterizations of 2p-2h

Red "Old": from Delorme et al.
(2p-2h π absorption)

the one used in:
Marteau, Delorme, Ericson, NIM A451 (2000) 76-80

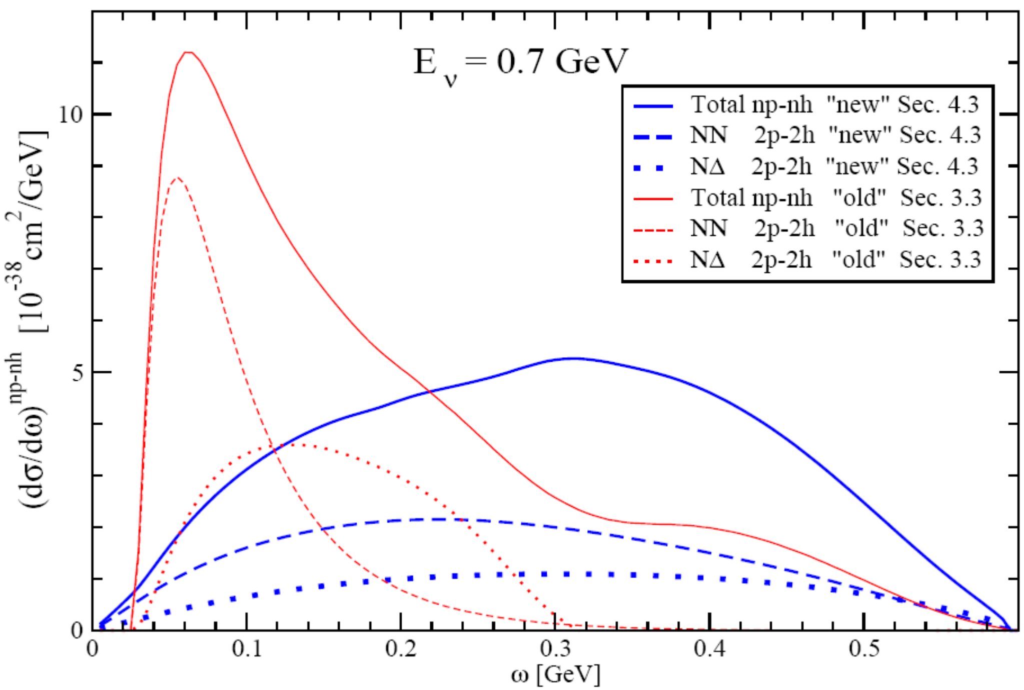

Blue "New": from Alberico et al.
(R_T of (e,e') ^{56}Fe rescaled)

in the next papers we have only considered the "New" parameterization

Our results vs experiment for other q values

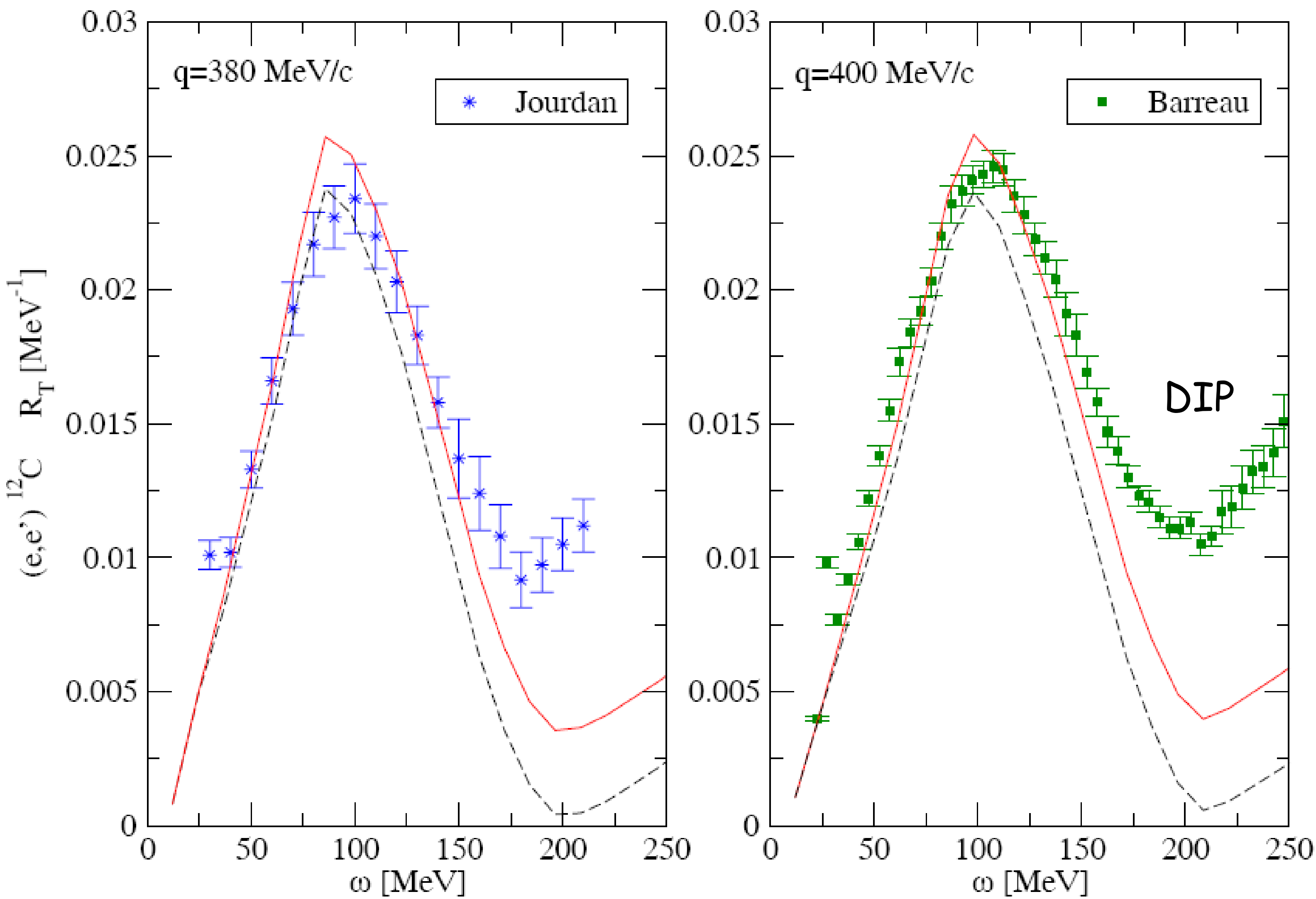

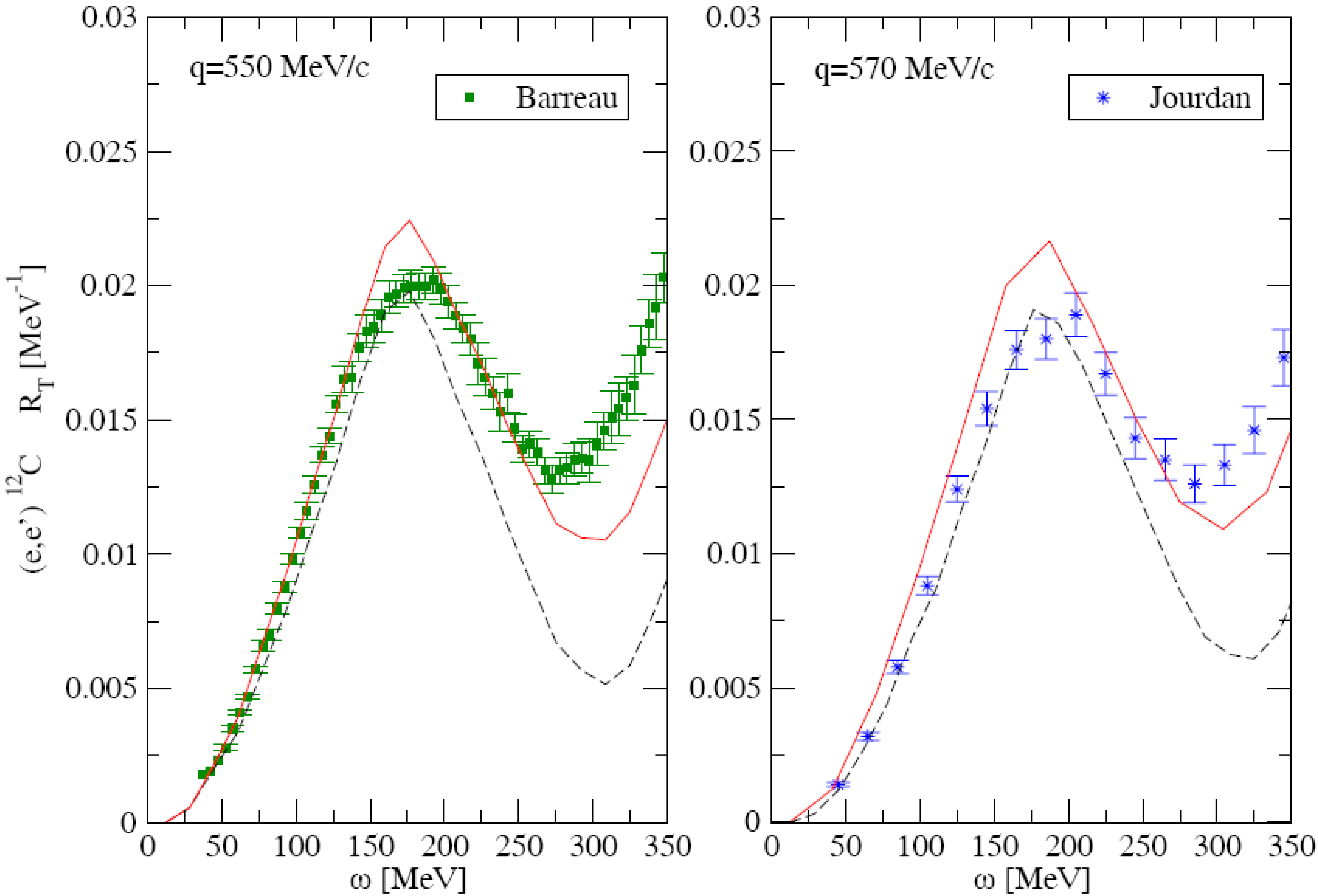

q=550 MeV/c
Barreau
q=570 MeV/c
Jourdan
(e,e') ^{12}C R$_T$ [MeV^{-1}]
ω [MeV]
ω [MeV]
0.03
0.025
0.02
0.015
0.01
0.005
0
0
50
100
150
200
250
300
350

Scaling approach in electron scattering

$$f_{\mathrm{L}}(\Psi) = k_{\mathrm{F}} \frac{q^2 - \omega^2}{q\, m} \frac{R_{\mathrm{L}}(\omega, q)}{Z\left(G_{\mathrm{E}}^{p}\right)^2 + N\left(G_{\mathrm{E}}^{n}\right)^2}$$

$$f_{\mathrm{T}}(\Psi) = 2\, k_{\mathrm{F}} \frac{q\, m}{q^2 - \omega^2} \frac{R_{\mathrm{T}}(\omega, q)}{Z\left(G_{\mathrm{M}}^{p}\right)^2 + N\left(G_{\mathrm{M}}^{n}\right)^2}$$

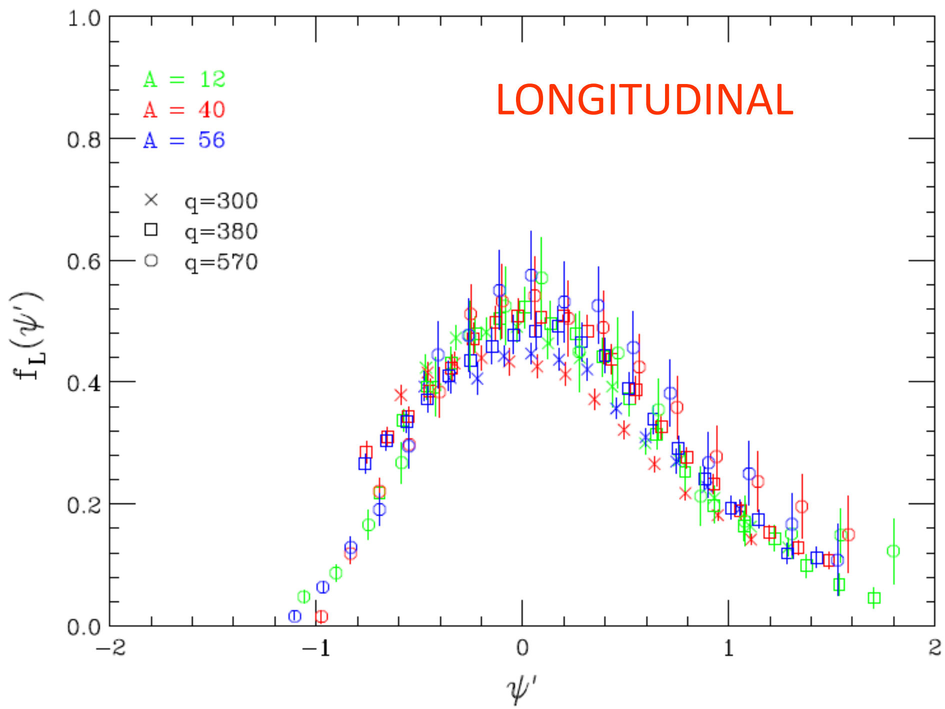

Donnelly et al. PRC 60 '99,…

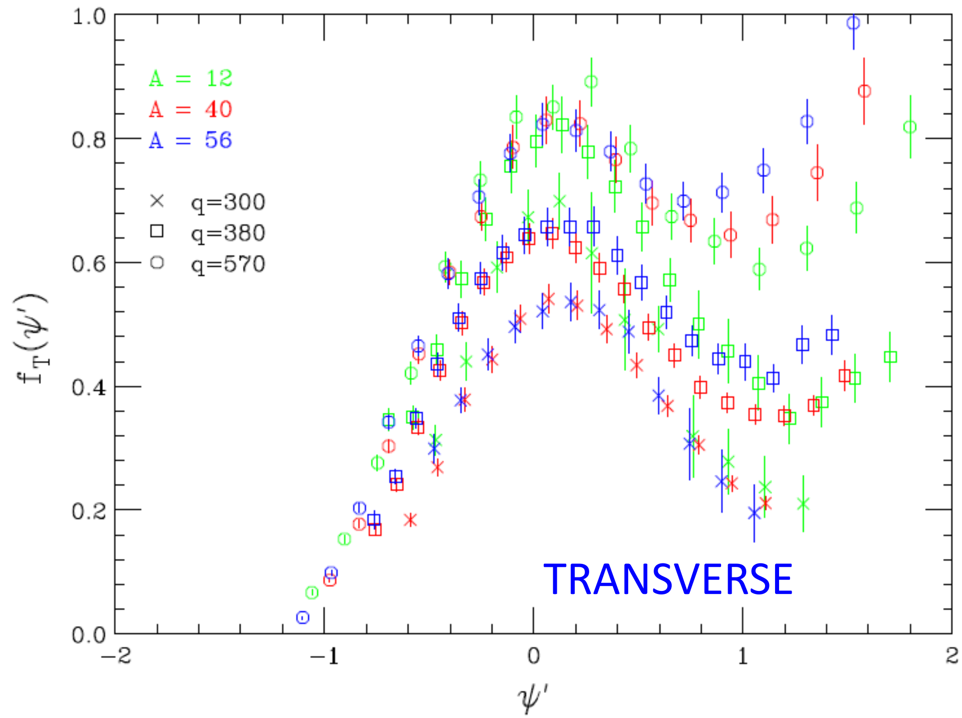

Superscaling: scaling with A and q

No superscaling: scaling with A, not with q

NB: the longitudinal superscaling function in used to study ν scattering in SuSA approach

Excess in the transverse channel likely due to 2-body currents (MEC and correlations)

A.Bodek et al. Eur.Phys.J. C71 (2011) :

parametrization of the enhancement in T channel in terms of correction to $G_M(Q^2)$

Total CCQE and comparison with flux unfolded MB

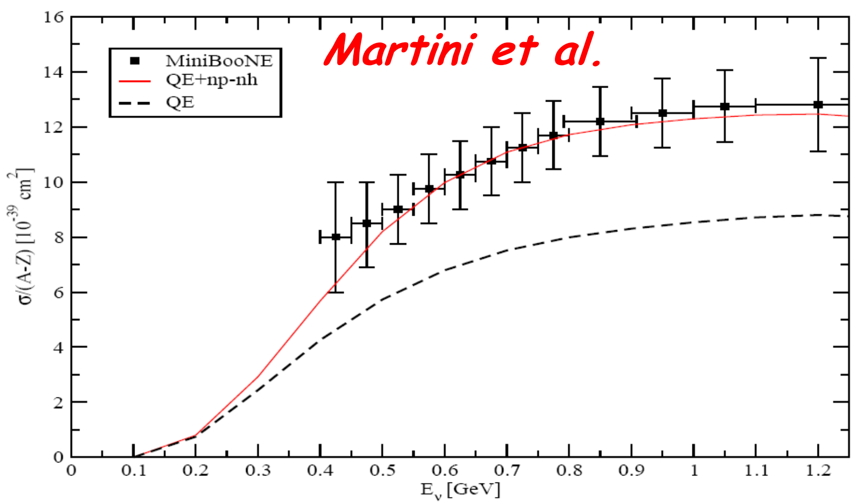

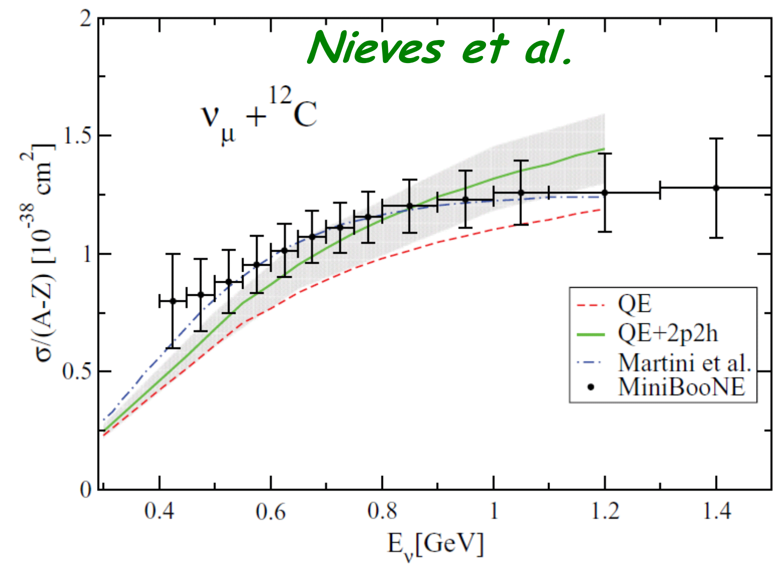

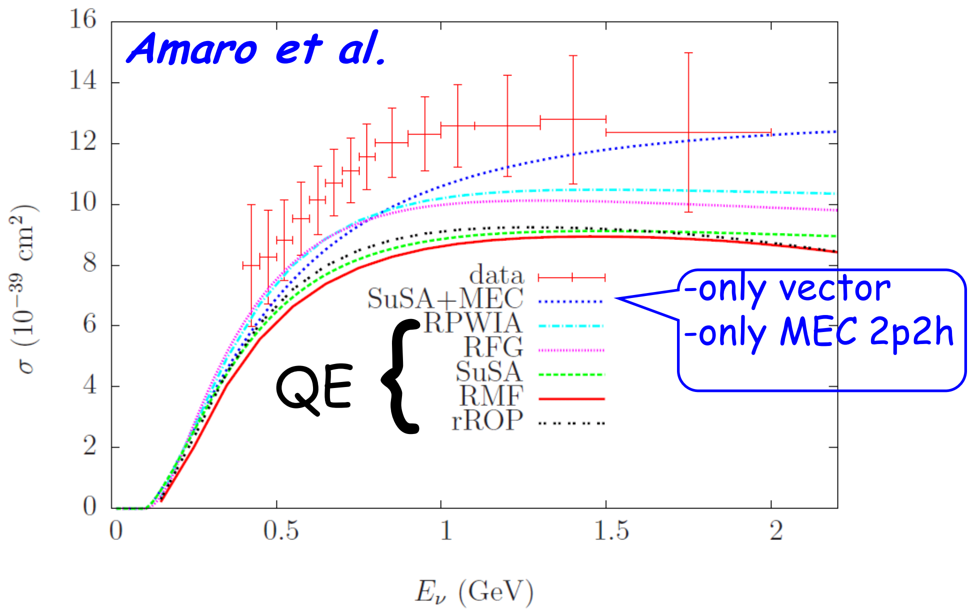

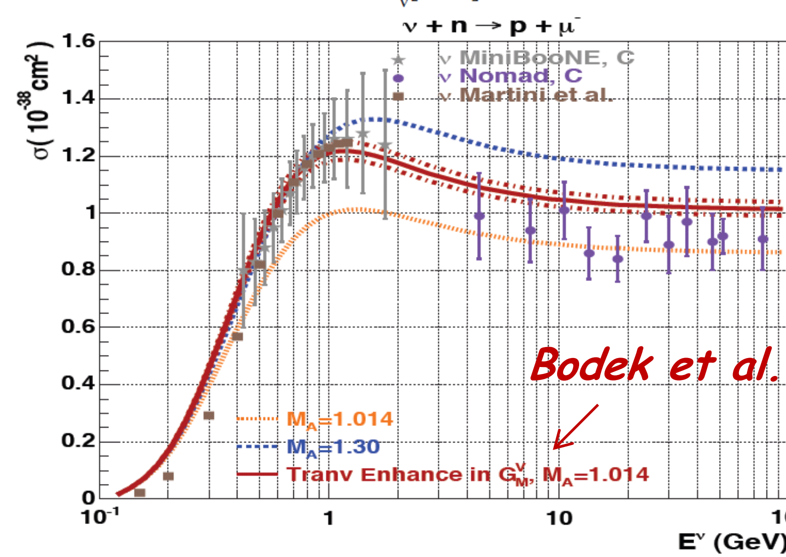

N.B. The experimental unfolding is model dependent

A. Bodek, H.S. Budd, M.E. Christy, arXiv: 1106.0340 (EPJC 2011)

$$G_{Mp}^{nuclear}(Q^2) = G_{Mp}(Q^2) \times \sqrt{1 + AQ^2 e^{-Q^2/B}}$$

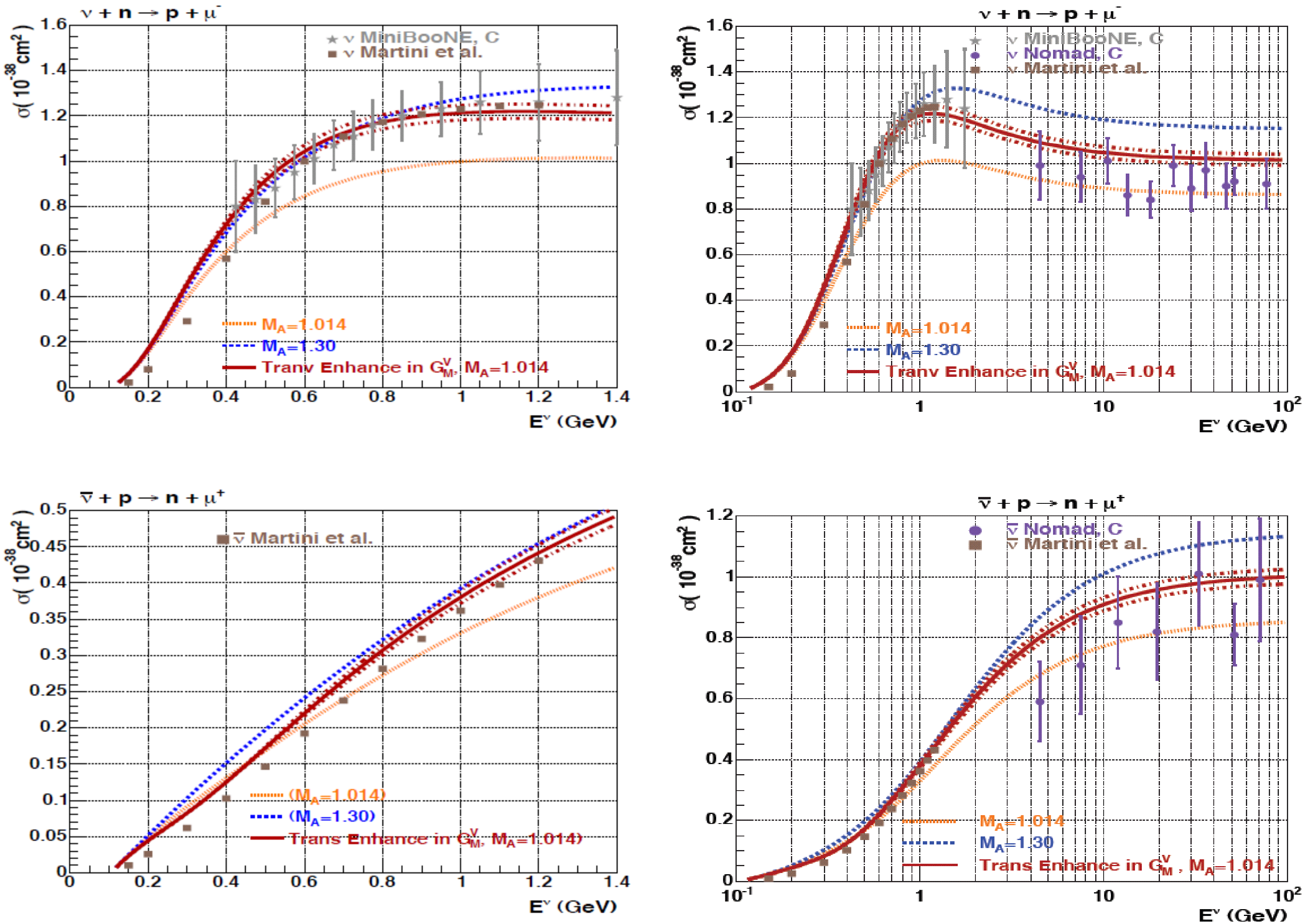

Various response contributions to the ν and $\overline{\nu}$ CCQE

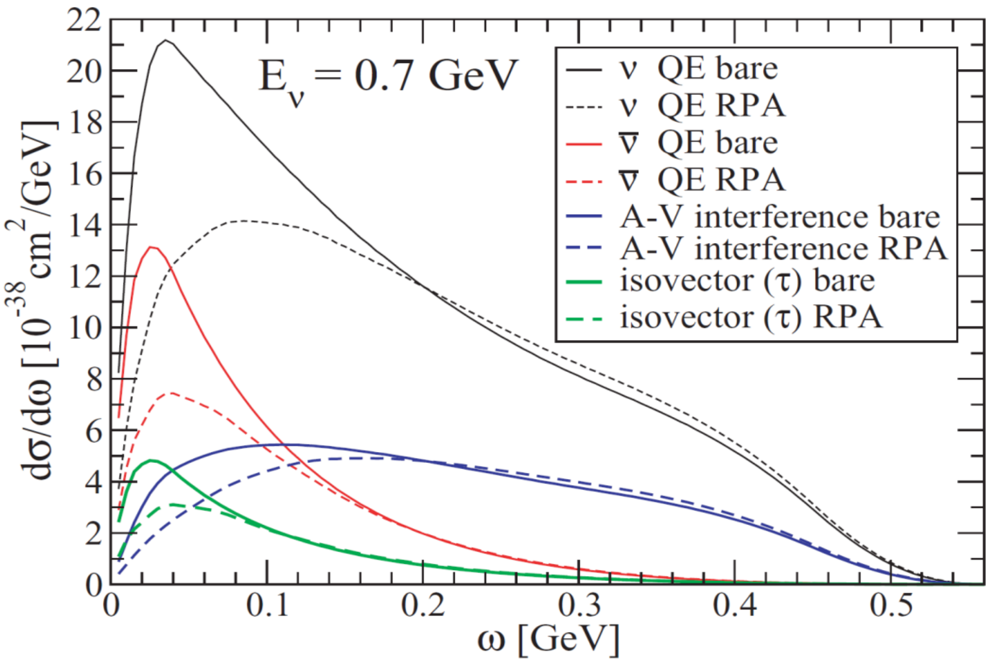

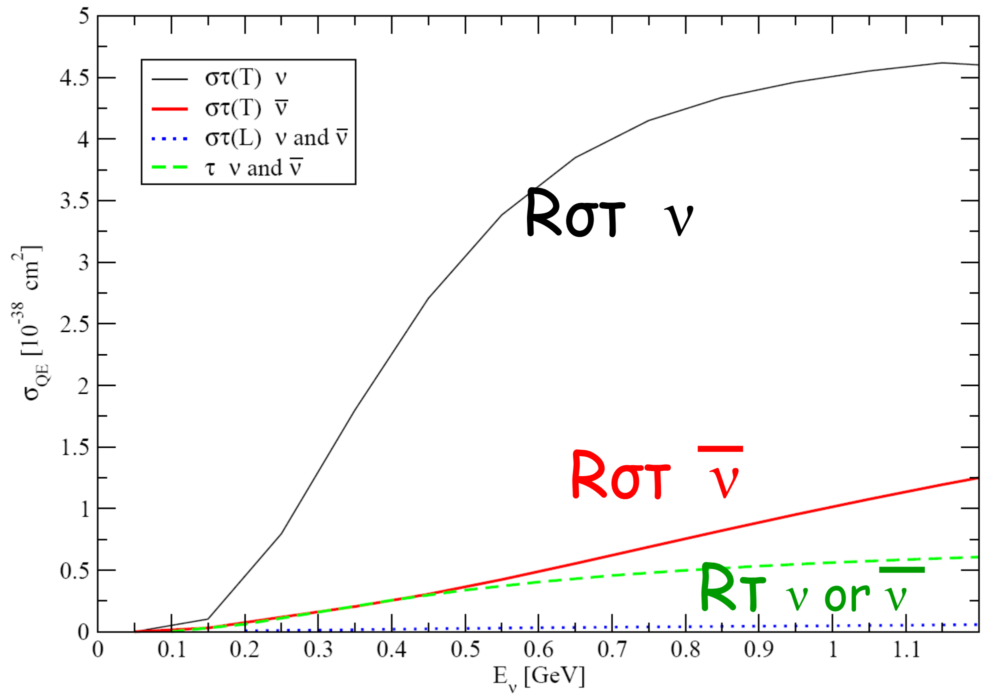

The role of interference term (in $G_A G_M$) is crucial:
it enhances the contribution of Rστ(T) for neutrinos.
For antineutrinos instead the destructive interference partially suppresses this contribution leaving a larger role for isovector Rτ which is insensitive to 2p-2h.

Hence the **relative** role of 2p-2h should be smaller for antineutrinos

M. Martini, M. Ericson, G. Chanfray, J. Marteau, Phys. Rev. C 81 045502 (2010)

Comparison of Models of Neutrino-Nucleus Interactions

S. Boyd*, S. Dytman†, E. Hernández**, J. Sobczyk‡ and R. Tacik§

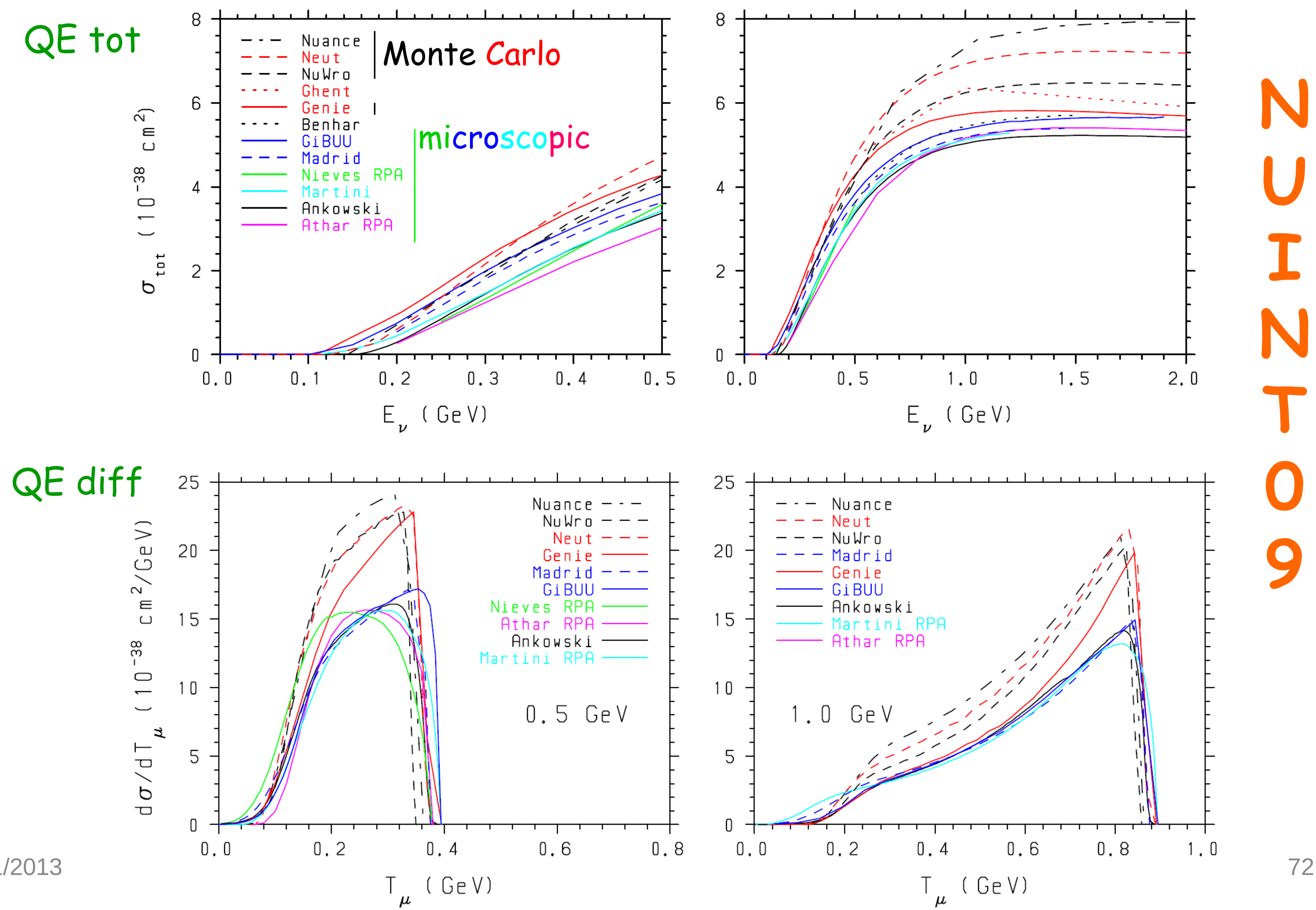

NUINT09

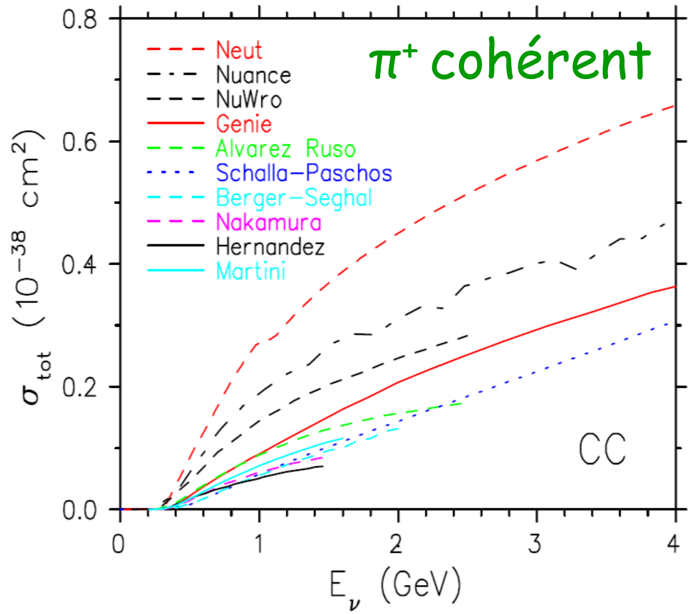

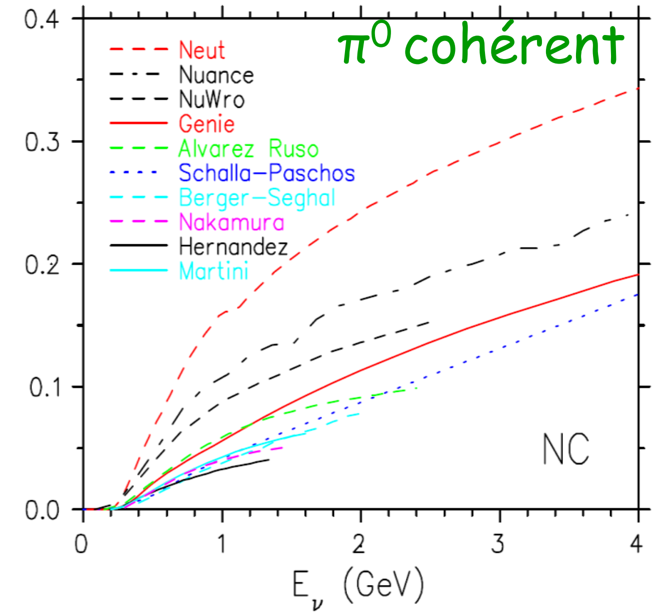

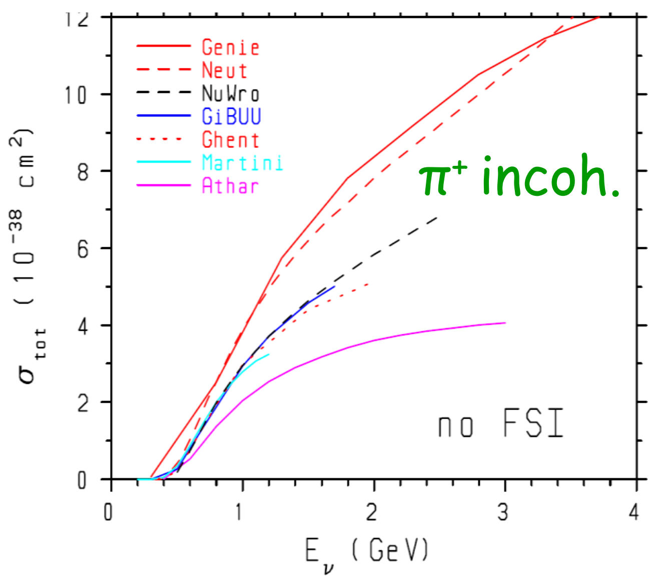

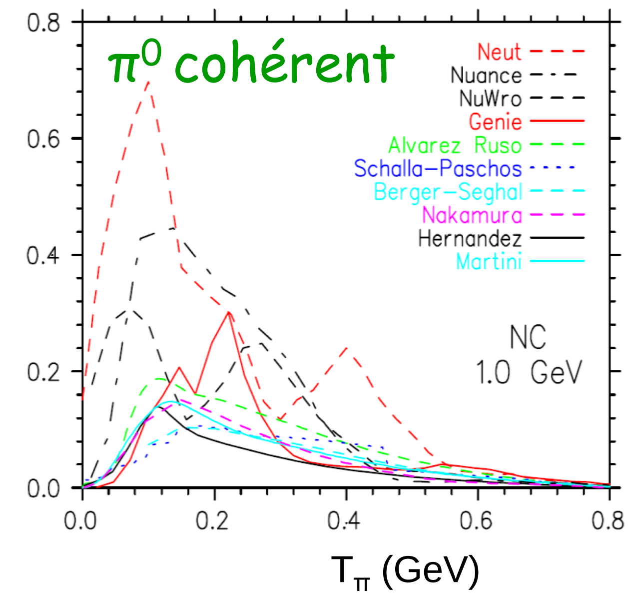

Monte Carlo

QE: Fermi Gas

π prod:Rein-Sehgal

- Neut: SuperKamiokande, K2K, T2K, SciBooNE
- Nuance: SuperKamiokande, MINOS, MiniBooNE
- Genie: T2K, MINOS, Minerva, NOvA, ArgoNEUT
- NuWro: Wroclaw theo. group

MC larger than microscopic models

Experience from electron quasielastic scattering on carbon suggests that multibody final states are dominated by initial-state np pairs [24,43,44]. This could lead to an expectation of final state pp pairs in neutrino quasielastic scattering and nn pairs in the analogous antineutrino channel. The vertex energy measurement, shown in Fig. 5, is sensitive to these effects. These data prefer the addition of a final state proton with less than 225 MeV kinetic energy in $25 \pm 1(\text{stat}) \pm 9(\text{syst})\%$ of the events. The corresponding result in the antineutrino mode [35], in contrast, prefers the removal of a final state proton in $10 \pm 1(\text{stat}) \pm 7(\text{syst})\%$ of the events. The systematic uncertainties for the two samples are positively correlated with a correlation coefficient of +0.7, implying that the observed difference is unlikely to be due to one of the systematic uncertainties considered. The systematic uncertainties are primarily from the detector response to protons and uncertainties in reactions in the target nucleus that absorb or create final state protons. Independent of models, elastic and inelastic nucleon reactions which might produce additional final state protons in the neutrino data should have analogous reactions in the antineutrino data, and the difference in the two results makes it unlikely that any modification of final state nucleon interactions can explain the discrepancy. Pion final state interactions (FSI), especially absorption, would produce more protons in the neutrino reaction and neutrons in the antineutrino reaction, but the associated uncertainties are included in the total systematic errors. The observed patterns in the neutrino and antineutrino channels, combined with the observation that electron quasielastic scattering with multinucleon final states in carbon produces primarily final state np pairs, suggests that an initial state of strongly correlated np pairs also may participate in the neutrino quasielastic interaction.

ν *PRL 111 022502 (2013)*

MINERνA

PRL 111 022501 (2013) $\bar{\nu}$

Transverse enhancement is included as a parametrization affecting the Q^2_{QE} dependence in our analysis but is thought to be due to underlying multinucleon dynamical processes [57–63]. Such processes could have an effect on the vertex and recoil energy distributions that we do not simulate. Motivated by these concerns and by discrepancies observed in our analysis of ν_μ quasielastic scattering [64], we have also studied the vertex energy to test the simulation of the number of low energy charged particles emitted in quasielastic interactions. Figure 5 shows this energy compared to the simulation. A fit which modifies the distributions to incorporate energy due to additional protons is not able to achieve better agreement. This might be explained if the dominant multibody process is $\bar{\nu}_\mu(np) \rightarrow \mu^+ nn$ [57,60,65] since MINERvA is not very sensitive to low energy neutrons. A similar analysis on neutrino mode data is consistent with additional protons in the final state [64].

ν *PRL 111 022502 (2013)*

MINERνA

PRL 111 022501 (2013) $\bar{\nu}$

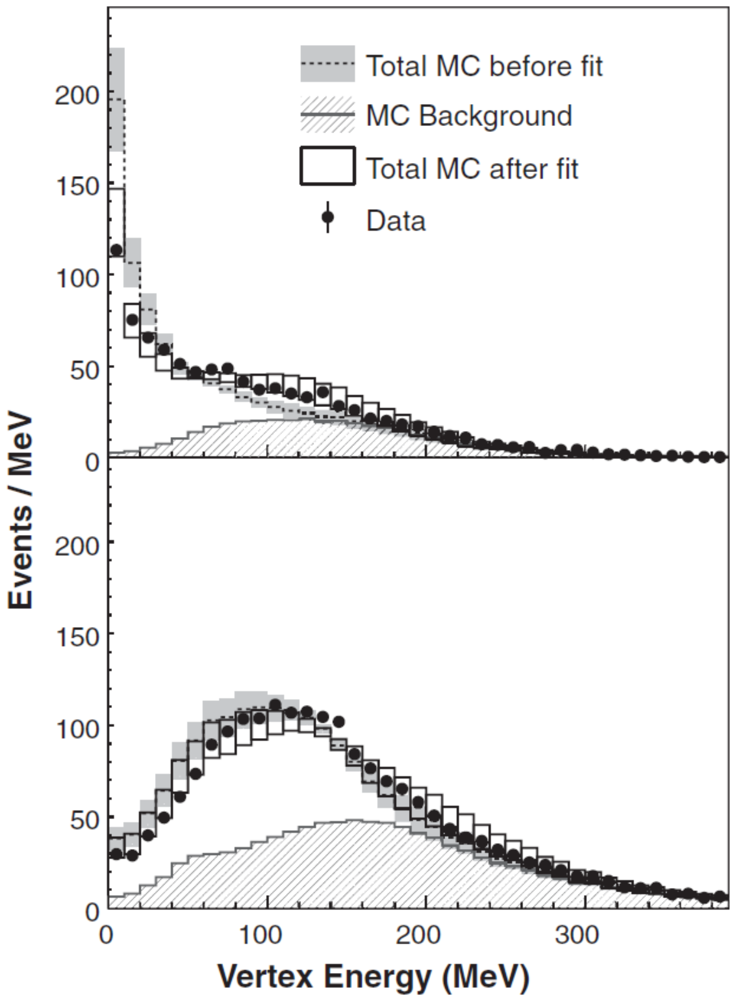

FIG. 5. Reconstructed vertex energy of events passing the selection criteria in the data (points with statistical errors) compared to the GENIE RFG model (shown with systematic errors) for $Q^2_{\mathrm{QE}} < 0.2\ \mathrm{GeV}^2/c^2$ (top) and for $Q^2_{\mathrm{QE}} > 0.2\ \mathrm{GeV}^2/c^2$ (bottom).

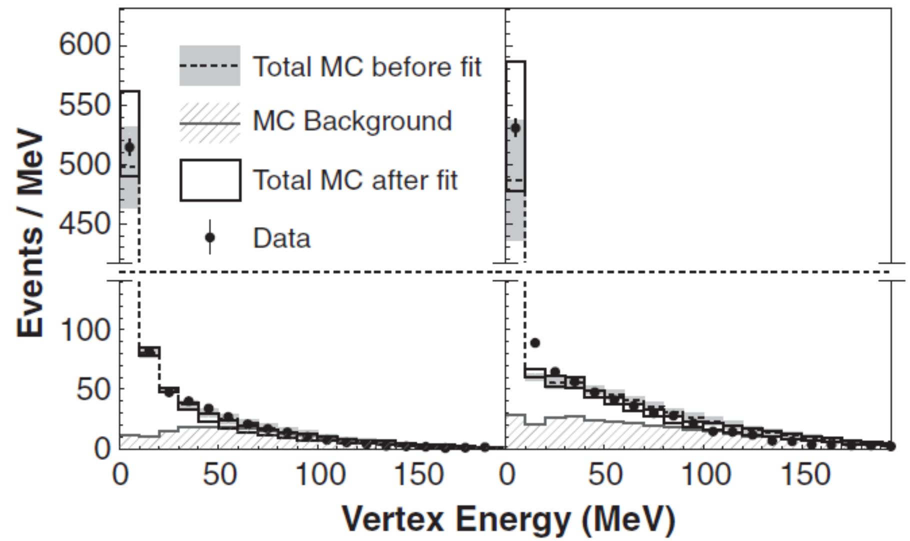

FIG. 5. Reconstructed vertex energy of events passing the selection criteria compared to the GENIE RFG model for $Q^2_{\mathrm{QE}} < 0.2\ \mathrm{GeV}^2/c^2$ (left) and for $Q^2_{\mathrm{QE}} > 0.2\ \mathrm{GeV}^2/c^2$ (right).

Comparison with ν data
pion production

Testing our model: pion-nucleus cross-section

$$\sigma^{tot}(\omega) = \left(\frac{g_r}{2M_N}\right)^2 \pi q_\pi \, R_L(\omega, q_\pi)$$

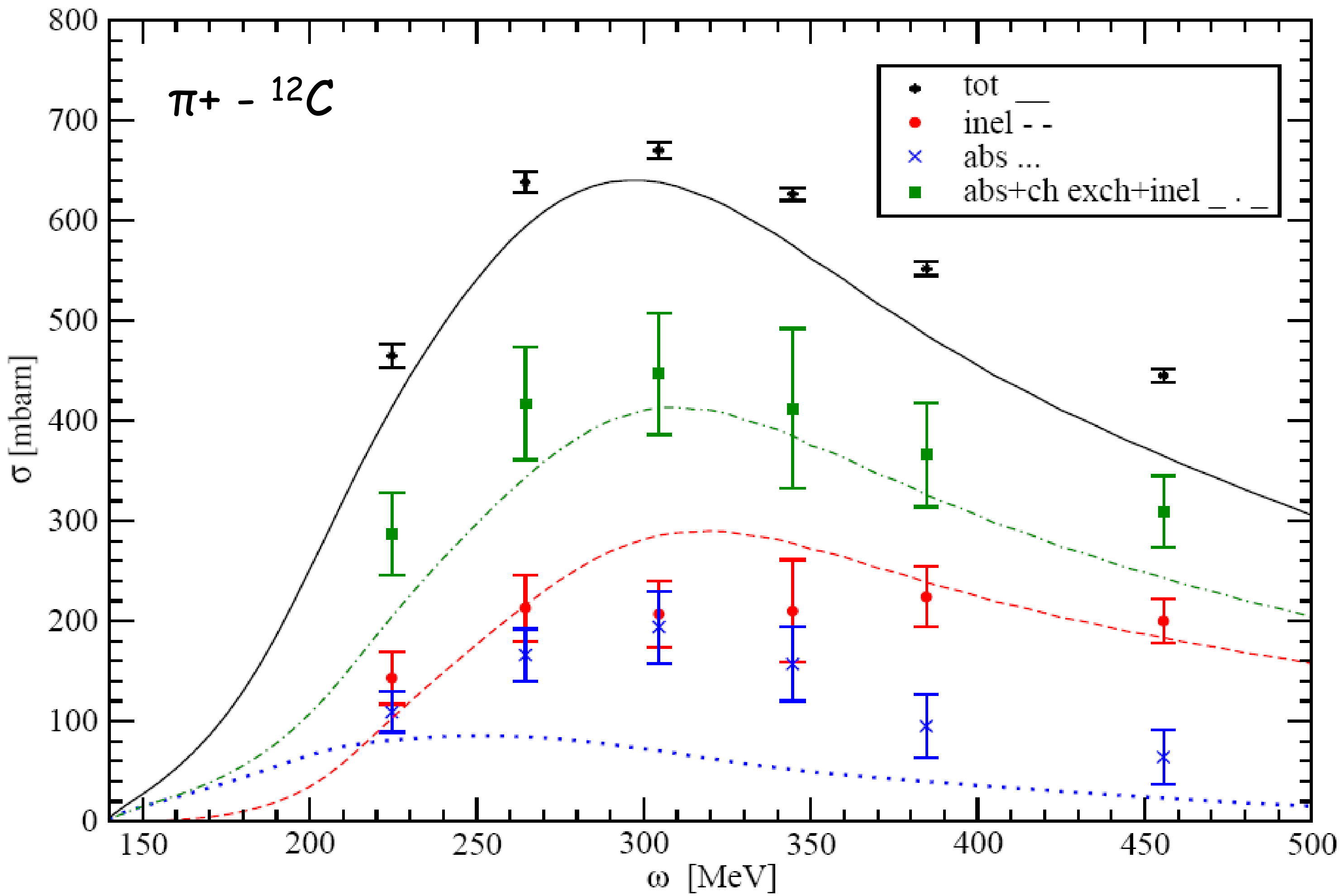

Overestimation of inelastic ch. in the peak region

Underestimation of absorption

Absence of π FSI

Coherent channel

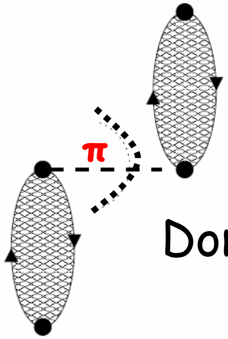

Dominated by $R_{\sigma\tau}$ longitudinal

Reshaped by collective effects

Softening of the responses

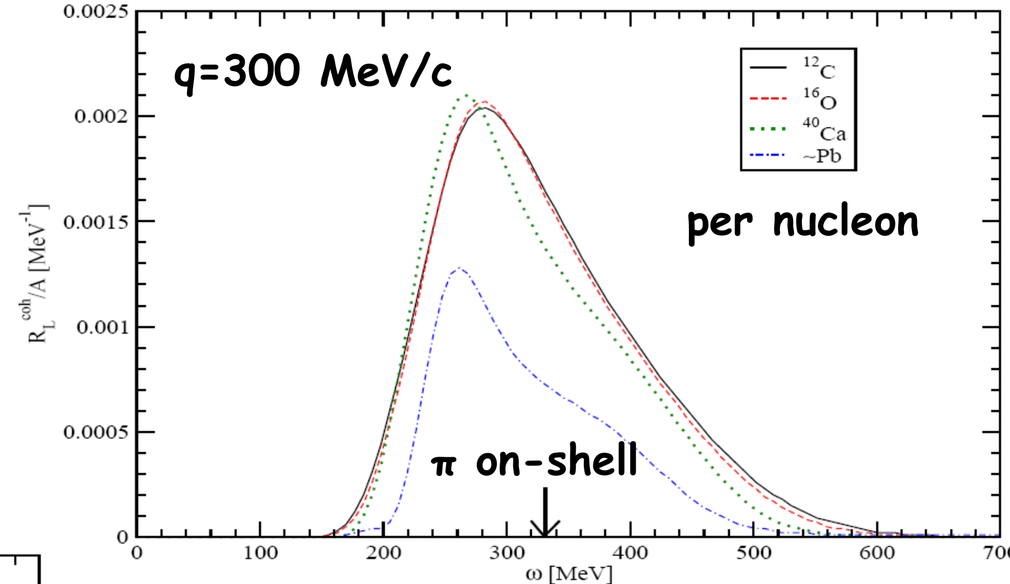

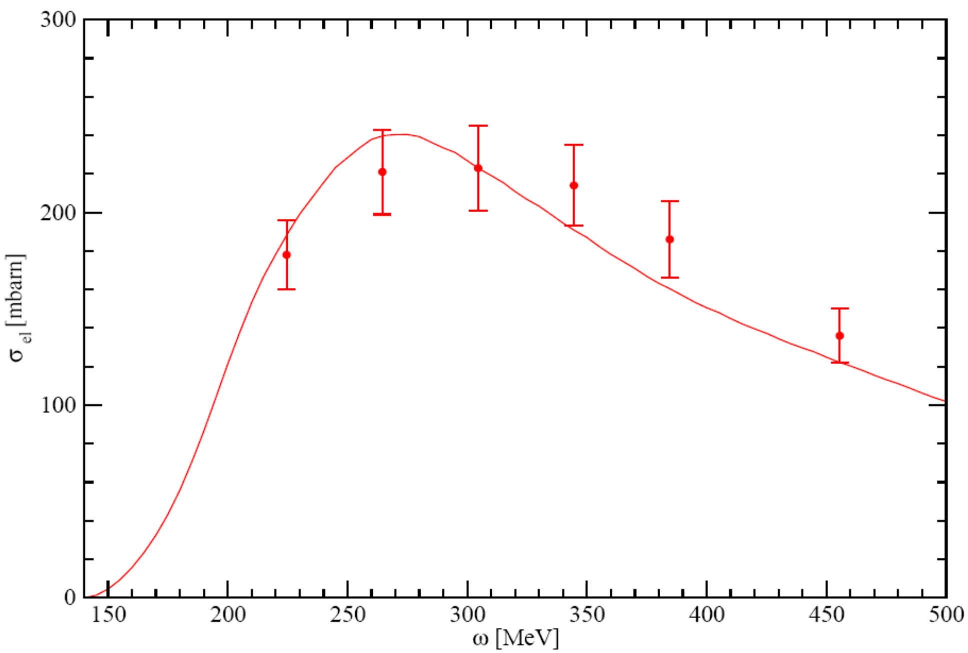

Test: π - ^{12}C elastic cross-section

$$\sigma^{elas}(\omega) = \left(\frac{g_r}{2M_N}\right)^2 \pi q_\pi \, R_L^{coh}(\omega, q_\pi)$$

$$q_\pi^2 = \omega^2 - m_\pi^2$$

Charged current total $1\pi^+$ production over QE ratio

MiniBooNE, Phys. Rev. Lett. 103, 081801 (2009)

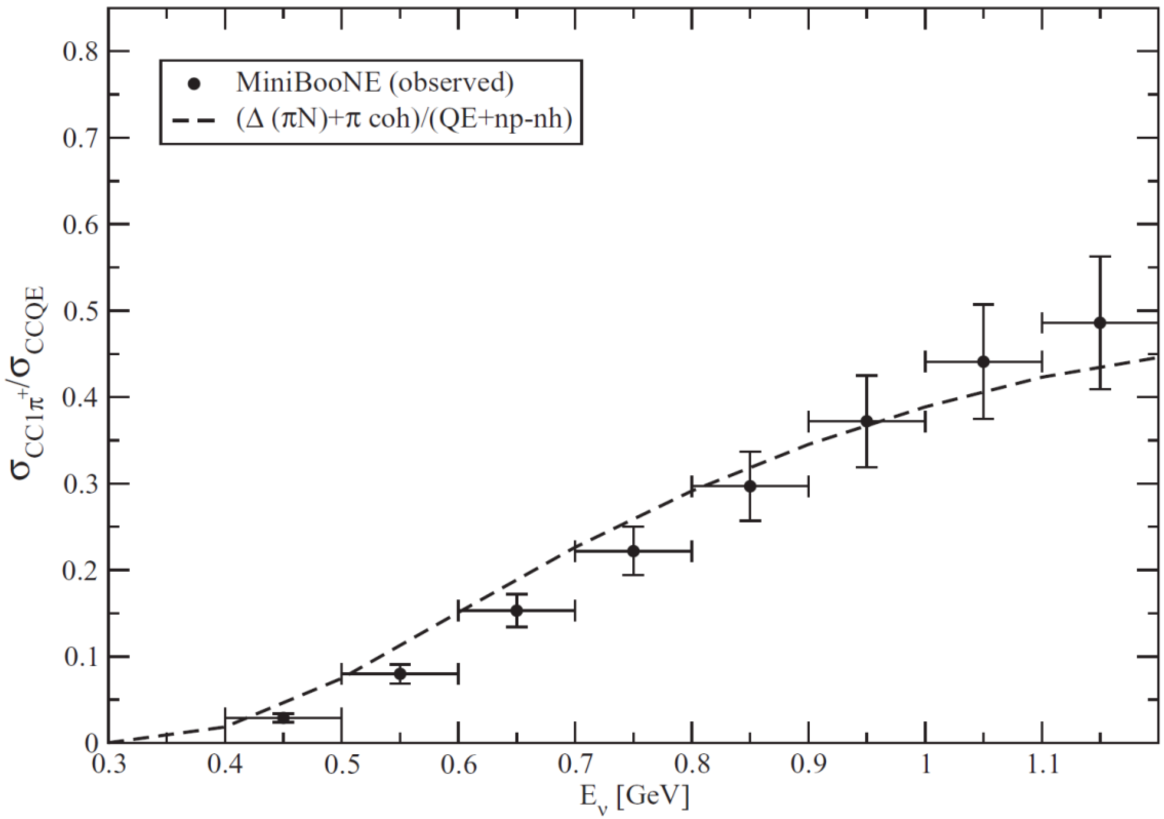

In our model π FSI are not included;
a reduction of ~ 15 % is expected

NC π^0 production cross sections

Total cross section	MiniBooNE PRD 81, 013005 2010 σ [10^-40 cm^2/nucleon]	Our model σ [10^-40 cm^2/nucleon]
ν @ 808 MeV	4.76 ± 0.05 st ± 0.76 sy	5.42
$\bar{\nu}$ @ 664 MeV	1.48 ± 0.05 st ± 0.23 sy	1.37

	Incoherent exclusive NC $1\pi^0$ corrected for FSI effects	Our model
ν @ 808 MeV	5.71 ± 0.08 st ± 1.45 sy	5.14
$\bar{\nu}$ @ 664 MeV	1.28 ± 0.07 st ± 0.35 sy	1.17

π0 total NC/ σ total CC	SciBooNE PRD 81 033004 '10	Our model
ν @ 1.1 GeV	(7.7 ± 0.5 st ± 0.5 sy) 10^{-2}	7.9 10^{-2} (without np-nh: 9.8)

Coherent pion production

Ratio of σ	Experiment	Our model
π+ coherent CC/ σ total CC	SciBooNE u.l.@ E_ν 1.1 GeV $0.67\ 10^{-2}$ PRD 78 112004 '08	$0.71\ 10^{-2}$ (without np-nh: 0.89)
π0 coherent NC/ π0 total NC	MiniBooNE $(19.5\pm1.1\pm2.5)\ 10^{-2}$ Phys. Lett. B 664,41 '08	$6\ 10^{-2}$
π0 coherent NC/ σ total CC	SciBooNE $(0.7\pm0.4)\ 10^{-2}$ PRD 81 033004 '10	$0.4\ 10^{-2}$ (without np-nh: 0.5)
π+ coherent CC/ π0 coherent NC	SciBooNE $0.14\ ^{+0.30}_{-0.28}$ PRD 81 111102 '10	1.5

coherent puzzle

Coherent puzzle

Boyd S. et al. AIP Conf. Proc. 1189 60 (2009)

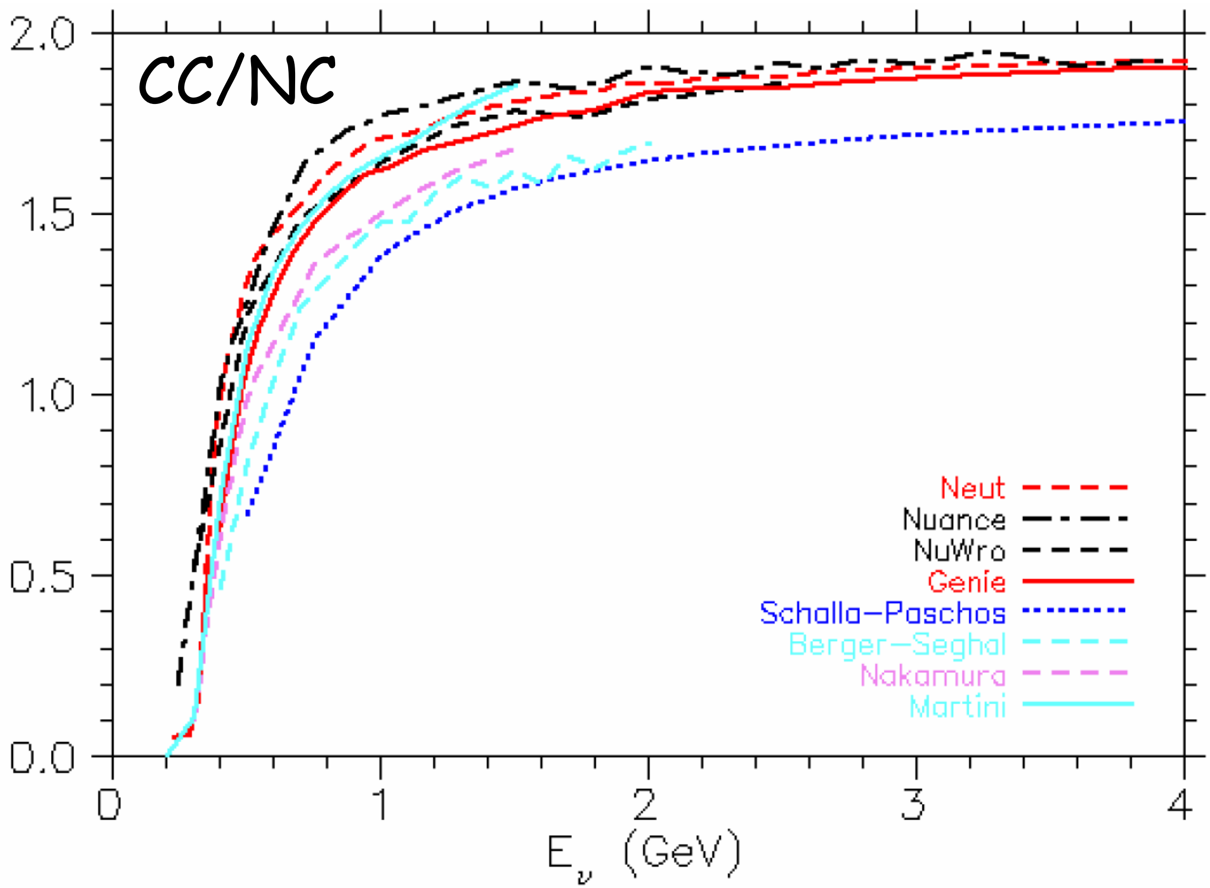

SciBooNE:

$$\frac{\pi\text{+ coh. CC}}{\pi 0 \text{ coh. NC}} = 0.14^{+0.30}_{-0.28}$$

Theoretical models:

$$\frac{\pi\text{+ coh. CC}}{\pi 0 \text{ coh. NC}} = 1.5 \sim 2 \;!!$$

ν_μ induced coherent pion production off ^{12}C

Differential cross section

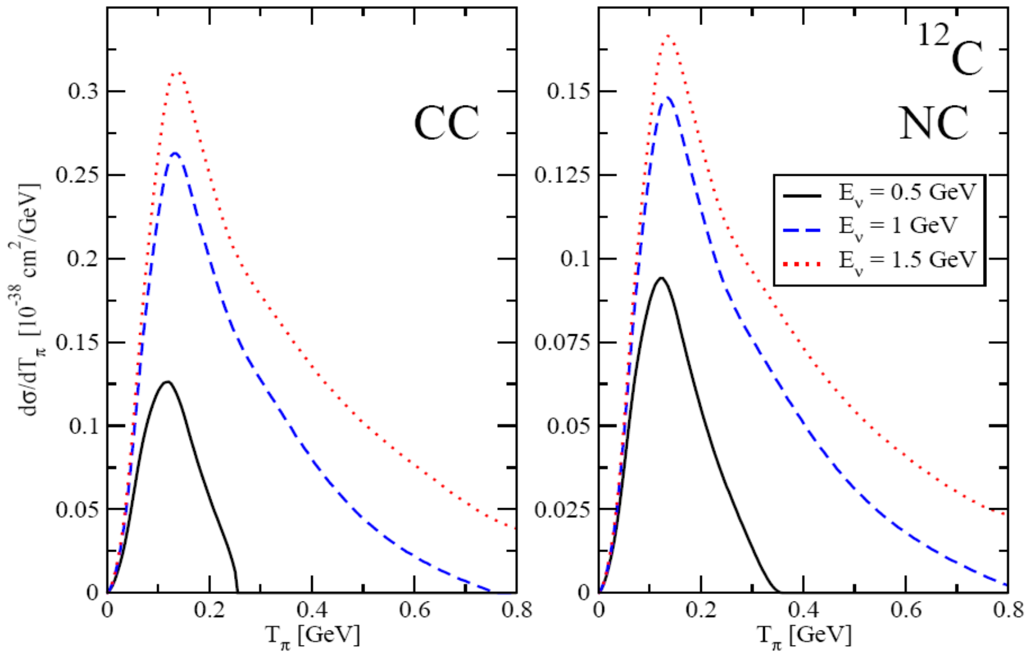

pion kinetic energy

Total cross section

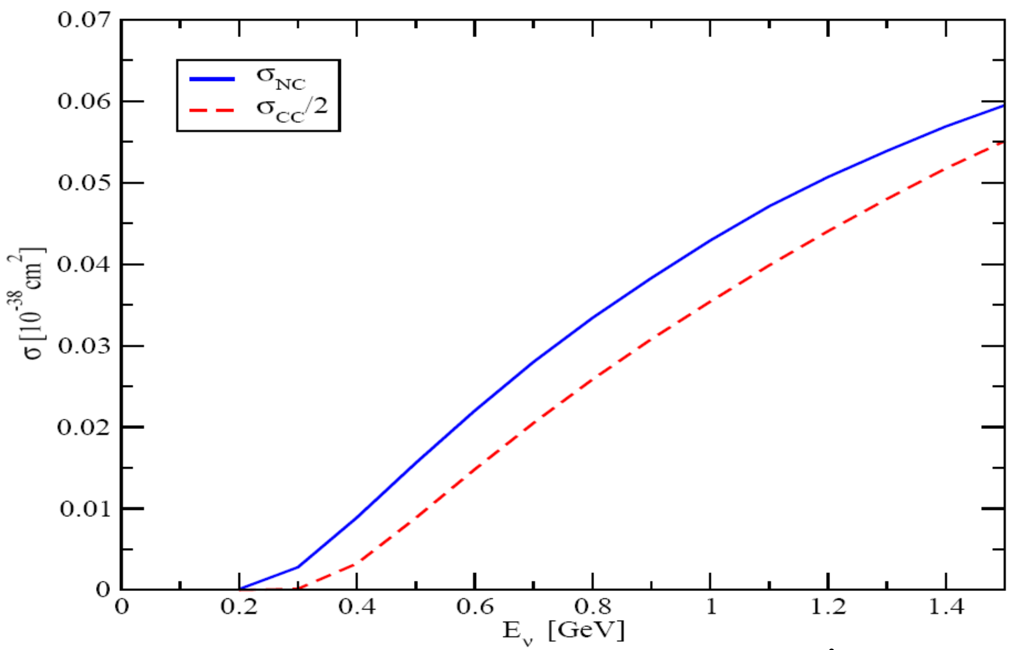

neutrino energy

ν_μ induced coherent pion production

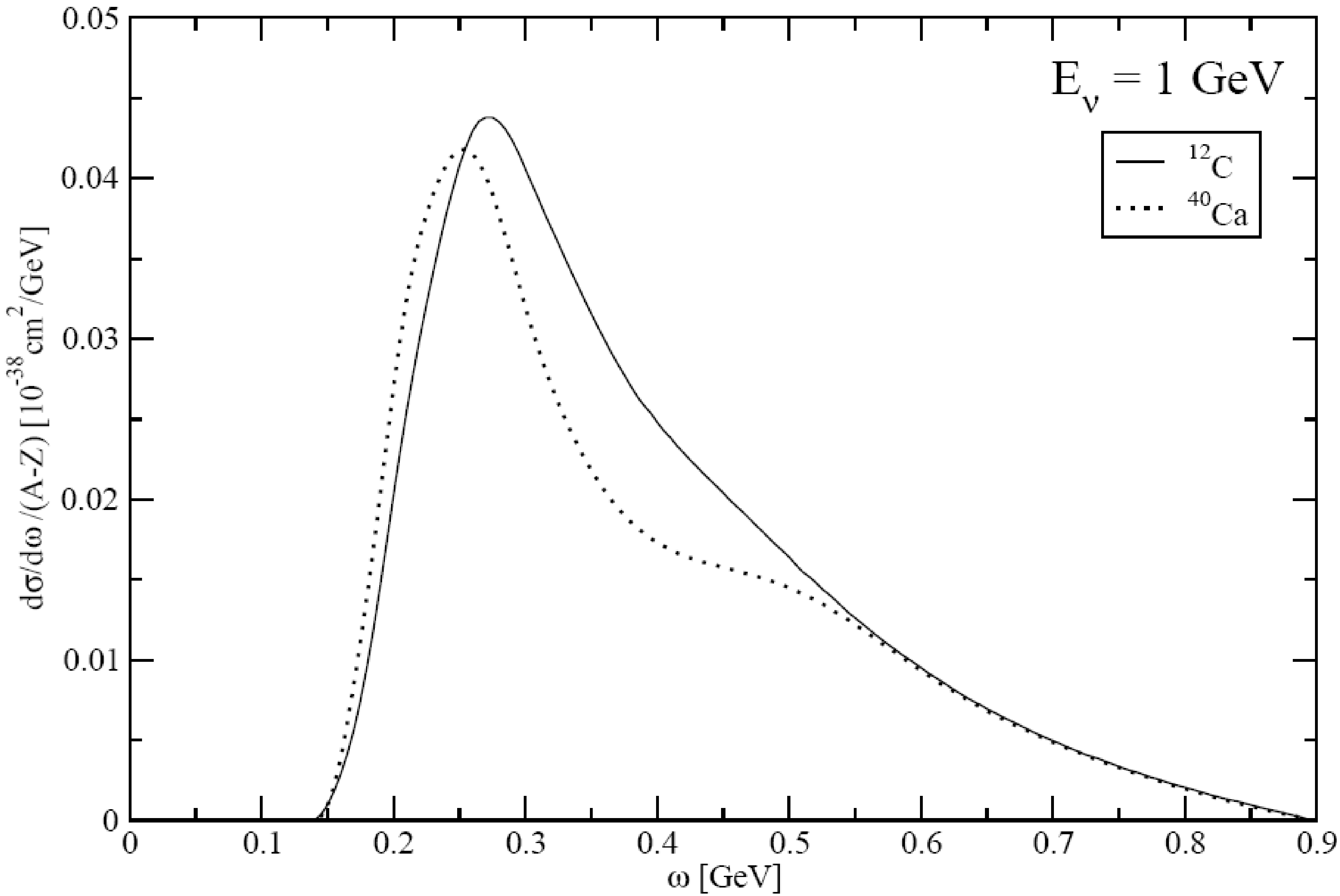

QE Scattering with free nucleon at rest: two-body kinematics

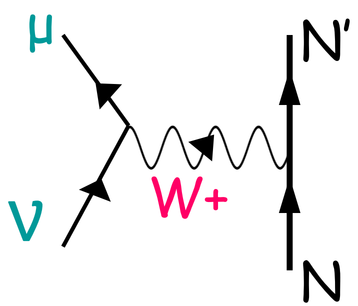

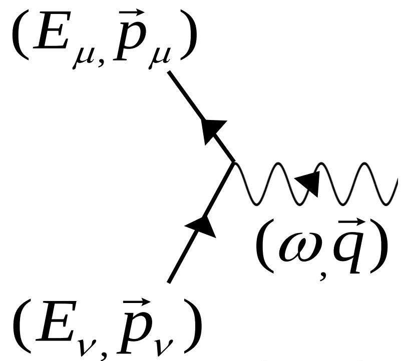

$$\omega = E_\nu - E_\mu$$

$$q^2 = E_\nu^2 + p_\mu^2 - 2E_\nu p_\mu \cos\theta$$

$$q^2 - \omega^2 = 4(E_\mu + \omega)E_\mu \sin^2\frac{\theta}{2} - m_\mu^2 + 2(E_\mu + \omega)(E_\mu - p_\mu)\cos\theta$$

The nuclear response function is proportional to the delta distribution

$$\delta\left[\omega - \left(\sqrt{q^2 + M^2} - M\right)\right]$$

The intercept of the **hyperbola** with the **QE line** fixes the possible ω and q values for given E_μ and θ.

Hence the neutrino energy is determined

$$\boxed{E_\nu = E_\mu + \omega_{\text{intercept}}}$$

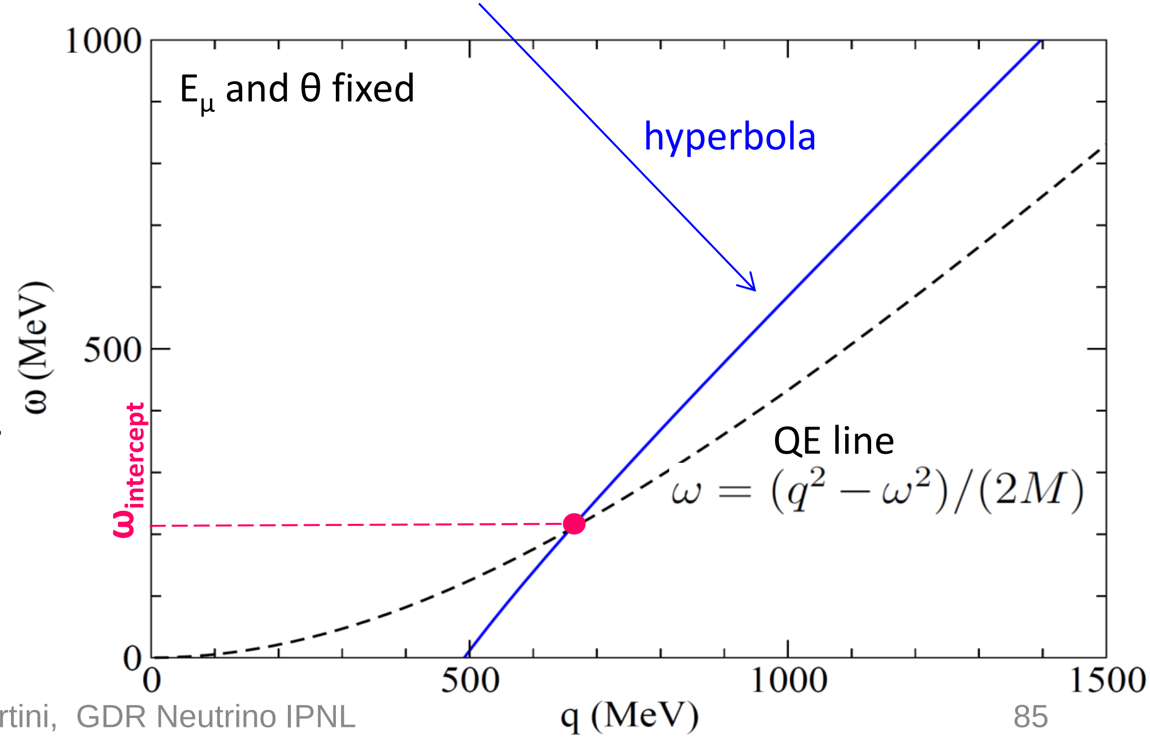

QE Scattering with nucleons inside the nucleus

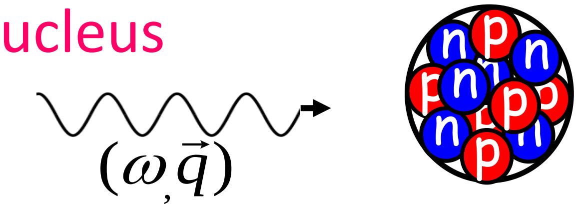

1 particle- 1 hole (p-h) excitation

$q < 2\, k_F$

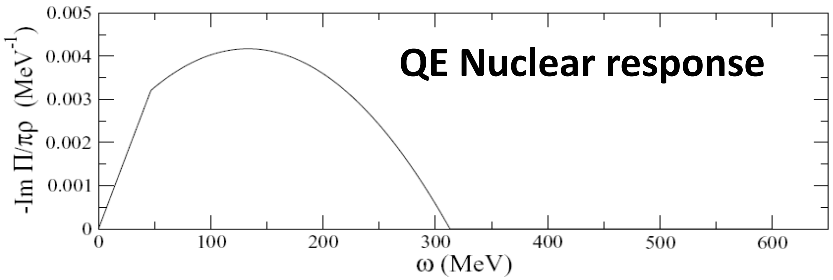

Fermi motion spreads δ distribution (Fermi Gas)

Pauli blocking cuts part of the low momentum nuclear response

RPA collective effects

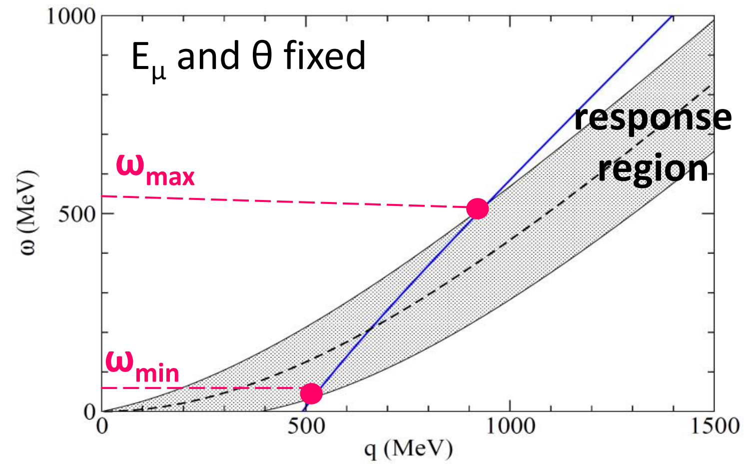

Broadening of the neutrino energy

$$\boxed{E_\nu = E_\mu + (\omega_{\min} \le \omega \le \omega_{\max})}$$

np-nh excitations

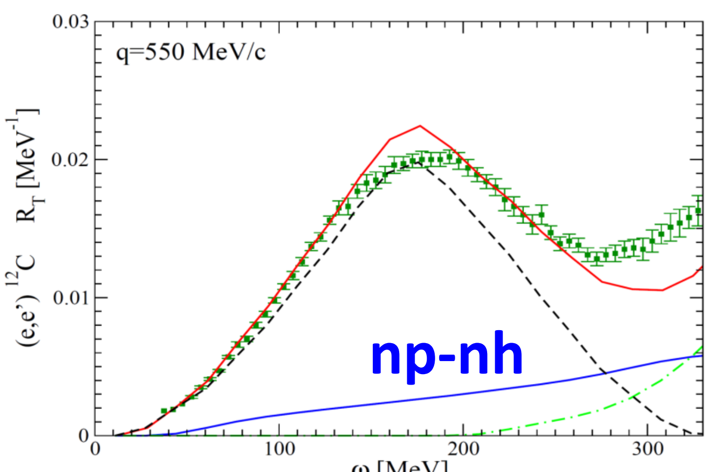

- np-nh creates a high energy tail above the QE peak
- np-nh enlarges the region of response to the whole (ω,q) plane

no reason to fulfill the QE relation for Ev reconstruction

A. Neutrino energy distributions with fixed muon variables (E_μ and θ)

$$f(E_\nu, E_\mu, \theta)dE_\nu = C\left[\frac{d^2\sigma}{d\omega\ d\cos\theta}\right]_{\omega=E_\nu-E_\mu}\Phi(E_\nu)dE_\nu$$

Neutrino flux
3 cases for example

Neutrino-nucleus double differential cross section

- Main ingredient of this calculation
- We consider our theoretical model which was quite successful in the reproduction of MiniBooNE QE data

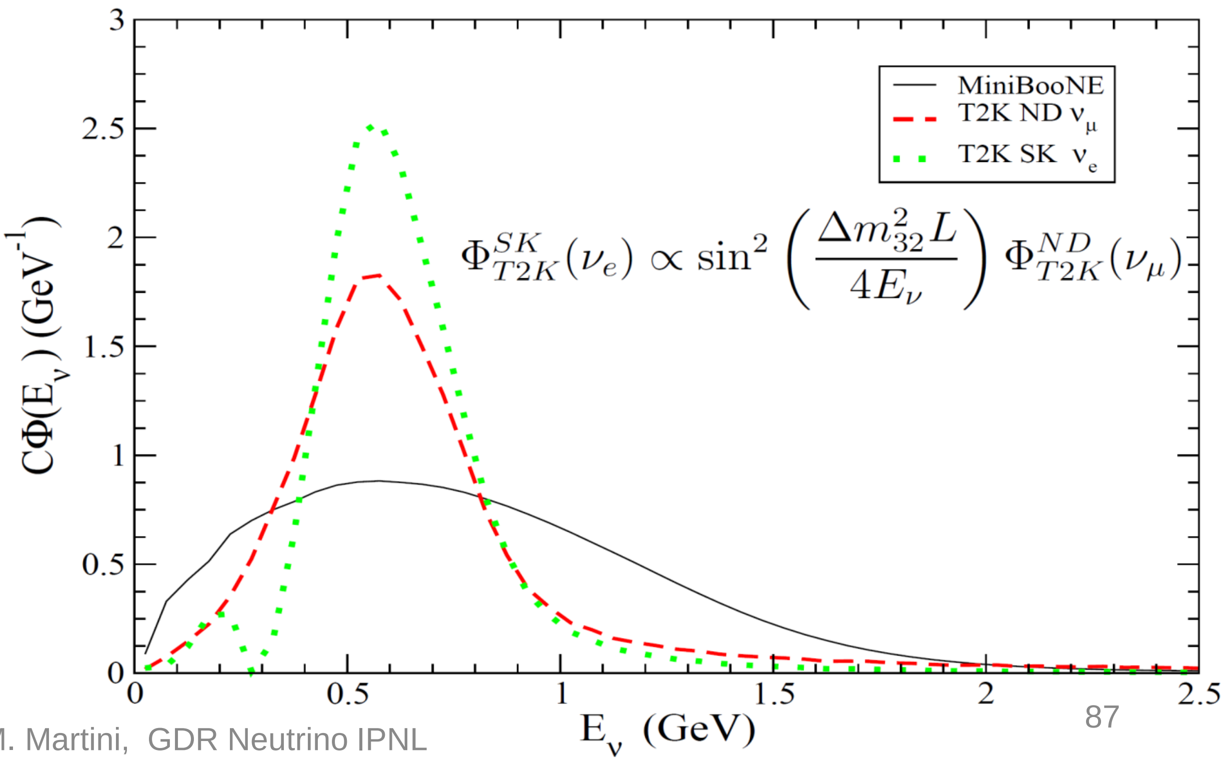

Given Eμ and θ ⟹ Unique $\bar{E}\nu$ reconstructed value (vertical green line) but a broadening of the true neutrino energy due to nuclear effects (Fermi motion, RPA, np-nh)

Neutrino energy distributions

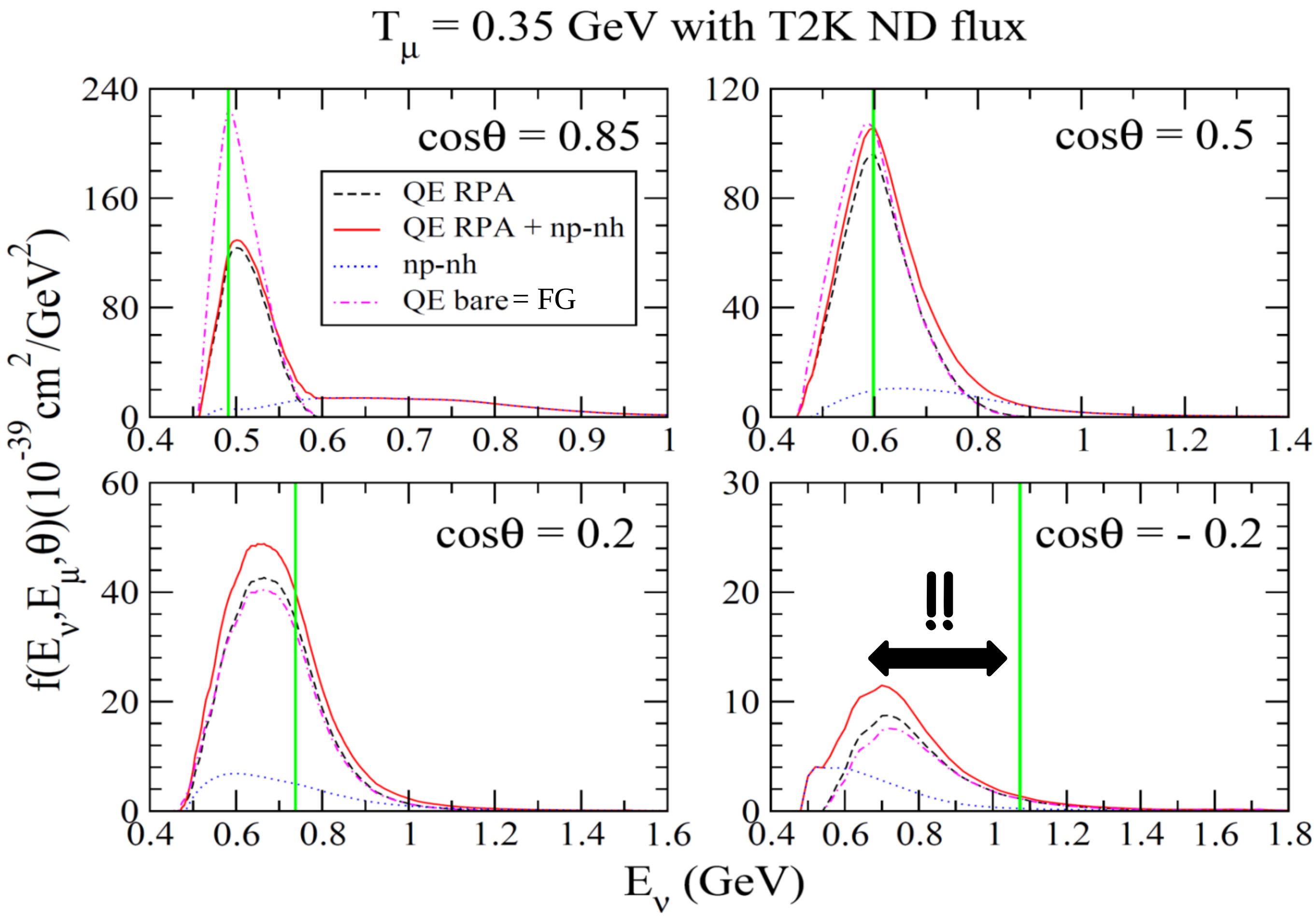

Sizeable deviations from the reconstructed energy

Hardening or softening depending on θ

Tails created by the np-nh contribution

Neutrino energy distributions with fixed Eμ and θ

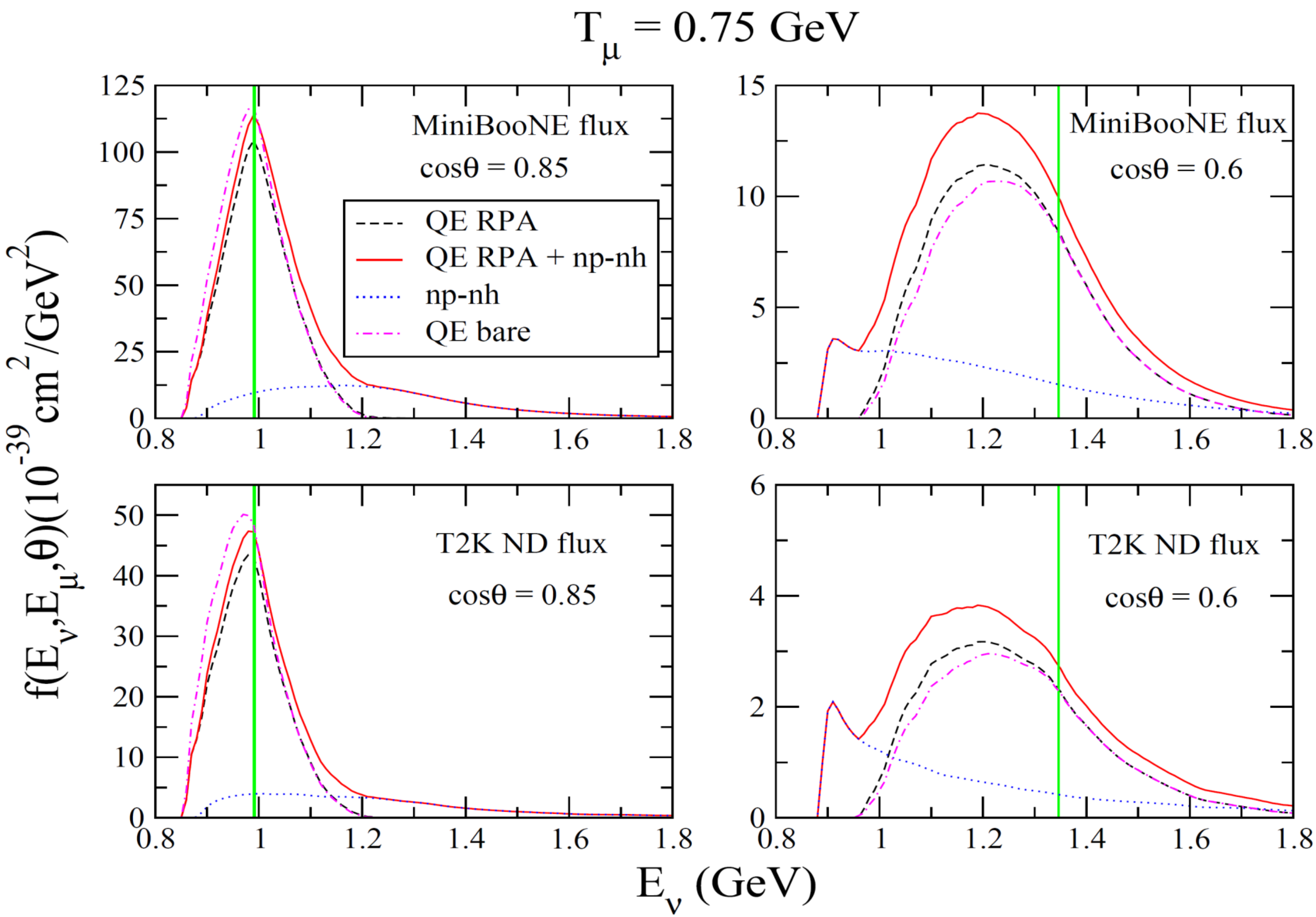

Remember: response region and hyperbolas

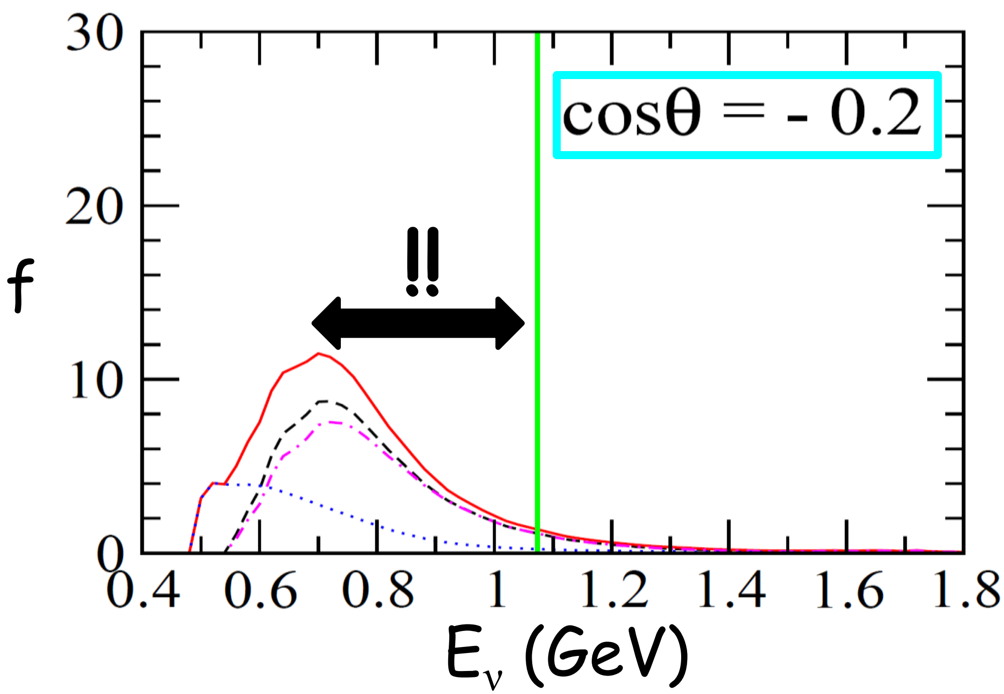

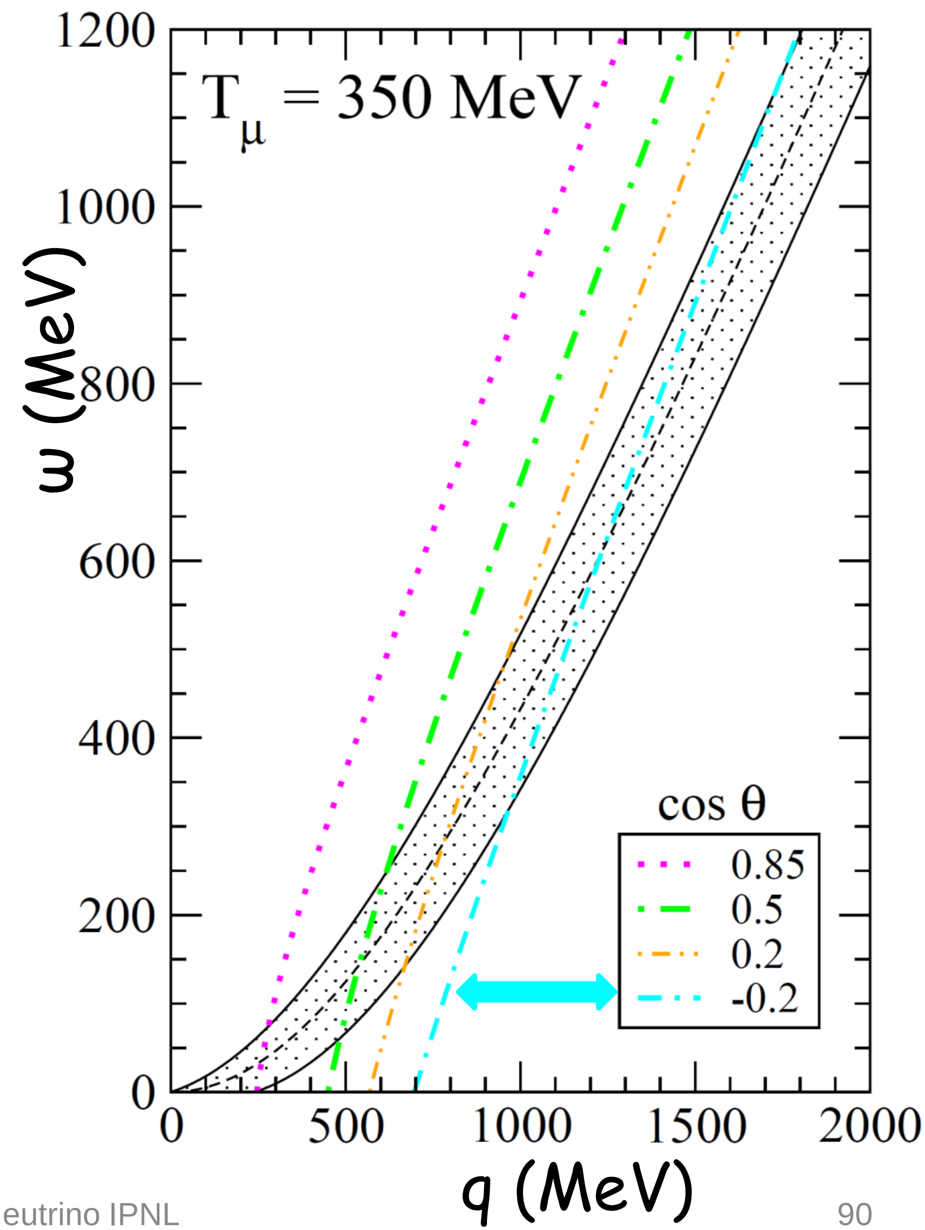

At large muon angle the portion of hyperbola inside the quasielastic region is very large

Response region and hyperbolas for several Tμ and θ

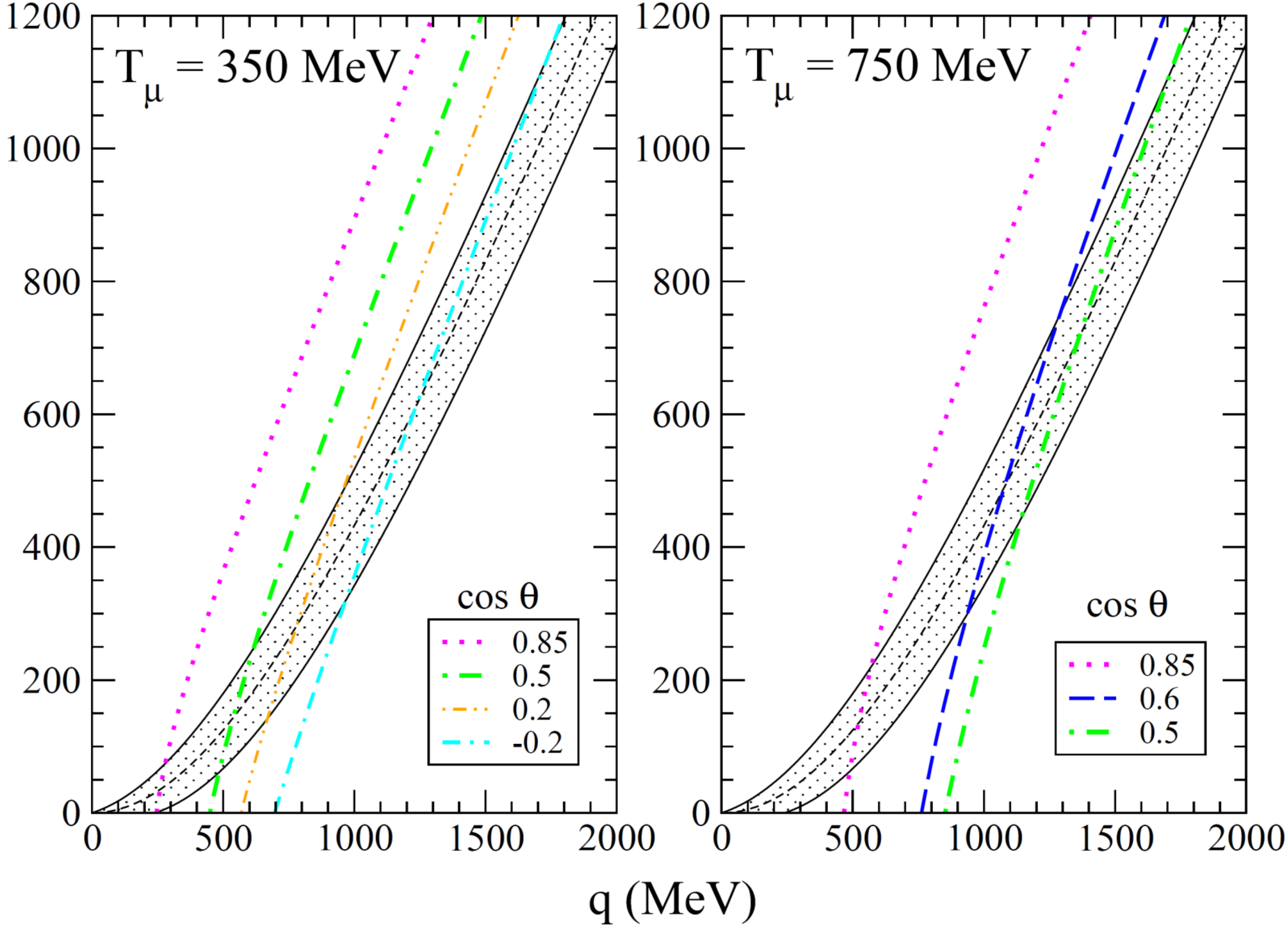

With increasing muon angle the portion of hyperbola inside the quasielastic region become very large

B. Neutrino energy distributions with no specification of lepton observables

Neutrino reconstructed energy **$\bar{E}\nu$ is fixed**

Many couples of Eμ and θ can lead to the same $\bar{E}\nu$

One has to sum over these couples

$$\overline{E_\nu} P_\mu \cos\theta + M(\overline{E_\nu} - E_\mu) - \overline{E_\nu} E_\mu + m_\mu^2/2 = 0 \Longleftrightarrow \overline{E_\nu} = \frac{E_\mu - m_\mu^2/(2M)}{1-(E_\mu - P_\mu\cos\theta)/M}$$

$\cos\theta(E_\mu, \overline{E_\nu})$ is the cosine solution of this equation for given $\bar{E}\nu$ and Eμ

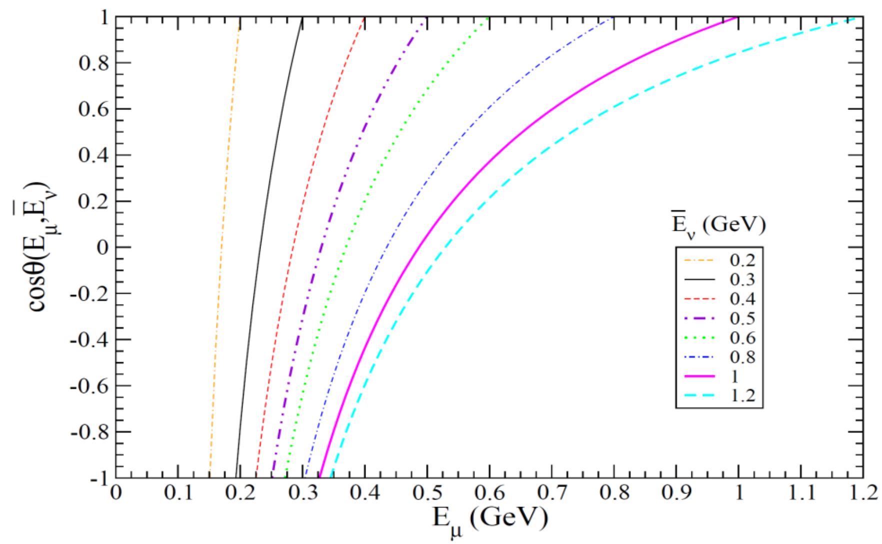

$$F(E_\nu, \overline{E_\nu}) = c\frac{\Phi(E_\nu)}{\int dE_\nu \Phi(E_\nu)} \int_{E_\mu^{\min}}^{E_\mu^{\max}} dE_\mu \left[\frac{d^2\sigma}{d\omega\ d\cos\theta}\right]_{\omega=E_\nu-E_\mu,\ \cos\theta=\cos\theta(E_\mu,\overline{E_\nu})}$$

Probability distribution before normalization

$$F(E_\nu,\overline{E_\nu}) = c\frac{\Phi(E_\nu)}{\int dE_\nu \Phi(E_\nu)} \int_{E_\mu^{\min}}^{E_\mu^{\max}} dE_\mu \left[\frac{d^2\sigma}{d\omega\ d\cos\theta}\right]_{\omega=E_\nu-E_\mu,\ \cos\theta=\cos\theta(E_\mu,\overline{E_\nu})} = cI(E_\nu,\overline{E_\nu})$$

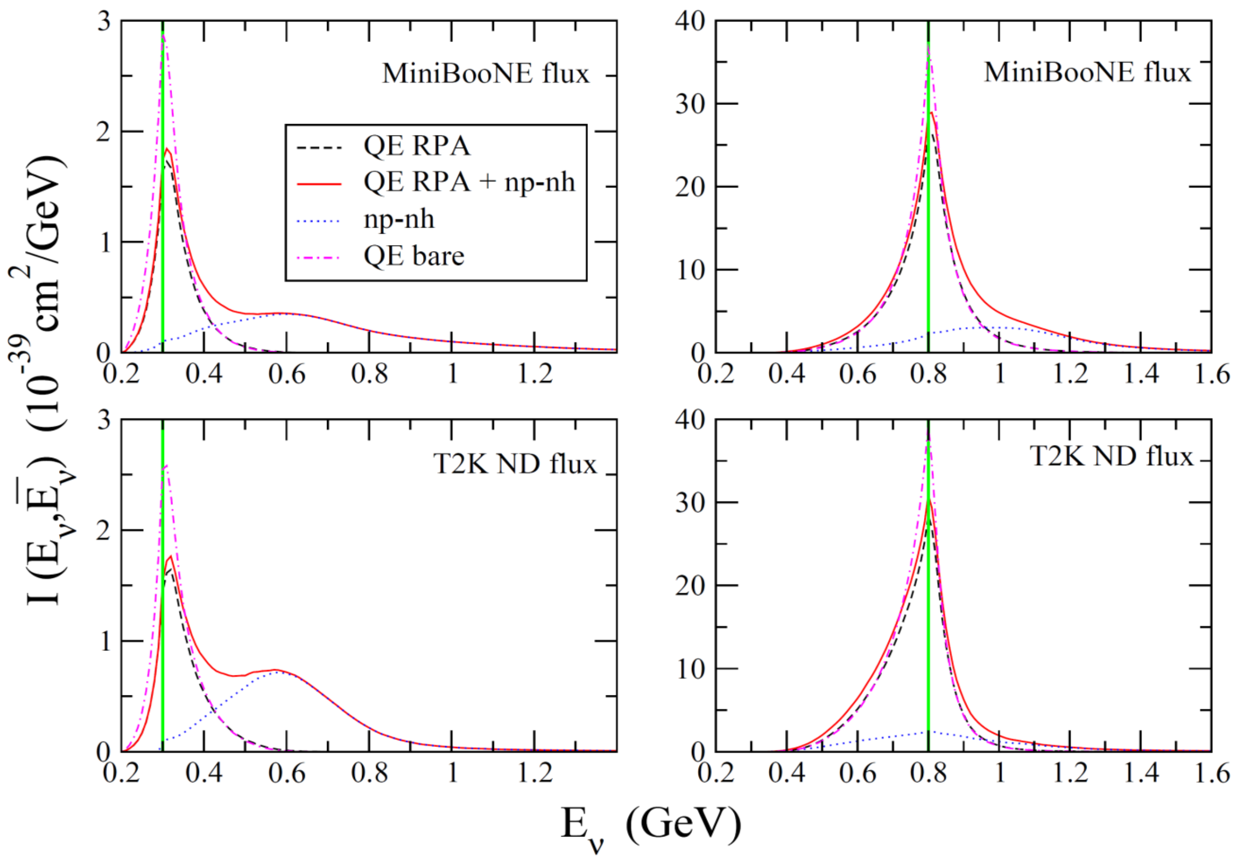

Probability energy distributions with no specification of lepton observables

$$F(E_\nu,\overline{E_\nu}) = c\frac{\Phi(E_\nu)}{\int dE_\nu \Phi(E_\nu)} \int_{E_\mu^{\min}}^{E_\mu^{\max}} dE_\mu \left[\frac{d^2\sigma}{d\omega\ d\cos\theta}\right]_{\omega=E_\nu-E_\mu,\ \cos\theta=\cos\theta(E_\mu,\overline{E_\nu})}$$

$$\int dE_\nu\ F(E_\nu,\overline{E_\nu}) = 1$$

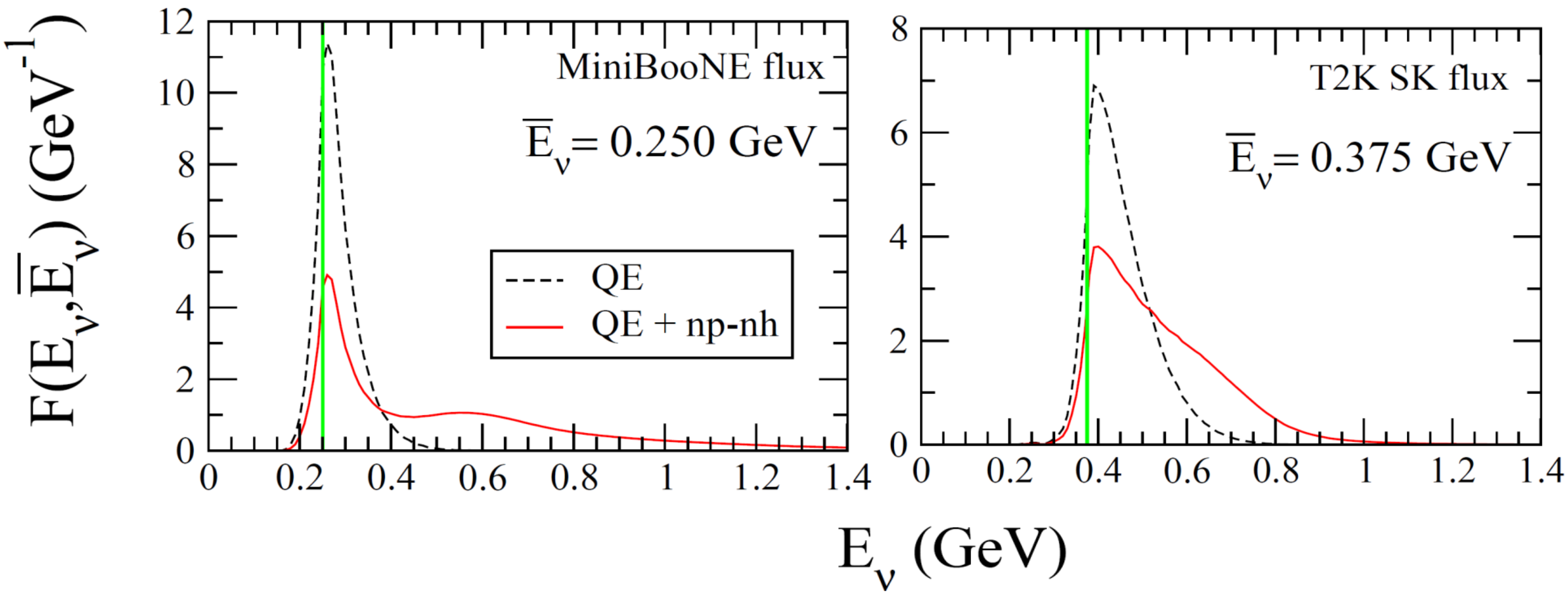

$\bar{E}\nu$: vertical green line

High energy tail due to the np-nh contribution

The average neutrino energy

$$(E_\nu)_{\text{average}}(\overline{E_\nu}) = \int dE_\nu \; E_\nu \; F(E_\nu, \overline{E_\nu})$$

	MiniBooNE		T2K ND	
$\overline{E_\nu}$ (MeV)	QE + np-nh	QE	QE + np-nh	QE
300	546	335	514	350
400	579	435	529	446
500	638	527	575	528
600	711	619	638	606
800	861	799	781	758
1000	1024	981	937	914
1200	1190	1164	1116	1104

Applications to actual data

Reconstructed energy $\Longrightarrow$ True neutrino energy

Experimental distributions are given in terms of reconstructed ν energy.
Experimental results change once plotted in terms of the true neutrino energy E_ν

The number of events $g(\overline{E_\nu})d\overline{E_\nu}$ in a bin of reconstructed energy $\overline{E_\nu}$

should be smeared by the function $\boxed{F(E_\nu, \overline{E_\nu})}$

leading to the following **distribution in terms of the real neutrino energy**:

$$G(E_\nu) = \int d\overline{E_\nu}\, g(\overline{E_\nu}) \underline{F(E_\nu, \overline{E_\nu})}$$

For practical reasons instead of continuous integral we have taken a discrete sum of 3 energy points in each bins (which explains the unphysical spikes of our next curves).

N.B.

Up to now any Monte Carlo used in ν experiments includes multinucleon emission

$\nu_\mu \rightarrow \nu_e$ T2K

Reconstructed energy ⟹ True neutrino energy

T2K PRL 107, 041801 (2011)

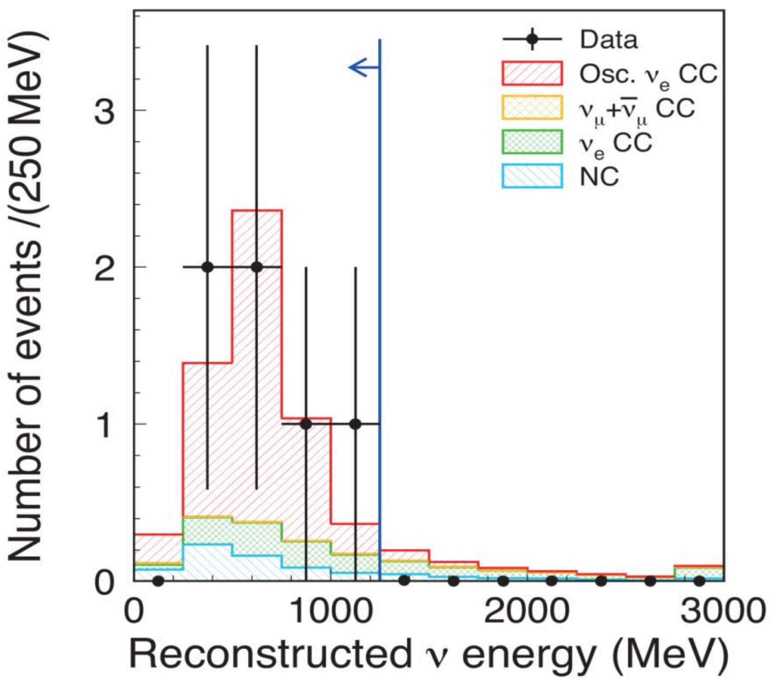

Our calculation

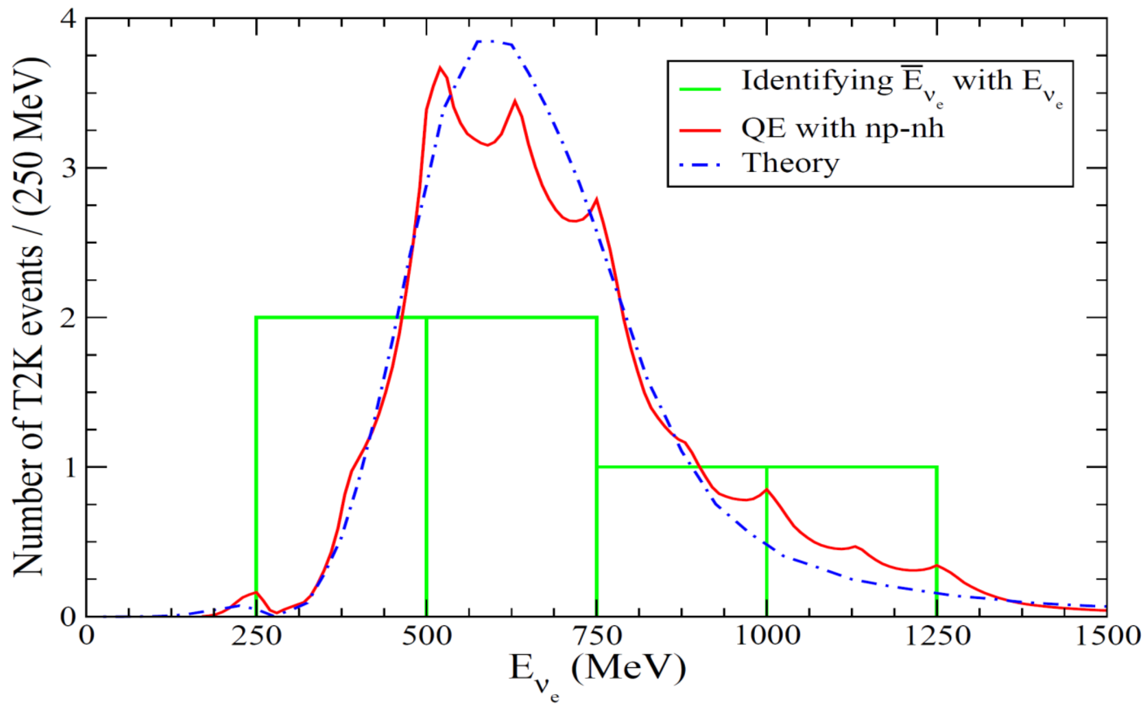

Narrowing of the smeared distribution
in agreement with
our theoretical prediction $\sigma_{\mathrm{QE+np\text{-}nh}}(E_{\nu_e})\Phi^{SK}_{T2K}(E_{\nu_e})$
normalized to same number of events

True neutrino energy ⇨ Reconstructed energy

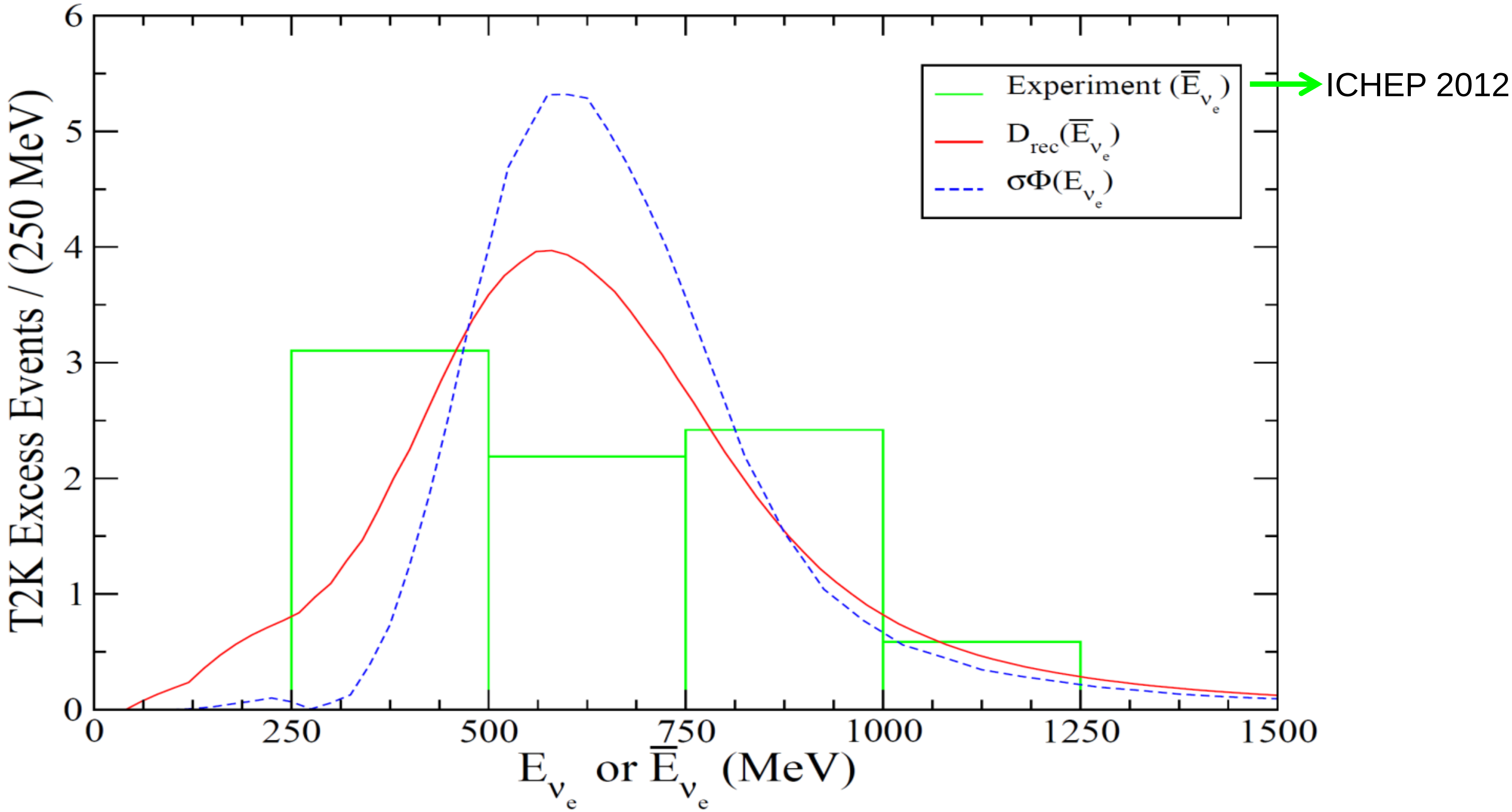

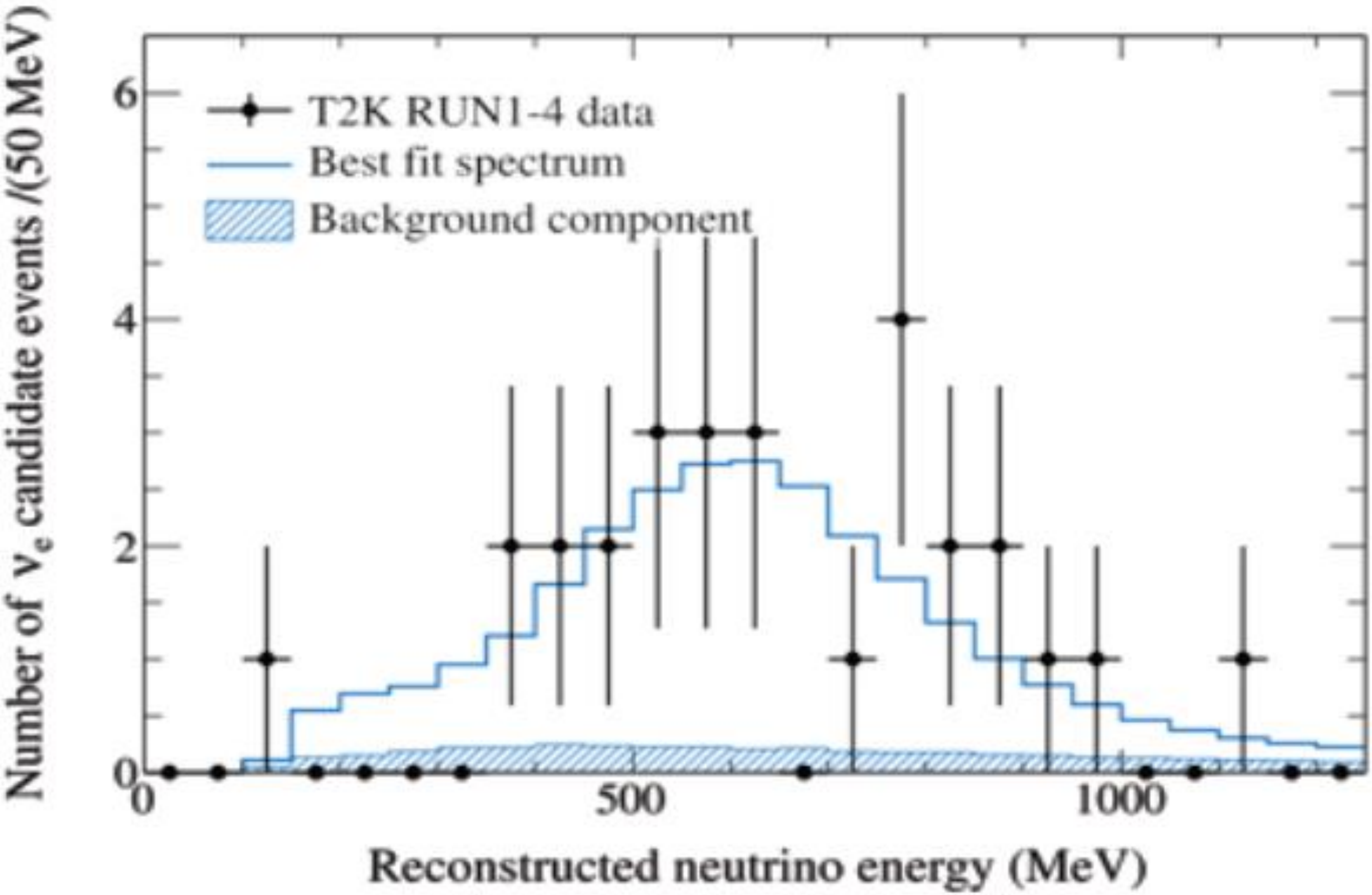

T2K RUN1-4 data
Best fit spectrum
Background component
Number of ν_e candidate events /(50 MeV)
Reconstructed neutrino energy (MeV)
0
2
4
6
0
500
1000

T2K ν_μ disappearance

T2K PRD 85, 031103 (2012)

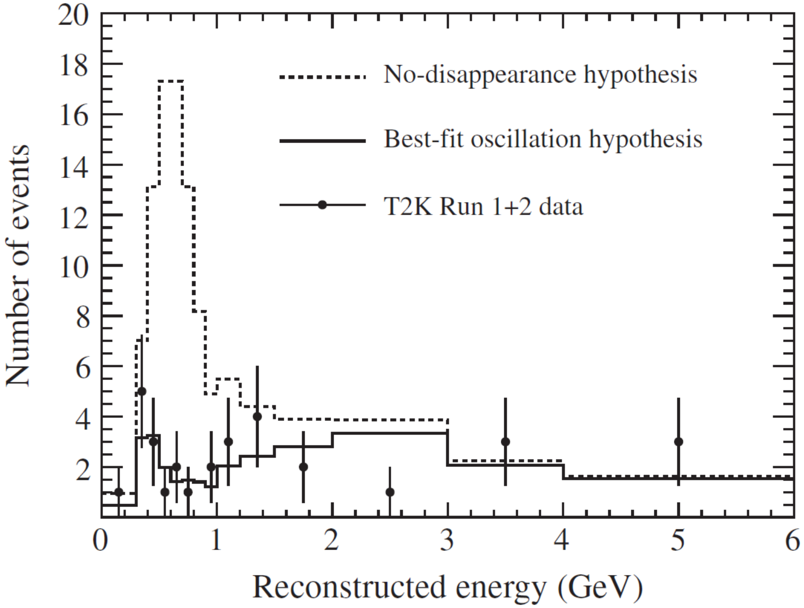

T2K arXiv 1308.0465 (2013)

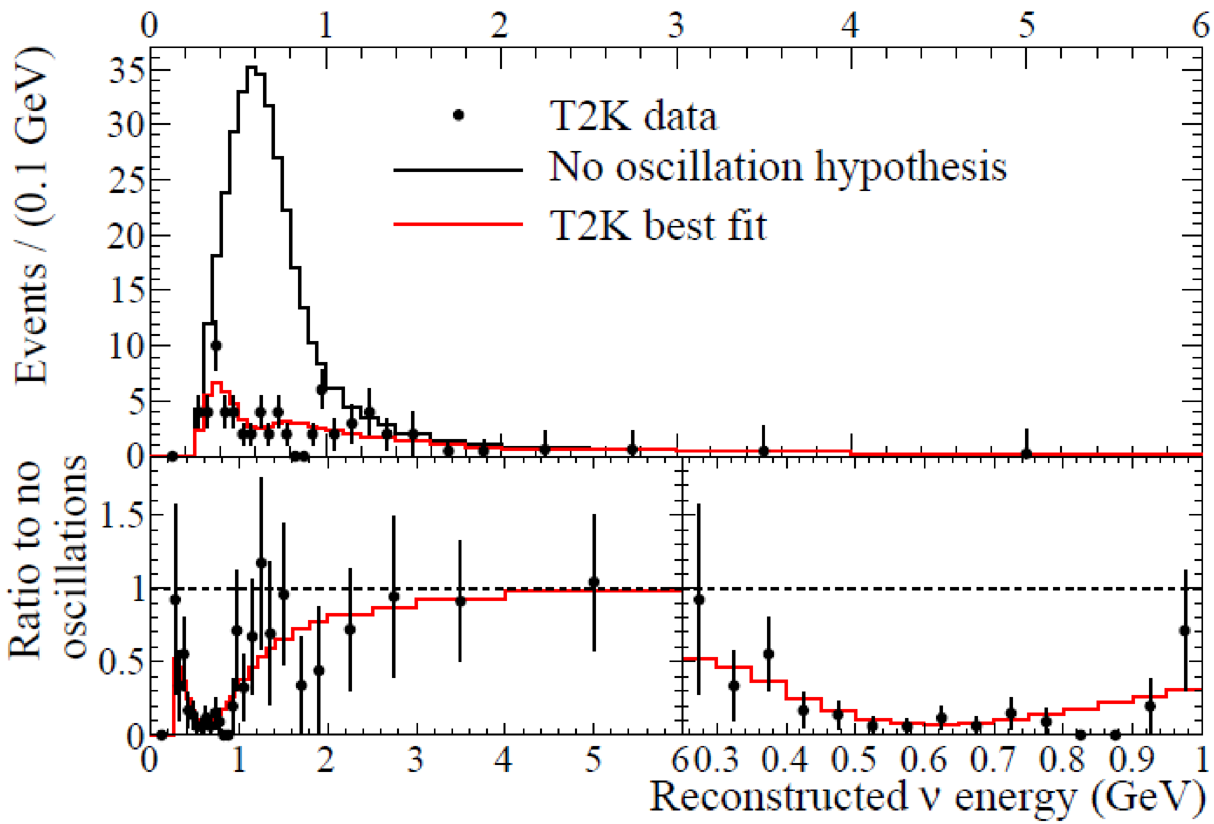

T2K ν_μ disappearance

T2K PRD 85, 031103 (2012)

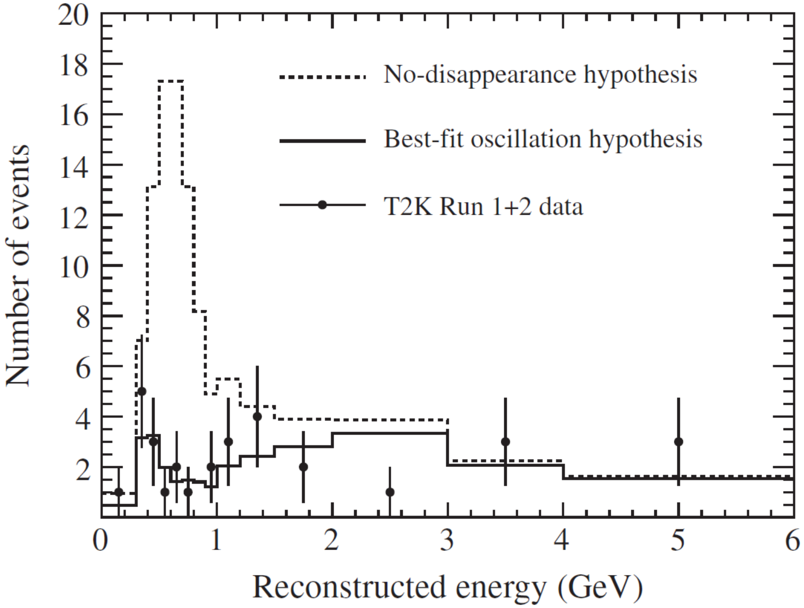

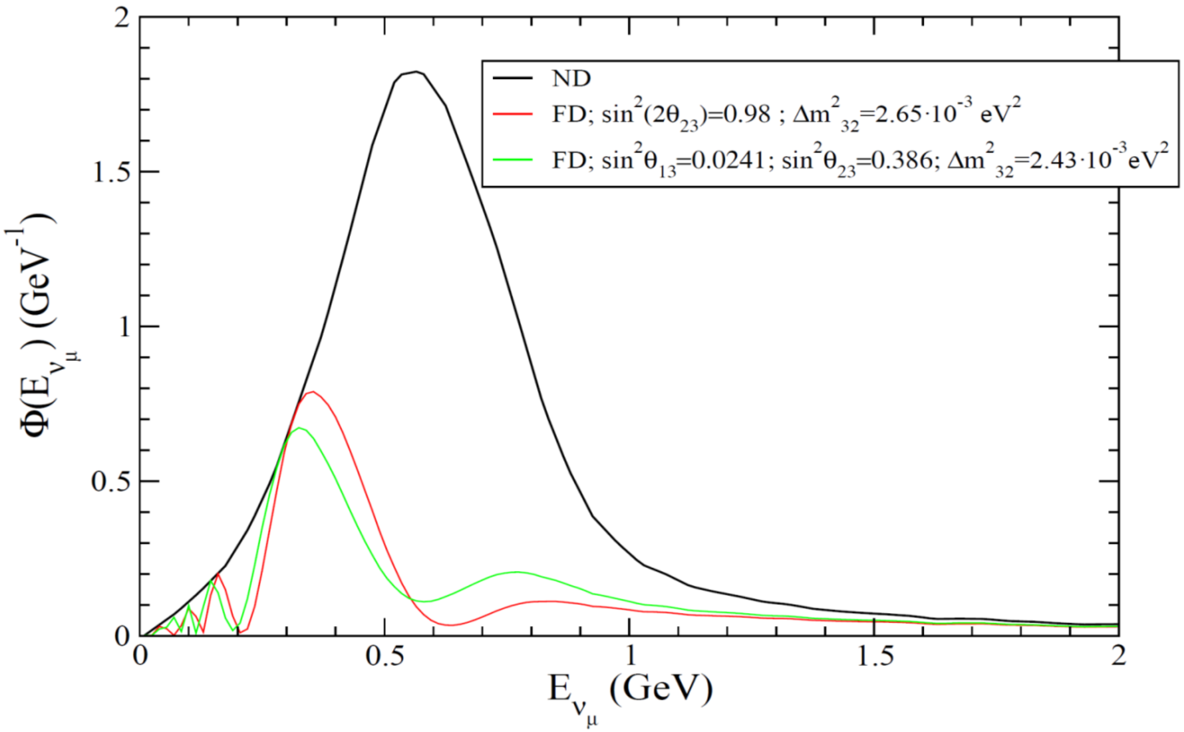

$$\Phi^{FD}_{\nu_\mu}(E_{\nu_\mu}) = \left[1 - 4\cos^2\theta_{13}\sin^2\theta_{23}(1-\cos^2\theta_{13}\sin^2\theta_{23})\sin^2\left(\frac{\Delta m^2_{32}L}{4E_{\nu_\mu}}\right)\right]\Phi^{ND}_{\nu_\mu}(E_{\nu_\mu})$$

Ratio of the distributions FD/ND

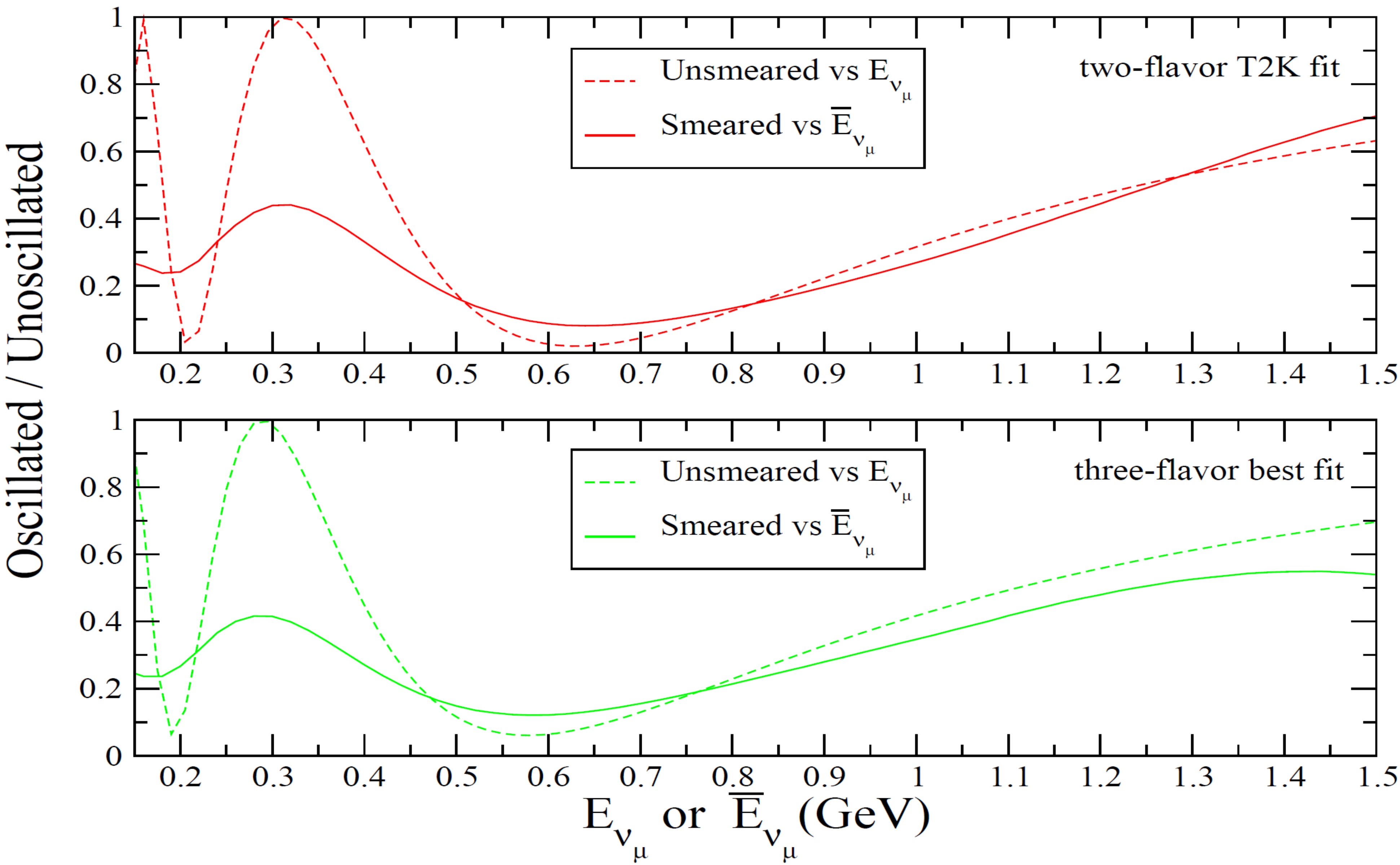

T2K far detector

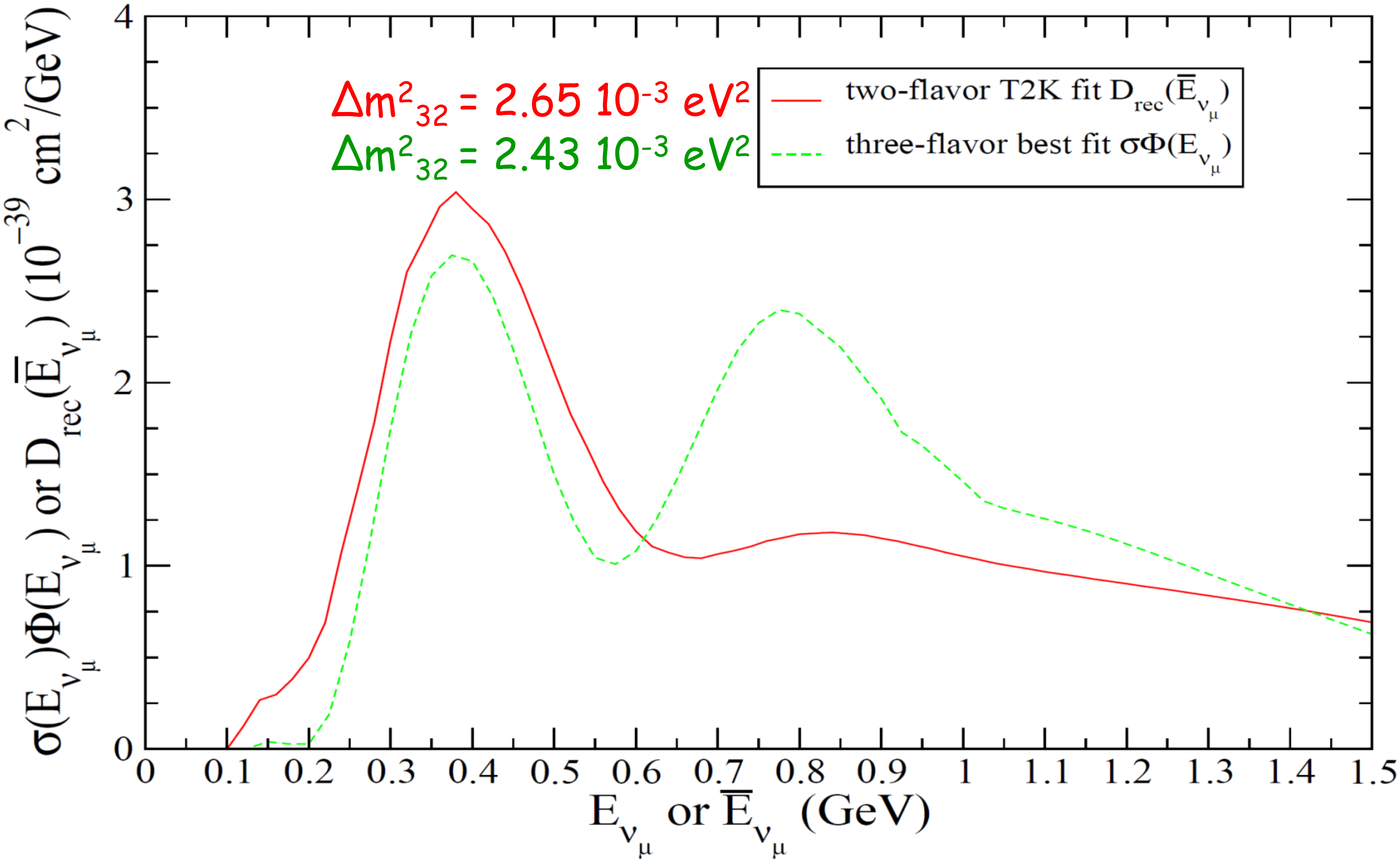

In the first peak region: the smeared curve can be reproduced in the unsmeared case with a lower value of the oscillation mass parameter

M. Martini, M. Ericson, G. Chanfray, PRD 87 013009 (2013)

O. Lalakulich, U. Mosel, K. Gallmeister, PRC 86 054606 (2012)

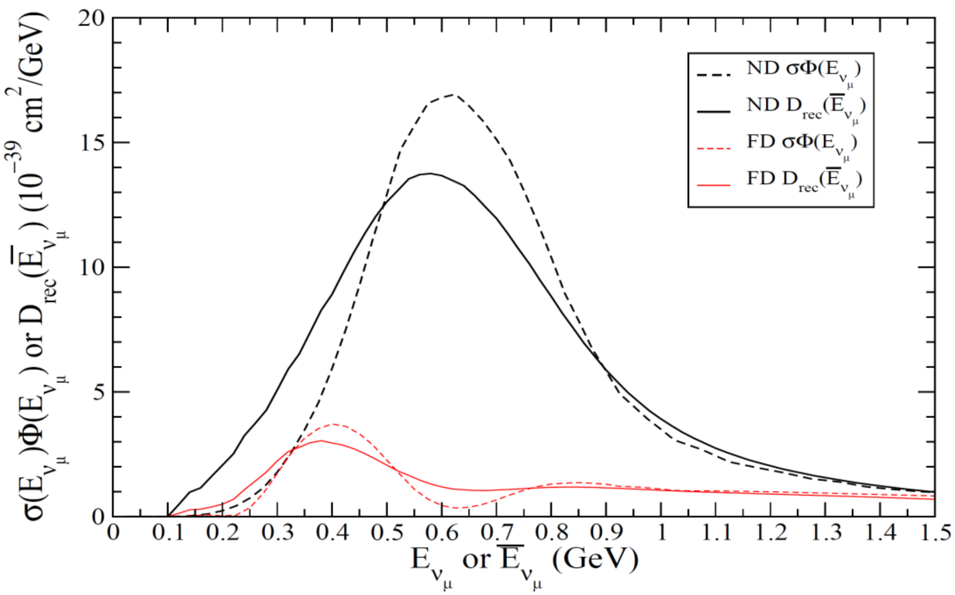

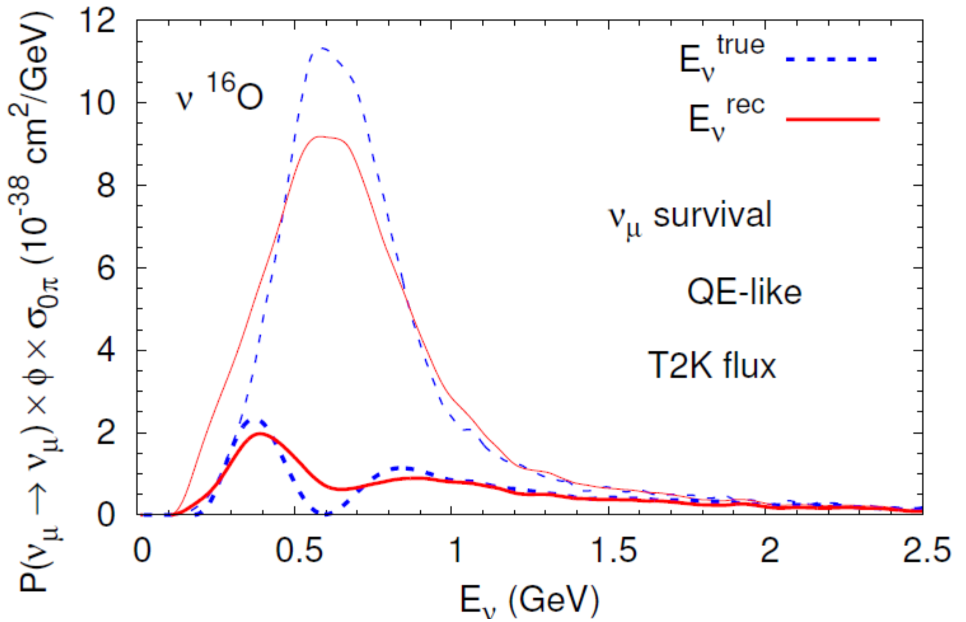

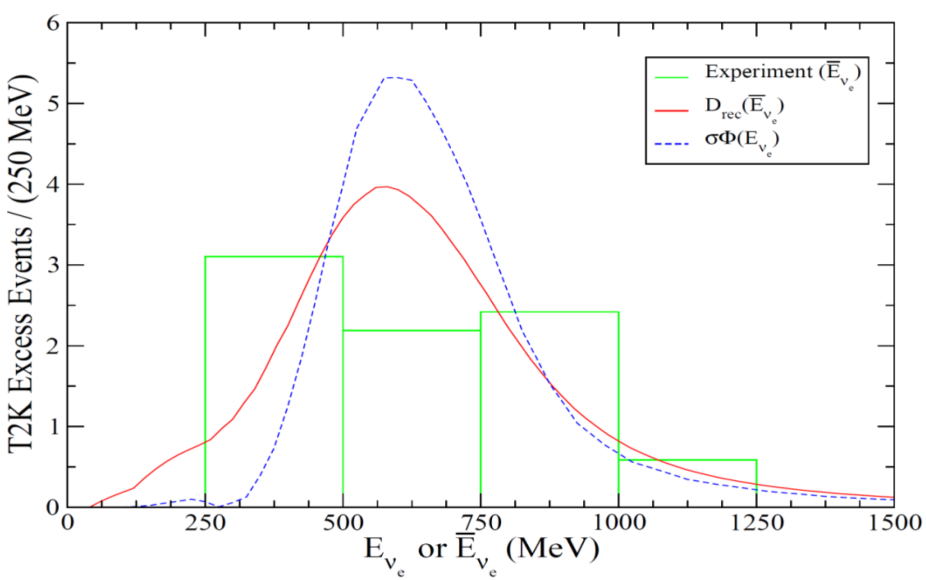

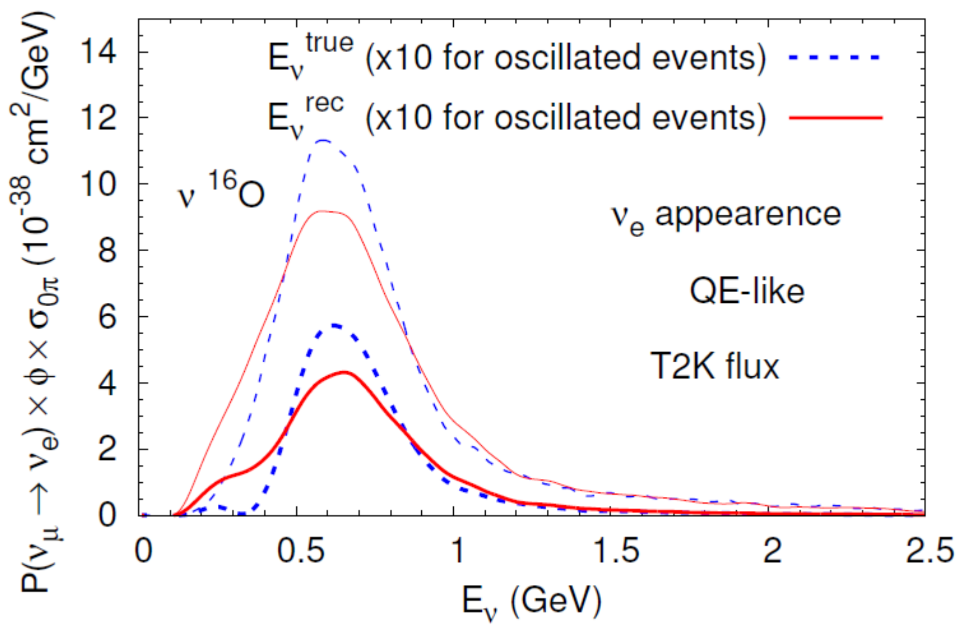

Oscillations induced by sterile neutrino; 3+1 hypothesis

$$\Phi_{\nu_e}(E_{\nu_e}) = \Phi_{\nu_\mu}(E_{\nu_\mu}) \sin^2(2\theta_{41}) \sin^2\left(\frac{\Delta m^2_{41} L}{4E_\nu}\right)$$

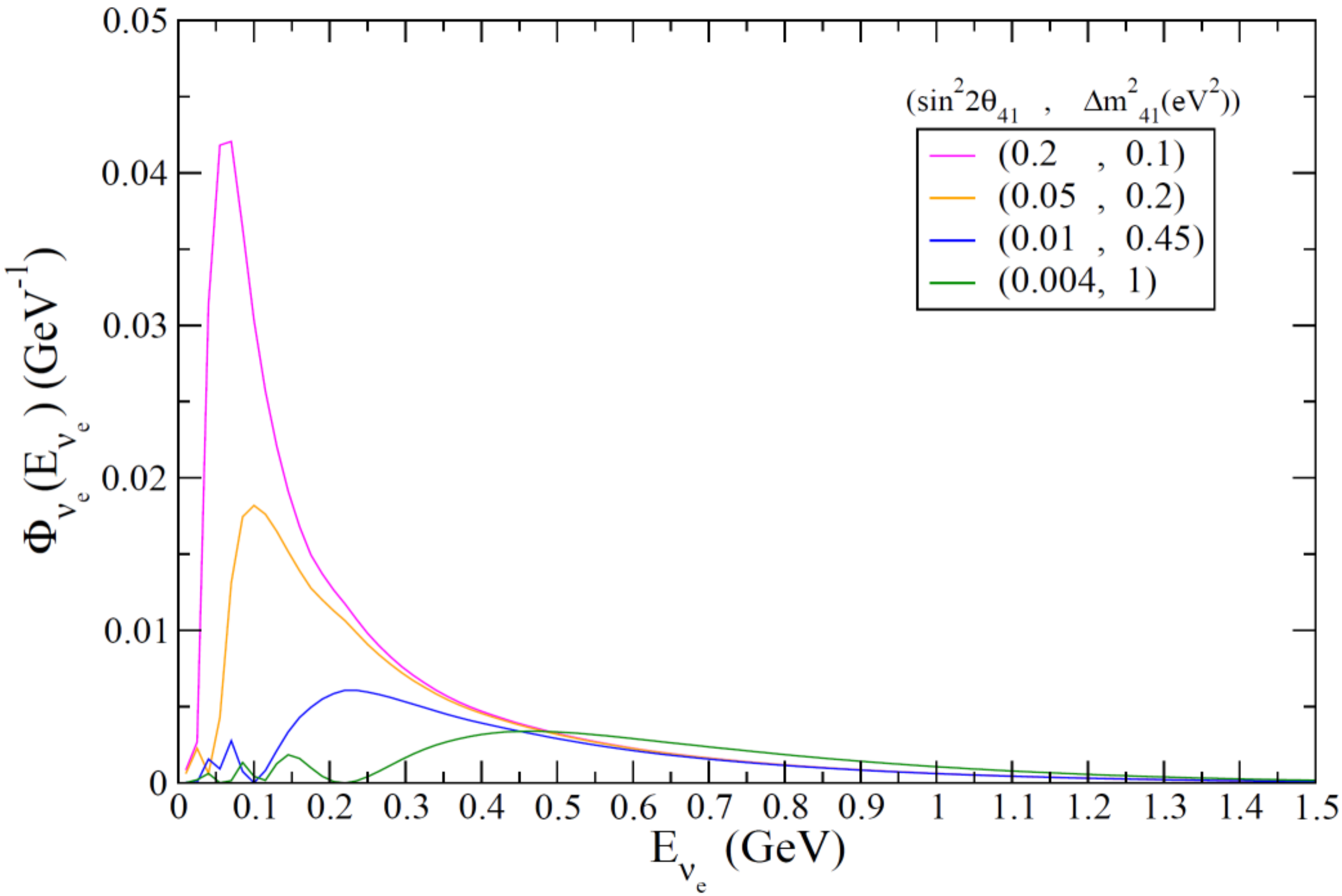

Some considerations on the oscillation parameters

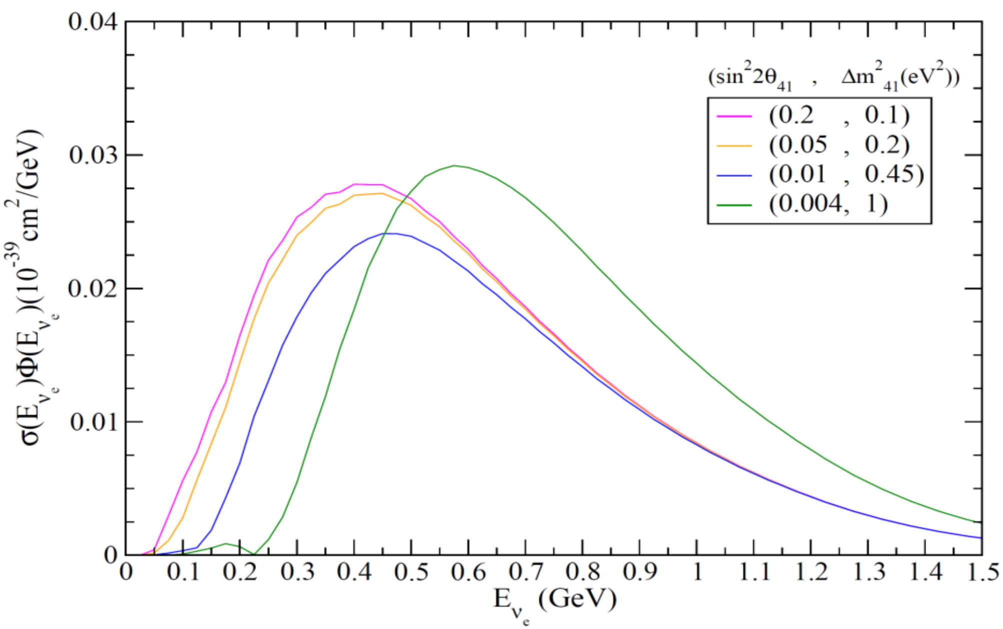

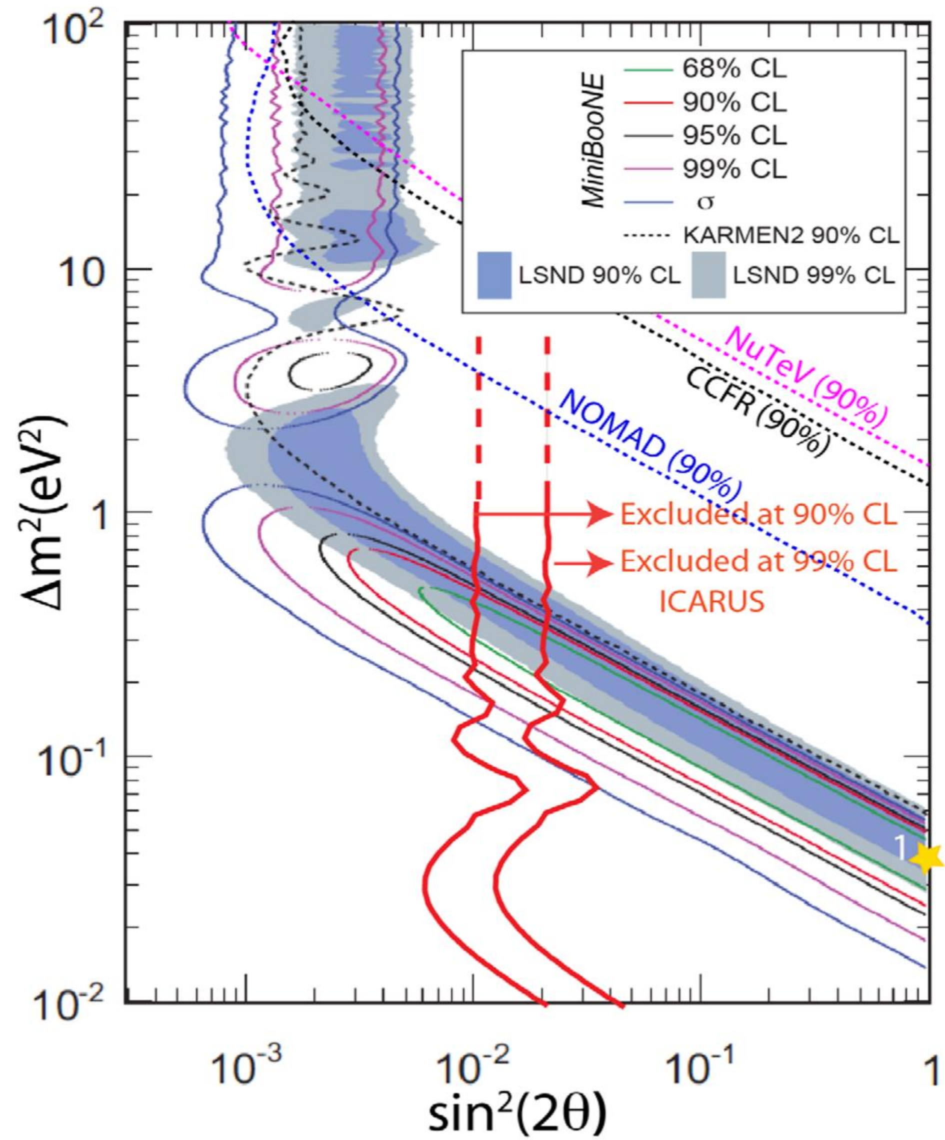

The low energy behavior of the MiniBooNE data favors small values of the mass parameter which concentrate the ν flux at low energies. But small values imply, in order to have enough events, large values of $\sin^2(2\theta)$ which are not compatible with the constraints from other sets of data.

The case of smaller mass values

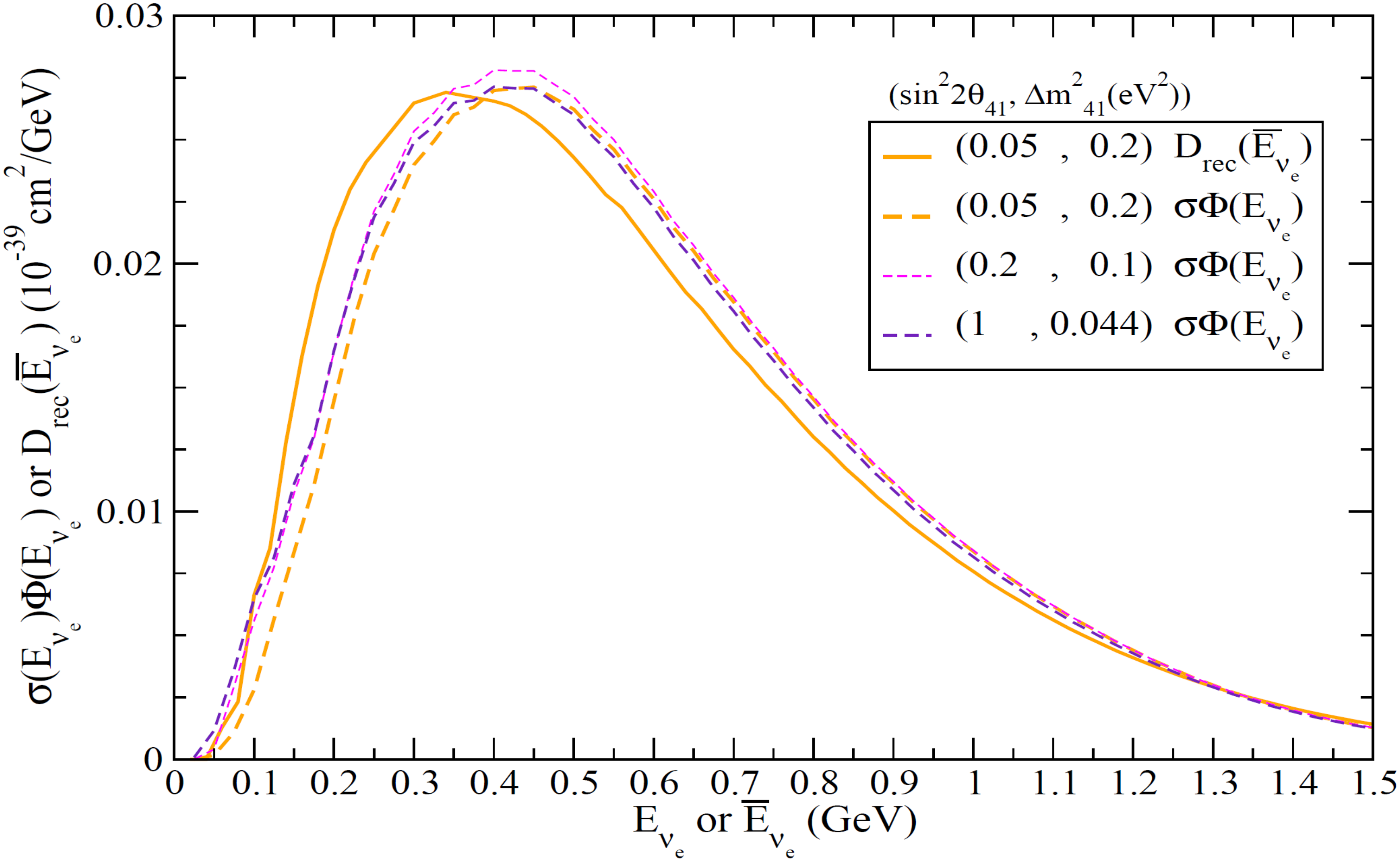

The smeared curve is shifted at lower energies (displacement of the peak ≈ 80 MeV).

It is impossible to reproduce the smeared curve with an unsmeared one even taking a very small mass.

Antineutrinos

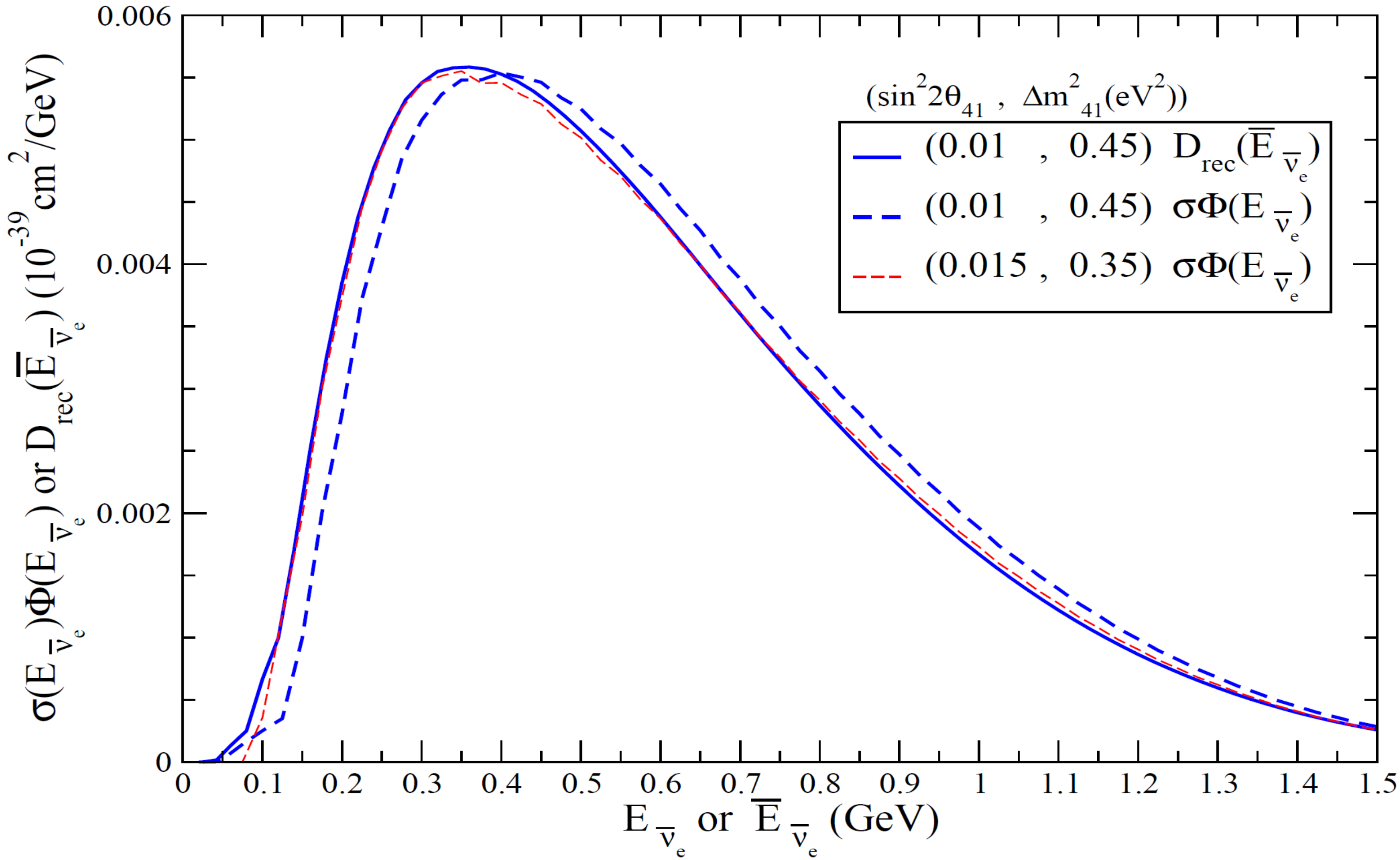

Similar effects, although less pronounced, are present for antineutrinos.

$\nu_\mu \longrightarrow \nu_e$ MiniBooNE

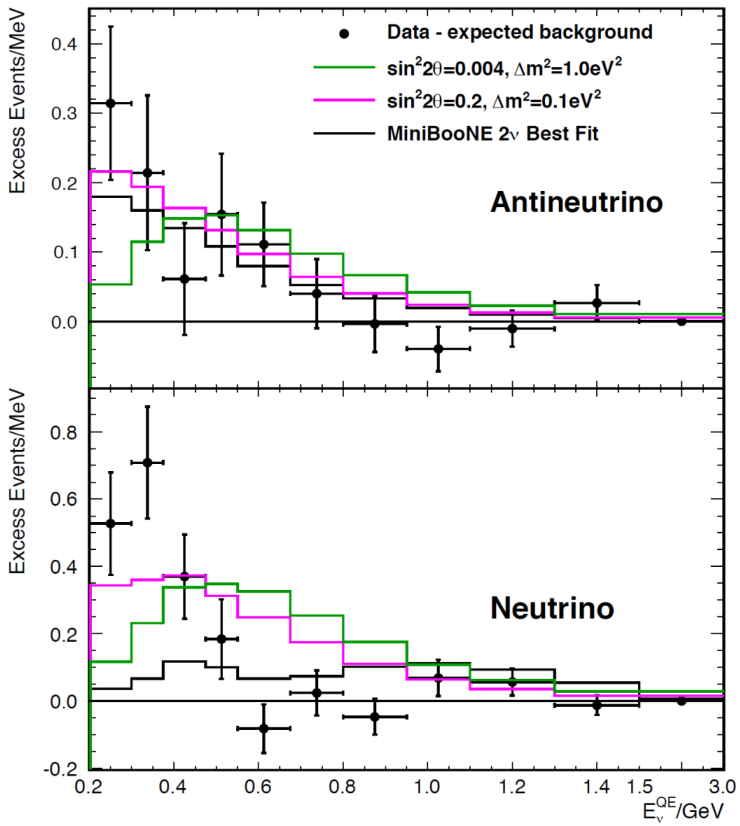

TABLE II: χ^2 *values from oscillation fits to the antineutrino-mode data for different prediction models. The best fit* $(\Delta m^2, \sin^2 2\theta)$ *values are (0.043 eV^2, 0.88), (0.059 eV^2, 0.64), and (0.177 eV^2, 0.070) for the nominal, Martini, and disappearance models, respectively. The test point* χ^2 *values in the third column are for* $\Delta m^2 = 0.5$ *eV^2 and* $\sin^2 2\theta = 0.01$. *The effective dof values are approximately 6.9 for best fits and 8.9 for the test points.*

Prediction Model	χ^2 values Best Fit	χ^2 values Test Pt.
Nominal $\bar{\nu}$−mode Result	5.0	6.2
Martini *et al.* [25] Model	5.5	6.5
Model With Disapp. (see text)	5.4	6.7

arXiv: 1303.2588

ν_e background
and
effective cross sections

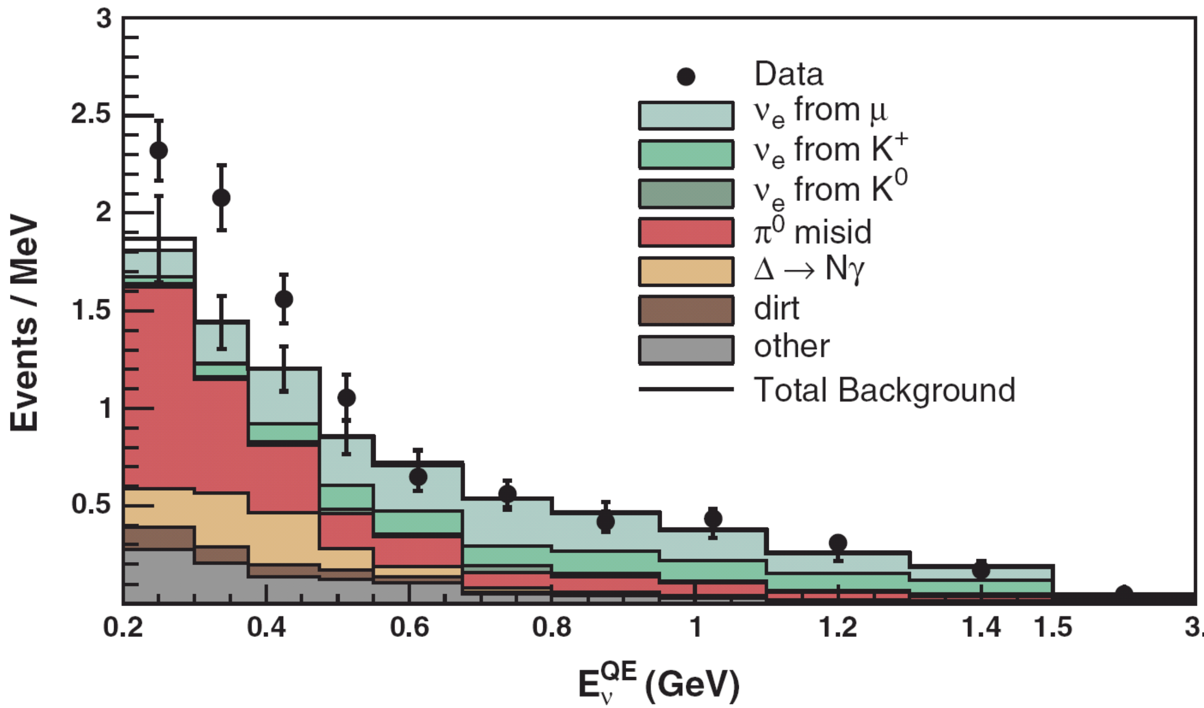

MiniBooNE electron events distribution for ν_e background

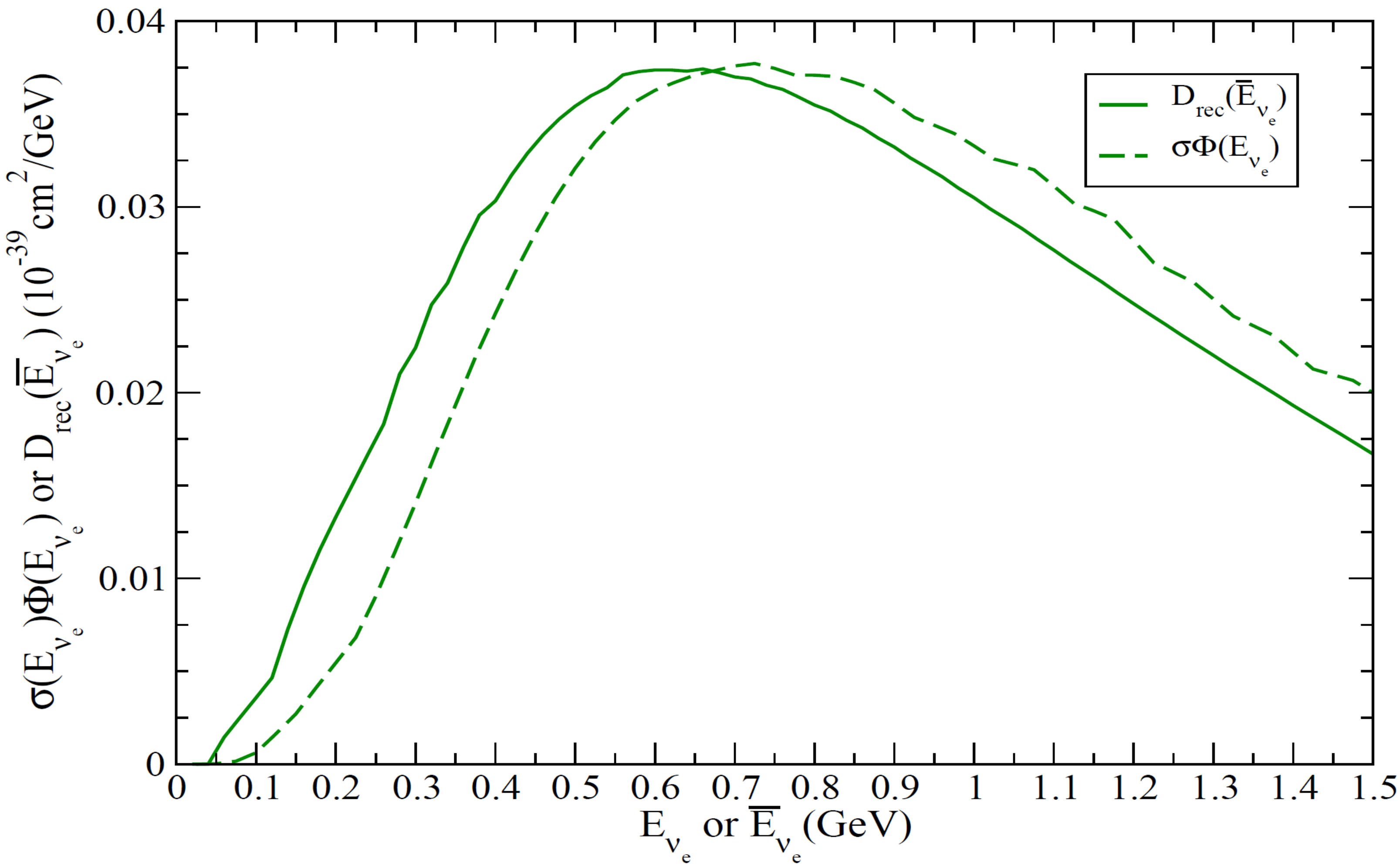

The electron event background is underestimated for low reconstructed neutrino energies E < 0.6 GeV and overestimated for larger ones

MiniBooNE muon events distribution

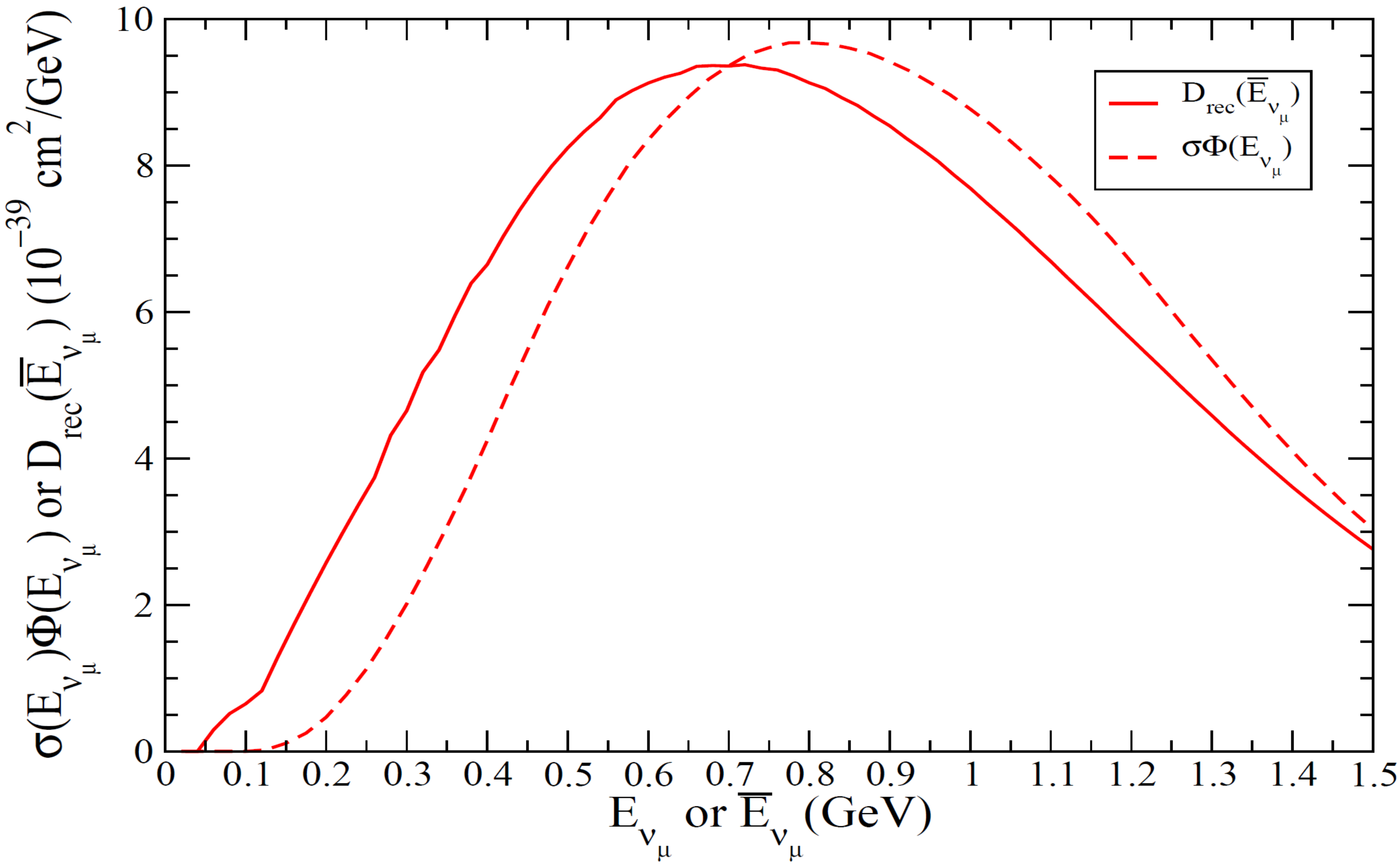

Real and effective cross sections for μ